NTNU – Trondheim
Norwegian University of
Science and Technology

Investigation of Water Injection Performance and Potential on Eldfisk

A Simulation Study

Christina Emilie Kittilsen

Petroleum Geoscience and Engineering
Submission date: December 2014
Supervisor: Jon Kleppe, IPT
Co-supervisor: Serap Ozoglu-Topdemir, ConocoPhillips

Norwegian University of Science and Technology
Department of Petroleum Engineering and Applied Geophysics

Acknowledgements

This thesis was written as the final product of the Master of Science program in Petroleum Engineering at the Norwegian University of Science and Technology (NTNU), Department of Petroleum Engineering and Applied Geophysics during the fall of 2014. It was carried out in cooperation with ConocoPhillips Scandinavia AS, which I would like to thank for providing me with the necessary data, office space and hardware/software as needed.

I am profoundly grateful to my mentor at ConocoPhillips, Serap Ozoglu-Topdemir, for her technical guidance and knowledge sharing, and her co-workers for their valuable inputs and discussions during this thesis work. I would also like to express my gratitude to my supervisor at NTNU, Jon Kleppe, for his feedback and support when needed.

A special thanks to Ole Eeg for his help and guidance throughout the semester.

Finally, I would like to express my deepest gratitude to my mother and grandmother for their confidence, patience and continuous support in pursuing this Master of Science degree.

Stavanger, December 2014

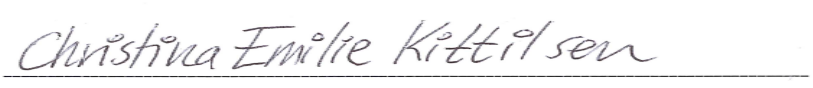

Christina Emilie Kittilsen

Abstract

The need to increase recovery efficiency in mature oil fields has become more evident with increasing costs, decreasing oil price and emerging competitive energy resources. At the same time the demand for energy continues to rise. The petroleum industry is currently the largest and most important sector in Norway's economy. As the Norwegian Continental Shelf (NCS) matures, improved oil recovery from known areas will play a significant role for the survival of the petroleum industry in Norway.

With increased maturity comes the benefit of enhanced understanding of the subsurface. This enables improvement of recovery strategies. The remaining resources after planned cessation of the fields on the NCS are of significant proportion. Incremental recovery of these would be of great value for the Norwegian society.

Eldfisk is one of the largest oil fields on the NCS and it is the focus of this thesis. To maintain production and increase the recovery of oil, water injection was successfully implemented in year 2000. Still, large volumes in the reservoir remain unflooded. In order to evaluate an optimized injection strategy for the future it is necessary to analyze the reservoir characteristics and the injection history. This thesis has used a combination of technologies to perform and evaluate reservoir model based studies in the effort to improve the efficiency of the waterflood operations on Eldfisk. The reservoir flow dynamics and the injector's performance have been investigated, which revealed influencing factors for efficient injection.

The objective of this thesis was also to investigate the potential for future water injection on Eldfisk. By the use of the reservoir model, infill injection targets were evaluated through existing and future producer locations. The change in fluid distribution was evaluated through investigation of saturations, pressure, production and streamlines. It resulted in valuable observations, important for reservoir management decisions.

Sammendrag

Behovet for å øke effektiviteten av utvinningen i modne oljefelt er blitt mer tydelig med økt kostnadsnivå, reduksjon i oljepris og utviklingen av konkurransedyktige energiressurser. Samtidig stiger etterspørselen etter energi. Petroleumsindustrien er for tiden den største og viktigste sektoren for norsk økonomi. Etter hvert som den norske kontinentalsokkel (NCS) modnes, vil økt oljeutvinning fra kjente områder spille en betydelig rolle for overlevelsen av petroleumsindustrien i Norge.

Med økt modenhet kommer fordelen av bedre forståelse av undergrunnen. Dette muliggjør forbedring av utvinningsstrategier. De gjenværende ressursene etter planlagt opphør av feltene på norsk sokkel er av betydelig andel. Økt utvinning av disse ressursene vil være av stor verdi for det norske samfunnet.

Denne oppgaven vil fokusere på Eldfisk, som er et av de største oljefeltene på norsk sokkel. For å opprettholde oljeproduksjonen og øke utvinningen i feltet, ble vanninjeksjon implementert i 2000. Likevel er store volumer i reservoaret fortsatt urørt av vanninjeksjonen. For å evaluere en optimalisert vanninjeksjonsstrategi for fremtiden er det nødvendig å analysere reservoaret og injeksjonshistorien. En kombinasjon av forskjellige teknologier har blitt brukt for å gjennomføre studier basert på reservoarmodellen til Eldfisk, med intensjon om å forbedre effektiviteten av vanninjeksjonen i feltet. Reservoarets strømningsdynamikk og injektorenes ytelse er blitt analysert, noe som viste viktige faktorer for å oppnå effektiv vanninjeksjon.

Målet med denne oppgaven var også å undersøke potensialet for fremtidig vanninjeksjon på Eldfisk. Ved bruk av reservoarmodellen, ble ytterligere lokasjoner for vanninjeksjon evaluert gjennom beliggenheten til eksisterende og fremtidige produsenter. Endringen i væskefordeling ble evaluert gjennom analyse av metninger, trykk, produksjon og strømlinjer. Det resulterte i verdifulle observasjoner som er viktige for optimalisering av reservoarstyringen.

Table of Contents

List of Figures

List of Tables

1 Introduction

1.1 Objectives

The Eldfisk waterflood started in year 2000 and the reservoir response has been very positive. Still, there remain significant portions of the reservoir to be targeted by water flooding. The purpose of this thesis is to investigate water injection performance and potential on Eldfisk using the reservoir model.

Understanding the reservoir characteristics and the injection history is necessary in order to evaluate an optimized injection strategy for the future. An analysis of the flow dynamics in the reservoir model and the injectors' performance will be an important part of this study. It can reveal influencing factors for efficient injection, using the reservoir simulation model to investigate historic and predict future reservoir performance. Streamline simulation will be used to visualize the results to further understand the communication between producers and injectors.

The scope of this thesis is also to look into additional locations for injection outside the established pattern, were conversions of existing and future producers will be used. The analysis will be conducted with the use of reservoir simulation. The output from the simulation runs will be used to generate streamlines to visualize the injection pattern. The focus will be to find locations that have potential for successful future water injection.

This thesis has the following configuration:

- Chapter 2 gives an overview of the Eldfisk field and the reservoir model.
- Chapter 3 introduces factors that are crucial for oil production on Eldfisk. It also gives a discussion about how to estimate recovery efficiency and the ultimate oil recovery factor.
- Chapter 4 summarizes the status of water injection on Eldfisk and the value of future water injection.
- Chapter 5 provides a study on reservoir flow dynamics and the process of modeling fractures.

- Chapter 6 presents an analysis of the injectors' performance.
- Chapter 7 includes results and discussions of the producer conversion study.
- Chapter 8 investigates the impact of fractures in the reservoir model.
- Chapter 9 summarizes the results of the work performed in this thesis and gives recommendations for future work.

1.2 Motivation

The world's energy map is changing. Improvements made to the development of unconventional hydrocarbon resources and renewable energy change our understanding of the distribution of energy resources throughout the world (IEA, 2013, p.23). Governing changes to global trends are emerging as a result of oil price volatility, shifts in economic growths and efforts to reduce greenhouse-gas emissions. At the same time, the world population is increasing and the average standard of living is improving. As a result the demand for energy continues to rise (NPD, 2014a, p.43-49).

Oil, natural gas and coal will be important resources in the effort to reduce the increasing gap between the supply and demand of energy in the foreseeable future. Norway was the 15th largest oil producer in 2012 and it is the 3rd largest gas exporter in the world (NPD, 2014a, p.43-45). The petroleum industry is currently the largest and most important sector of Norway's economy, measured in value creation, exports and State revenues. The industry creates ripple effects both locally and regionally, and it employs a substantial segment of the Norwegian population (NPD, 2014a, p.12-13).

The cost of operation, investment and other spending on the Norwegian Continental Shelf (NCS) has increased significantly, especially in the past 10 years. This is shown in **Fig. 1.1**. As the NCS is maturing, the growth in costs has been met with an overall decline in production. The result is an increase in the operating cost per unit produced (NPD, 2014b, p.16-17).

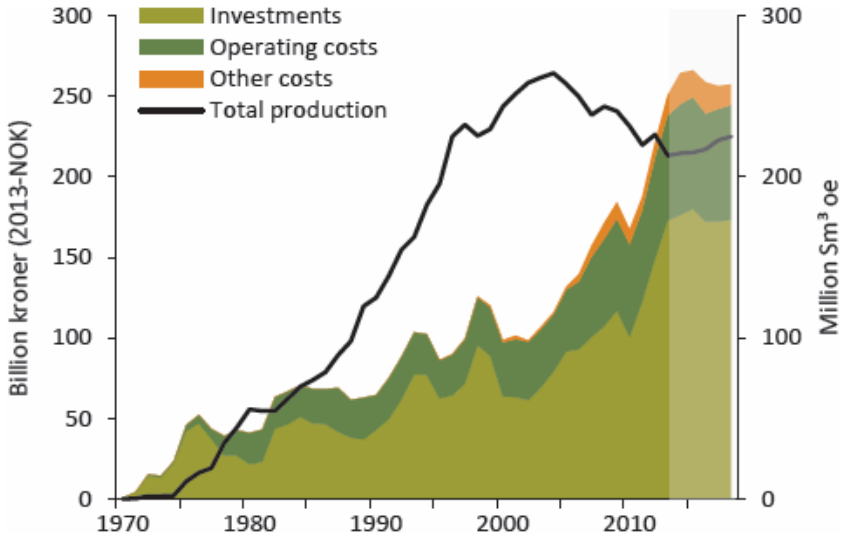

Fig. 1.1 Development in costs on the NCS. *The figure shows an increase in operating costs, investments and other spending on the NCS (2013-2018 is a forecast). There has been a significant increase, especially in the last 10 years. The growth in costs has been met with an overall decline in production as the NCS is maturing, which in turn increases the operating cost per unit produced (NPD, 2014b, p.16-17).*

In recent years, the oil price has been on a historical high which has helped the industry in a period with increasing costs. In the last few months, there has been a significant drop in the oil price. As of December 8th 2014, the Brent crude oil price was 65.64 $ (EIA, 2014). This has created concerns about the future of the petroleum industry. The change of Brent crude oil price with time is shown in **Fig. 1.2**.

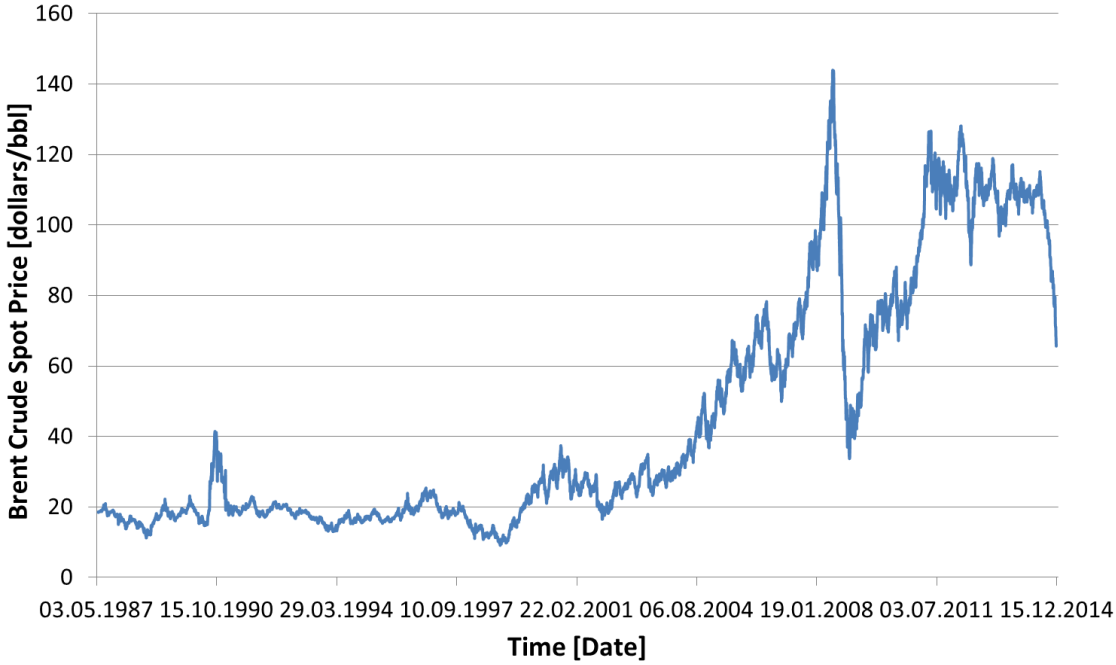

Fig. 1.2 Fluctuations in the oil price. *The figure shows the change in the Brent crude oil price since 1987 (EIA, 2014). The oil price has been on a historical high in recent years, but has reduced significantly in the last few months. This has caused concerns about the future of the oil industry.*

The profitability of future projects is threatened by the growth in costs and reduction in oil price. Both improved recovery from mature fields and the development of discoveries has become more demanding with the current market conditions. Still, remaining resources in fields and discoveries are substantial. This represents an important motivation for the industry, the suppliers and the government to work together to overcome this challenge and continue the value creation from the remaining reserves on the NCS (NPD, 2014b, p.9).

To maintain oil production, pressure support is provided through water and/or gas injection in most mature oil fields on the NCS. Systematic data acquisition, production data and reservoir information increase the understanding of the reservoir characteristics throughout the production phase. Enhanced modeling of fluid flow distribution enables improvement of recovery strategies in the hydrocarbon fields. There is a significant potential to improve oil recovery from known resources on the NCS, as shown in **Fig. 1.3**. The figure shows an overview of the recovery status of the 25 largest oil fields (NPD, 2014b, p.19).

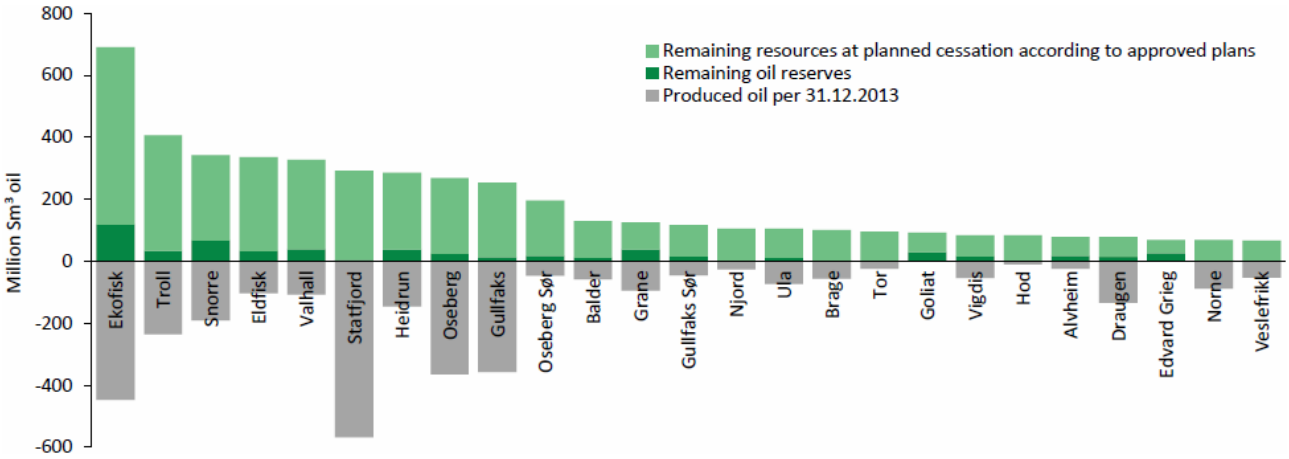

Fig. 1.3 Recovery status of the 25 largest oil fields on the NCS. *The figure reflects the significant potential for improved oil recovery from known hydrocarbon resources on the NCS (NPD, 2014b, p.19). The grey bar represents the produced oil per 31.12.2013, the dark green bar the remaining oil reserves and the light green bar the remaining resources at planned cessation according to approved plans. ConocoPhillips operates the Ekofisk, Eldfisk and Tor fields. The Eldfisk field has the 4th largest volume of remaining oil reserves and resources according to approved plans on the NCS, and it is the focus of this thesis.*

ConocoPhillips is operating the Ekofisk, Eldfisk and Tor fields. The focus of this thesis is the Eldfisk field, where waterflood was successfully implemented in year 2000. As can be seen in Fig. 1.3, there will be a large volume of remaining hydrocarbon resources left in the underground at planned cessation of the field. This reflects a significant potential for increased oil recovery. The intention of the studies performed in this thesis is to improve the

understanding of the performance of the current waterflood and to investigate the potential for future water injection in the Eldfisk reservoir. This will be done by the use of a combination of technologies to create a new angle of approach compared to current practice. It will hopefully contribute to the effort of increasing the efficiency of the waterflood operations on Eldfisk, which will ensure good resource utilization and create socio-economic benefits.

2 The Eldfisk Field

The Eldfisk field is located in the southern part of the Norwegian Sector of the North Sea, in Block 2/7 and Production License 018 (PL018). ConocoPhillips operates the lease with a 35.112% working interest. It is a fractured oil and gas chalk reservoir with two northwest-trending anticlines, Alpha and Bravo, and a minor domal structure, East Eldfisk (ConocoPhillips, 2012, p. 6 and 11).

2.1 Development History

The Eldfisk field was discovered in 1970 and the initial field development started in 1975 with the installation of three platforms, Eldfisk 2/7-A, 2/7-FTP and 2/7-B. Production start-up was in 1979 and Eldfisk produced with natural depletion until 1999. Solution gas drive and reservoir compaction were key reservoir drive mechanisms (COPNO, 2014a). Because of encouraging waterflood results at Ekofisk, a similar program was developed for Eldfisk. A water injection platform, 2/7-E, was built and production wells were converted to water injectors. The associated seawater injection was initiated in 2000 with a horizontal line drive pattern in both Alpha and Bravo (ConocoPhillips, 2012, p.7). The horizontal wells frequently cross the many faults located in Eldfisk. These faults, and their associated fracture system, play an important role in non-matrix flow in relation with waterflooding (ConocoPhillips, 2012, p.15).

Gas injection was initiated in year 2000 (after waterflood start-up) as a means of dealing with gas handling constraints at the Ekofisk 2/4-J platform. Gas injection has never been an appreciable recovery mechanism (ConocoPhillips, 2012, p.9), and is therefore not part of the scope of this thesis.

Eldfisk is in the Greater Ekofisk Area, which consists of the Ekofisk, Eldfisk, Embla and Tor fields. The oil and gas production from platform 2/7-A is processed at the 2/7-FTP platform and then sent to a sales line. Production from the 2/7-B platform is sent to processing on platform Ekofisk 2/4-J. A schematic of the facilities and transportation infrastructure in the Greater Ekofisk Area is included in {**error:broken figure reference**} in Appendix A (ConocoPhillips, 2012, p.7).

2.2 Reservoir Description

Eldfisk has a total productive area of approximately 10 600 acres (43 km2) and is comprised of three formations (Ekofisk, Tor and Hod). Top structure maps with cross sections showing the Alpha and Bravo stratigraphy are depicted in **Fig. 2.1**.

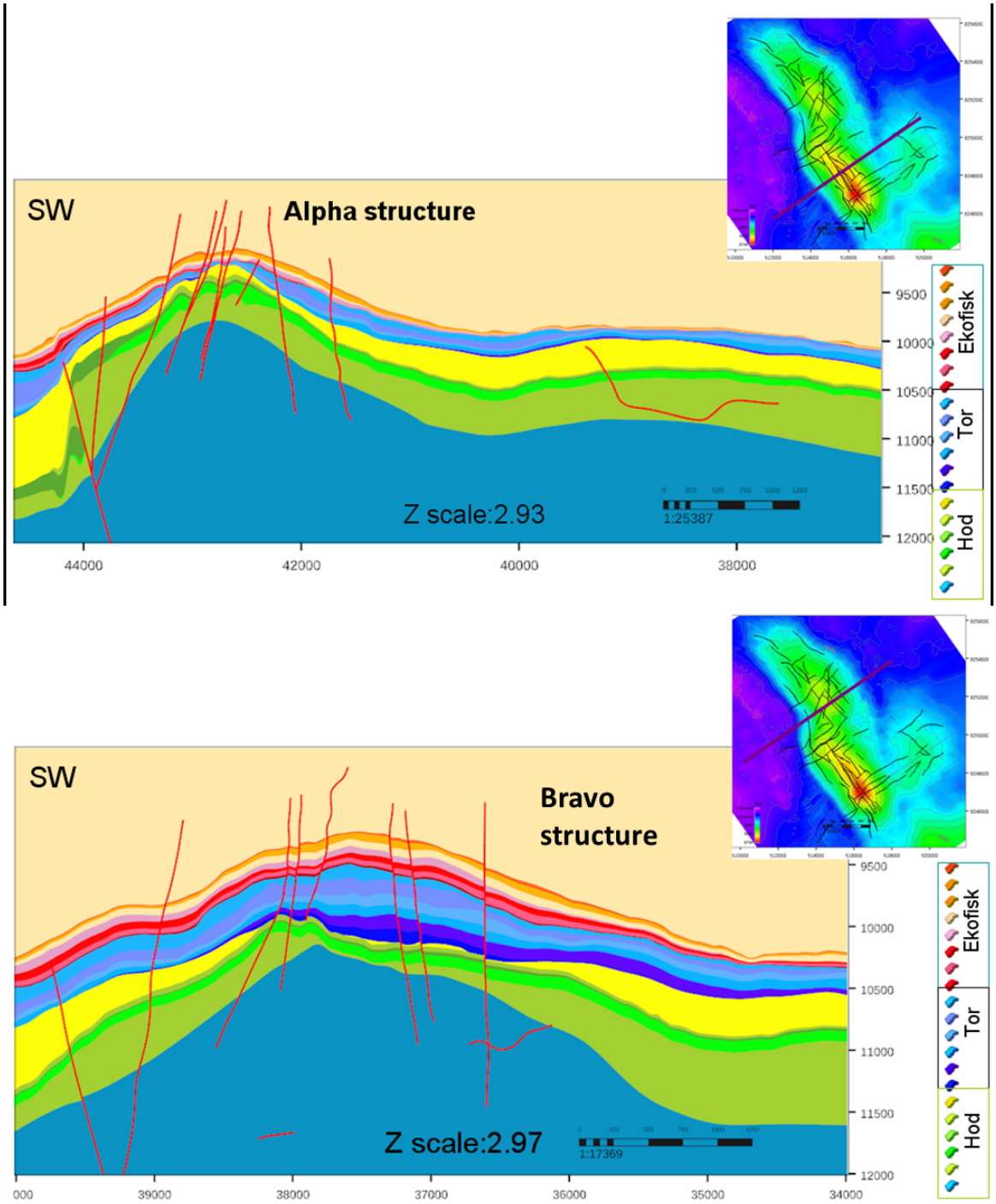

Fig. 2.1 Alpha and Bravo stratigraphy. *Top structure maps with cross sections showing the Eldfisk Alpha and Bravo stratigraphy (ConocoPhillips, 2012, p. 85 and 86). The red lines in the cross sections are interpreted locations of faults. The red line in the structure map shows the location of the cross section.*

Top of structure elevation in the Alpha structure is 8770 ft (2673 m) and it has a maximum thickness of 400 ft (122 m), while Bravo top of structure is 9220 ft (2810 m) with a maximum thickness of 800 ft (244 m). The chalk reservoir is heterogeneous with productive areas having an average porosity of 28 % (15-45 % range). The initial water saturation is less than 10 %. The average matrix permeability is less than 1 mD, but the chalk formation is highly fractured causing an average effective permeability of approximately 4 mD (ConocoPhillips, 2012, p.6).

The free water level (FWL) is tilted, with depths ranging from 9839 ft to 10 218 ft. The original oil-in-place (OOIP) is estimated to 2775 MMSTB (MMSTB = 10^6 STB) and 3488 MM STBOE. **Table 2.1** shows the OOIP by structure (ConocoPhillips, 2012, p.6).

Table 2.1 OOIP by structure and formation. The table shows the estimated original oil-in-place (OOIP) in total and by structure on Eldfisk. It is observed that approximately 90 % of the hydrocarbons in place are located in the Ekofisk and Tor Fm (ConocoPhillips, 2012, p.6 and 57). Also, calculations show that the Alpha, Bravo and East Eldfisk structures contain 52%, 39% and 8% of the OOIP, respectively.

Structure	Formation	OOIP [MMSTB]	OGIP [BCF]	OHIP [MMBOE]
Alpha	Ekofisk	735	1104	919
Alpha	Tor	485	711	604
Alpha	Hod	233	301	283
Bravo	Ekofisk	547	1012	716
Bravo	Tor	520	866	664
Bravo	Hod	23	35	29
East Eldfisk	Ekofisk & Tor	232	247	273
	Total	2775	4276	3488

The initial reservoir pressure is in general reported as 6835 psia at a depth of 9400 ft (2865 m) subsea, but pressure measurements vary across the Eldfisk field suggesting a degree of compartmentalization. The field contains a volatile oil, with log interpretations showing small crestal gas caps in the Bravo structure (ConocoPhillips, 2012, p.10).

Due to shallow gas in the overburden, the crestal parts of the Alpha and Bravo structures are seismically obscured. This makes it problematic to map faults and monitor waterflood

progression with the use of seismic analysis. This complicates the development drilling efforts (ConocoPhillips, 2012, p.12).

The Eldfisk field is summarized with key information in **Table 2.2**.

Table 2.2 Eldfisk key information. The table shows important information about the Eldfisk field.

	Eldfisk
Discovered	1970
First Oil	1979
Waterflood Start	2000
Structure	double anticline + EE dome
Area (acres)	10600
Rock Type	Fractured chalk
Source	Upper Jurassic Shales
Productive Intervals	Ekofisk, Tor, Hod
TVDSS ft Crest	8770 (Alpha), 9220 (Bravo)
Thickness, ft	400 (Alpha), 600-800 (Bravo)
Recovery Mechanisms	depletion, compaction, waterflooding
Porosity	15-45%
Swi %	<10
FWL, ft	9839-10318 (tilted)
Matrix Perm mD	<1 (avg)
Eff. Perm mD	4 (avg)
Initial Pressure psia	6835
Datum TVDSS ft	9400
Est. OOIP MMSTBO	2775
Oil Type	volatile
Initial Oil API deg	38-39
Initial Pb psia	4813-5610
Initial Res Temp deg F	245
Initial GOR SCF/STB	1350/1650
Current Pb psia	3770-4930
Historical Completions	134
Peak Rate MSTBD	128
Well Type	Horiz & Dev
ConocoPhillips WI%	35.112
End of Prod Liscence	31 Dec 2028
Wells to be drilled	~40-110
Well Life yrs	14
Stim Technique	acid
Seismically Obscured Area	Yes

2.3 Reservoir Management

Primary depletion, compaction and waterflood have been recognized as the main recovery mechanisms in the Eldfisk field to this date. All three structures have aquifer support, but its overall impact is of less importance. With field maturity, the waterflood has become the dominant recovery mechanism (ConocoPhillips, 2012, p.20).

2.3.1 Waterflood Management

The waterflood was initially managed to maximize injection in order to re-pressure the reservoir. The focus was to maximize oil production for the immature flood and to minimize subsidence. As the waterflood on Eldfisk became more mature, new work flows were developed to optimize all aspects of waterflood management (COPNO, 2011, p.56). Strategic practices were established to maximize the economic value by balancing oil rate, resource recovery and cost. The current strategic waterflood management for Eldfisk is summarized in the following bullet points (ConocoPhillips, 2012, p.30):

- Replace cumulative produced voidage with injected water to maintain reservoir energy.
- Optimize oil recovery while minimizing water production by using appropriate water injection targets.
- In the effort to attain the regional reservoir pressure target, the pattern level voidage replacement ratio (VRR) should be ≥ 1.
- Based on injector/producer interaction analysis, individual well injection targets should be set to avoid overburden injection and/or matrix bypass.
- To prolong the life of surface infrastructure, employ water injection in the effort to minimize subsidence.
- Individual well injection targets should be adjusted as necessary to avoid offset drilling risk.

Introduction of seawater to topside, downhole and in the reservoir causes complex processes that are important to take into account in reservoir management. On Eldfisk, important aspects of the waterflood include (ConocoPhillips, 2012, p.20):

- Spontaneous imbibition.
- Water weakening, resulting in significant permeability reductions at high water saturation.
- Non-matrix flow due to fractures and conductive faults.
- Compaction, causing a high mechanical wellbore failure rate and seabed subsidence.
- Scale deposition.

Spontaneous imbibition and water weakening is important for oil recovery on Eldfisk, and will be explained in chapter 3.2. The water injection status and future value on Eldfisk will be presented in chapter 4.

2.3.2 Compaction and Subsidence

Water injection has reduced the compaction and subsidence rate on Eldfisk, but due to water weakening these processes are still a challenge. The compaction and subsidence on Eldfisk is not as severe compared to the implications that have been encountered in the Ekofisk field. Still, they are important factors as they can impact numerous facets and strategies associated with recovery operations. Examples are reservoir pressure, injection fluid selection and water injection targets (ConocoPhillips, 2012, p.17). Also, it is important to predict compaction to ensure safe operations, provide reservoir management guidance and mitigate risk of wellbore failure and damage to surface facility infrastructure (ConocoPhillips, 2012, p.18).

There are two subsidence bowls in the Eldfisk field - one over the Alpha structure and one over the Bravo structure. These are depicted in **Fig. 2.2**. The picture shows that the maximum subsidence in the Bravo structure is approximately 15 ft (5 m), while the maximum subsidence in the Alpha structure only is about 7 ft (2 m) (ConocoPhillips, 2012, p.18).

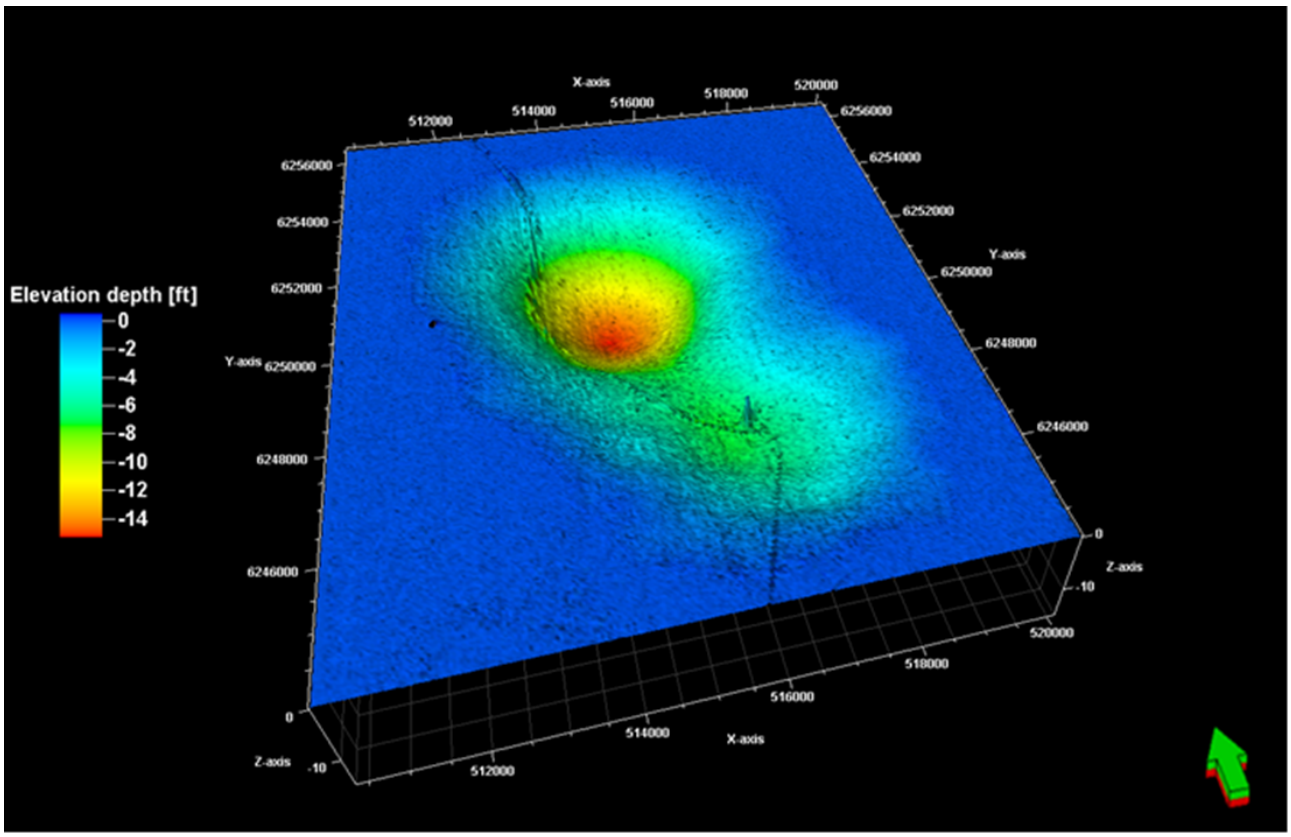

Fig. 2.2 Eldfisk subsidence map. *The figure shows the two subsidence bowls on Eldfisk - one over the Alpha structure and the other over the Bravo structure. The areal dimensions are provided in meters, while the elevation is shown in feet. The dark line that runs in a north-south direction is a footprint of a pipeline (ConocoPhillips, 2012, p.90).*

2.3.3 Eldfisk Phase II

The scope of the initial waterflood on Eldfisk was focused on higher quality rock, mostly situated in the Tor Fm. Still, large portions of the reservoir remain unflooded. The Eldfisk II project is a redevelopment of the Eldfisk field, and it will expand existing waterflood operations. Platform 2/7-A, 2/7-B and 2/7-E will undergo modifications that will prolong their functional life until at least the end of current license period in 31/12/2028. The project also consists of a new 40-slot platform, 2/7-S, located over the Alpha structure. There are 29 Alpha structure targets, 10 Bravo structure targets and one cuttings disposal well planned to be drilled from 2/7-S. The project is justified by a 259 MMBOE of incremental production by the end of the license period. Start-up of oil production from the new 2/7-S wells is expected to be in 2015 (ConocoPhillips, 2012, p.7).

2.4 Reservoir Model

Reservoir models are used to optimize reservoir management decisions by integrating geology, geophysics, petrophysics and reservoir surveillance. They are key tools that provide long-term reservoir performance forecasts and are used to address reservoir management issues. Modeling of the Eldfisk field is challenging because of its structural complexity, rapidly varying chalk sedimentology, natural fractures, faulting, diagenesis and reservoir compaction. SET II, the current Eldfisk reservoir model, incorporates these complexities as a full field PSIM model (ConocoPhillips, 2012, p. 15).

SET II is an implicit reservoir model and it uses a corner plot geometry grid with (i, j, k) dimensions of (125, 200, 19). The correlations between the reservoir and the model layers are given in **Table 2.3**. The average cell length and width is 1812 ft (552 m) and the thickness is 41 ft (13 m), in the hydrocarbon column. The model grid in the aquifer is coarsened to minimize simulation run time (ConocoPhillips, 2012, p. 16 and 178).

Table 2.3 Correlation between reservoir and model layers. The reservoir model is split into 19 layers. The table shows the correlation between model layers and layers in the reservoir.

	Reservoir Zone	Subgrid
Upper Ekofisk Fm	EU1	1
	EU2	2
	EU3	3
Middle Ekofisk Fm	EM1	4
	EM2	5
Lower Ekofisk Fm	EL1	6
	EL2	7
	EL3	8
Tor Fm	T1	9
	T2	10
	T3	11
	T4	12
	T5	13
	T6	14
Hod Fm	M1	15
	N1	16
	N2	17
	N3	18
	N4	19

The reservoir model is divided into regions and super regions to be able to investigate the change in the different formations and structures with time. The definitions of the regions and super regions are given in **Table 2.4**.

Table 2.4 Regions and super regions in the reservoir model. These are used to investigate the change in the different formations and structures with time.

Region	Reservoir Zone
1	Alpha Ekofisk Fm
2	Alpha Tor Fm
3	Alpha Hod Fm
4	Bravo Ekofisk Fm
5	Bravo Tor Fm
6	Bravo Hod Fm
7	Eldfisk East

Super region	Reservoir Zone
1	Alpha
2	Bravo
3	Field

The initial reservoir volumetric parameters and permeabilites for the Alpha, Bravo and Eldfisk East structures are summarized in **Table B.1 - Table B.3** in Appendix B. The process of permeability mapping in the model is explained in chapter 3.1. Black oil PVT properties were calculated using Peng-Robinson equation of state. The fluid properties vary both areally and vertically (ConocoPhillips, 2012, p. 11). A summary of the black oil properties for the different structures is given in **Table B.4** in Appendix B.

The Eldfisk reservoir model is a single porosity model. To incorporate the fracture/matrix fluid exchange, the model uses pseudo-relative permeability functions. This will be explained in chapter 3.1.2 about relative permeability in fractured reservoirs.

2.4.1 The Base Case

The Base Case of this study is based on the 2014 LTF for Eldfisk Phase II, with end of simulation in 01/01/2050. It uses a history matched file (HM_2014.restart) until 01/01/2014, when the forecast starts. The history match is presented in **Fig. A.2 - Fig. A.7** in Appendix A. The focus of this study is to analyze reservoir flow dynamics, evaluate the value of existing and future injectors and to investigate the reservoir potential for WI through producer locations. Therefore, the Base Case of this study have certain alterations from the original LTF:

- The injector well life constraints are based on statistical analysis of well life history. These are taken out for the injectors in order to investigate the full potential of the WI locations.
- In the LTF, all Alpha injectors and one Bravo injector are re-drilled from the S-platform with a different name. These events are taken out. Instead, the Alpha injectors are re-introduced with the same name after the platforms are SI. This is to prevent having different names for the same injector location. The other Bravo injectors are not re-introduced because they are replaced by new injectors in the model. In the Base Case, these wells are set to have a start-up date equal to the SI of the original Bravo injectors.
- The LTF has a future event to add an injector to replace A-30 B. This is taken out because this thesis includes a study including sensitivity runs that convert all existing producers to injectors.
- Re-drills of future producers (in the same location) are taken out to simplify the drilling schedule (only one well name per location through time). This is assumed to be a valid alternation because the purpose of this thesis is to investigate the well locations, and their potential. In SplicerXL, the well life constraints of the future producers were updated to be equal to the initial value plus the value of the well life constraint of the re-drill. Re-drills of good Alpha producers are kept in the model.
- B-15 is on reduced rate control (6000 bbl/day) in the start of 2014 because of a massive water breakthrough (WBT) event in B-18 B in 2011 and to prevent WBT in B-17 AT3. In the LTF, the rate is set to an increased value of 16 000 bbl/day in 01/01/2015. In the Base Case the rate is set to 16 000 bbl/day from 01/01/2014 because in reality this decision was made, but it is not yet included in the LTF.

To summarize, the reservoir model contains:

- Existing wells
- Future wells drilled from the S-platform (Eldfisk Phase II)
- Re-drills of good Alpha producers
- Eldfisk North wells

Compared to the LTF, the Base Case of this study has higher:

- ultimate recovery of oil
- cumulative water injection

This is mainly caused by the removal of well life constraint for the injectors in the Base Case. The WI rate is especially higher before the Bravo platform shuts in (01/01/2022), which indicates that the Bravo wells have high injection potential. A map of the existing and future injectors is given in **Fig. 2.3**. A map of existing injectors and their presence in the Ekofisk and Tor Fm is given in **Fig. C.1** in Appendix C. An overview of injectors and producers in 2026 in the Base Case is given in **Fig. A.8** in Appendix A.

Injectors naming convention

The injectors will be the focus of this thesis. To make the analysis easier to read, a shorter version of the existing injectors name will be defined here:

A-4 AT2I = A-4

A-5 BT2I = A-5

A-7 BT2I = A-7

A-13 BT2I = A-13

B-8 BI = B-8

B-15 AI = B-15

B-20 BI = B-20

B-22 I = B-22

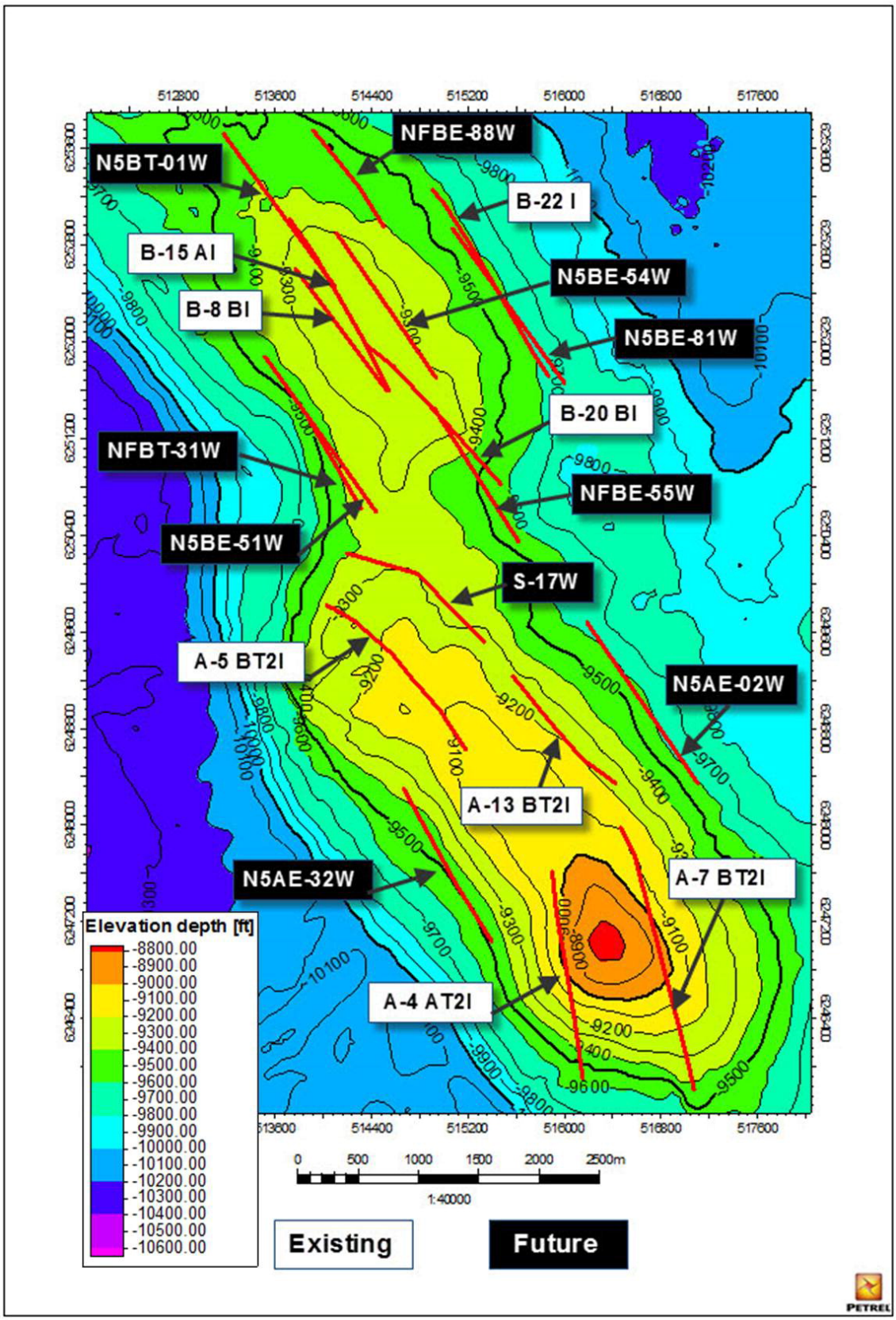

Fig. 2.3 Map of existing and future injectors. *The location of existing (white labels) and future (black labels) injectors.*

2.4.2 Software Overview

PSim 2012
PSim was used to run simulations of fluid flow on Eldfisk. This 3D reservoir simulation model was developed by ConocoPhillips. It can be used to solve three-phase black oil and compositional problems as single-porosity reservoirs. PSim has been tested against SPE Comparative Solution Project problems and has proved to be efficient and accurate in a numerous of field studies. Impes (default) and implicit formulations are included in the model, and it uses Peng-Robinson and Soave-Redlich-Kwong equations of state (ConocoPhillips, 2013b, p.23).

The reservoir simulations performed in this study were conducted through a remote desktop login on ConocoPhillips reservoir engineering cluster in Houston.

CView
CView is a ConocoPhillips-developed post-processing software. It is used to analyze results from the reservoir simulator, PSim. For the purpose of this study, CView was used to process:

- .PVWV-files: A binary file created by the reservoir simulator. It can be used to visualize the reservoir with array data through time.
- .PLTDAT-files: An ASCII file created by the reservoir simulator. It includes rates, cumulative production, WOR and other well and field data in time.
- .region_superregion: An ASCII file with a summary of regions and super regions data. CView can be used to generate XY plots of this data (ConocoPhillips, 2013a, p.249).

SplicerXL
This application was developed by the North Sea Business Unit of ConocoPhillips. It uses data loaded into an Excel workbook to create input dek-files for PSim simulation runs. The worksheets in SplicerXL can be manipulated to generate a complex set of changes whose logic can be defined (ConocoPhillips, 2014b).

SPARK
The Suite of Processes to Advance Reservoir Knowledge (SPARK) is an uncertainty quantification system, developed by ConocoPhillips. As scenario based planning has become

more common in the industry, it is desirable with uncertainty workflows. SPARK has an Excel interface, and it is possible to generate a large amount of sensitivity forecast runs with the integration of SplicerXL (ConocoPhillips, 2014a). By inputting a number of control variables in SPARK, SplicerXL recalculates any internal values dependent on these control variables before it generates a PSim dek-file. SPARK then launches PSim, which runs the simulations. When the results are ready, it is also possible to post-process these in SPARK. The process repeats as required (ConocoPhillips, 2014b). The workflow is illustrated in **Fig. 2.4**.

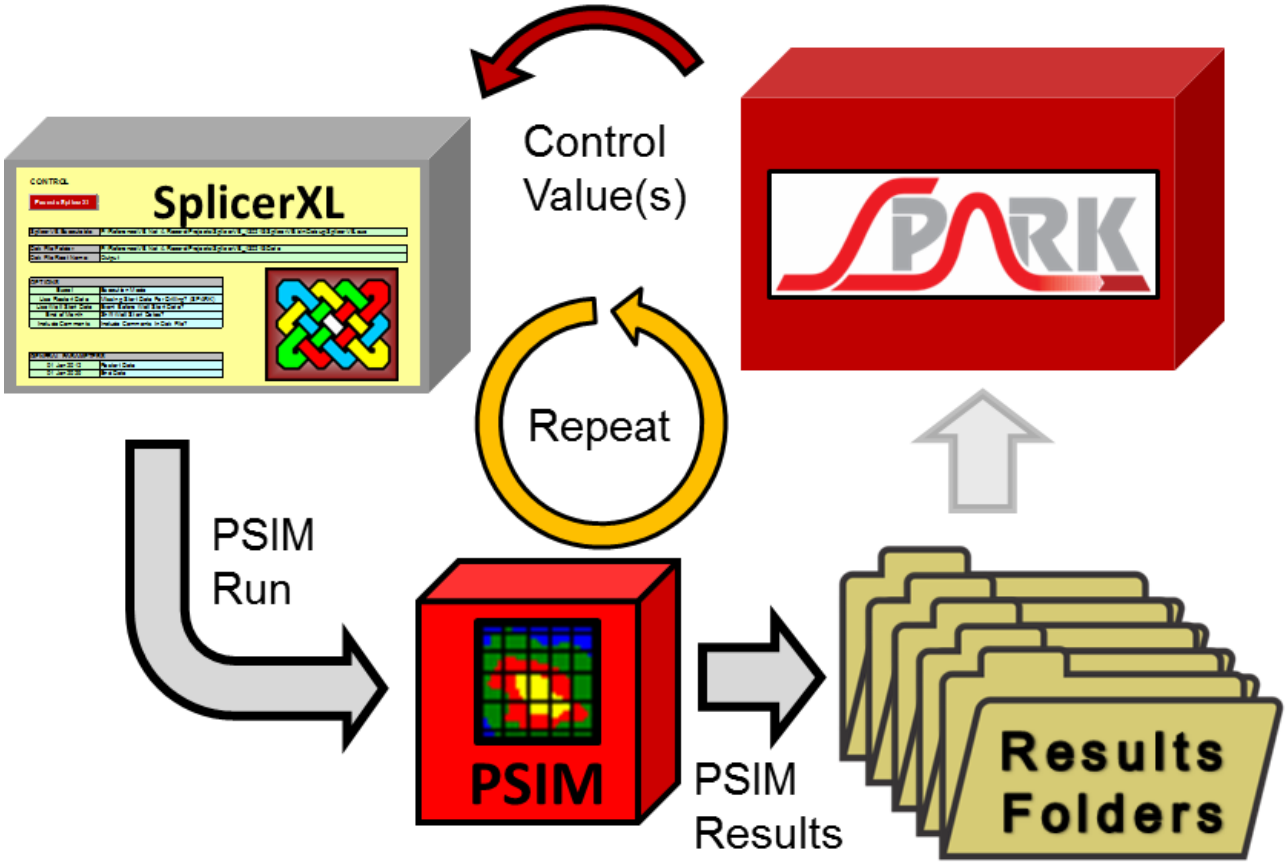

Fig. 2.4 SPARK/SplicerXL workflow. *Work flow illustration of SPARK and Splicer (ConocoPhillips, 2014a). SPARK is used to input variables in the SplicerXL workbook, which then generates the desired number of dek-files for reservoir simulation. SPARK can also be used as a post-processor.*

StudioSL

StudioSL is a tool developed by Streamsim Inc. Output files from reservoir simulation are used to compute flow-based Well Allocation Factors (WAF) between injectors and producers and to generate streamlines (Streamsim Inc., 2014).

3 Reservoir Properties Fundamentals

Hydrocarbon reservoirs are complex systems of water, oil and gas contained inside a porous medium. The hydrocarbons in place and the oil recovery factor is dependent on factors such as e.g. porosity, permeability, fluid saturations, wettability, flow physics and other fluid and rock properties (Dake, 1985). The displacement of oil in the reservoir is the fundamental basis of oil recovery mechanisms. It involves the interplay of transport, flow, rock/fluid interactions and thermodynamic processes. To have a clear description of static and dynamic reservoir properties is crucial in the effort to maximize oil recovery. This should be done on various scales, ranging from a pore scale to a field scale as described in **Fig. 3.1** (Zitha et al., 2011).

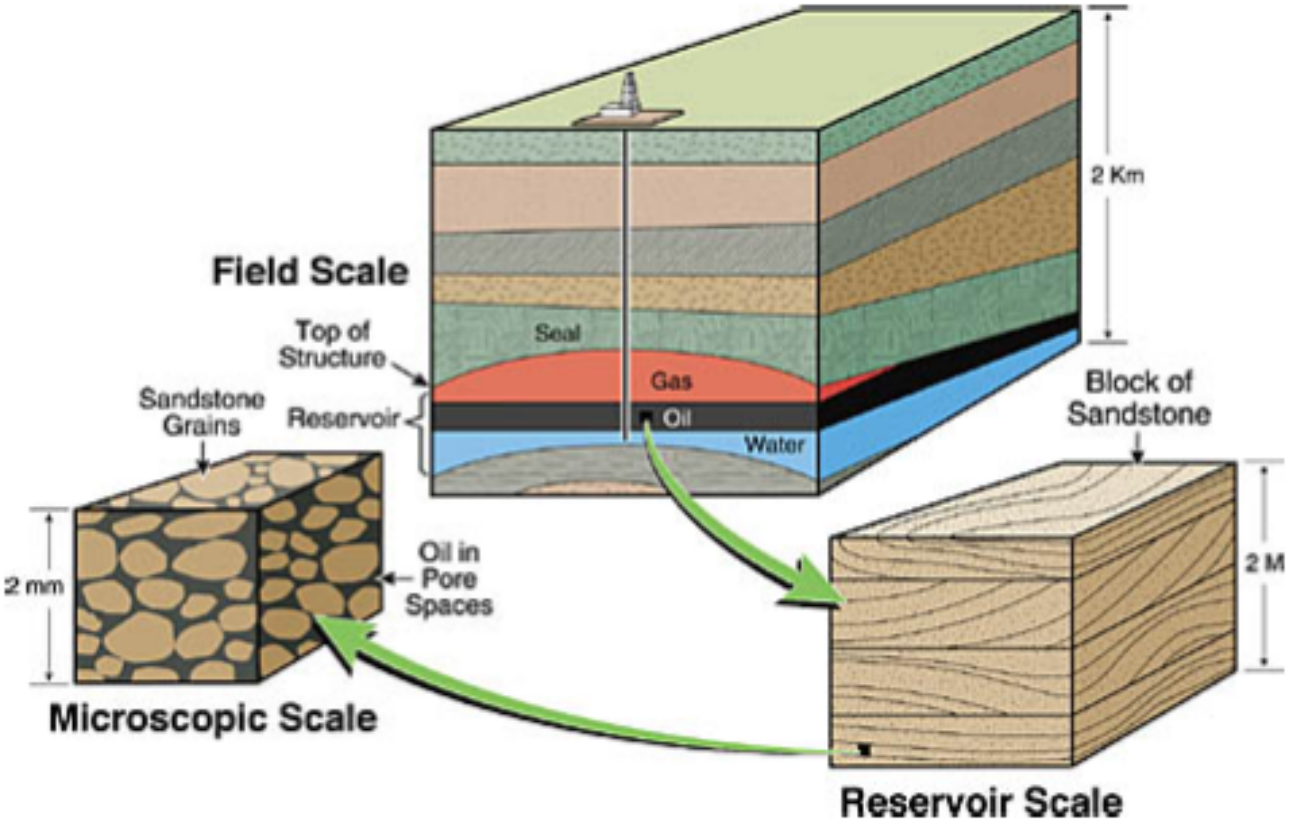

Fig. 3.1 Scales of observation. *Representation of the reservoir is done on different scales - from a microscopic scale to a field scale (Zitha et al., 2011).*

Factors that are crucial in waterflooding and therefore oil production on Eldfisk, will be discussed in this chapter. Also, a discussion about how to estimate recovery efficiency and the ultimate oil recovery factor will be given.

3.1 Permeability

Permeability is one of the most important sources of data when it comes to determining fluid flow in the reservoir. The permeability is defined as the ability of a porous medium (such as a reservoir rock) to transmit fluids. It is typically measured in darcy (D) or millidarcies (mD). Absolute permeability is the measurement of permeability when a single fluid (or phase) is present in the rock, while the effective permeability is the ability to preferentially transmit a particular fluid when other immiscible fluids are present in the rock (Schlumberger, 2014). The relative permeability is the ratio of effective to absolute permeability of a particular fluid, as described in **Eq. 3.1** (Ezekwe, 2011, p.15):

$$k_{ri} = \frac{k_i}{k_a} \qquad \text{.....(3.1)}$$

Where:

- k_{ri} = relative permeability of the porous medium to fluid *i*
- k_i = effective permeability of the porous medium for fluid *i*
- k_a = absolute permeability of the porous medium

Measurement of permeability can be done at different scales. The main sources of permeability data are (listed with increasing volume of reservoir investigated): core samples, well logs and pressure transient tests. Before the data is integrated and used for reservoir analysis, the difference in range of investigation among the sources of permeability data should be considered (Ezekwe, 2011, p.17).

Permeability data, especially relative permeability data, are important inputs in numerical reservoir simulation models. The relative permeability is strongly related to the fluid saturations and can be presented graphically in plots called relative permeability curves (Ezekwe, 2011, p.23). A discussion about relative permeability mapping in Eldfisk is given in chapter 3.1.2. First, chapter 3.1.1 introduces effective permeability mapping in fractured reservoirs.

3.1.1 Effective Permeability in Fractured Reservoirs

To identify the different types of fractures that can be found in the fracture network along the reservoir is one of the main challenges in understanding how the fracture network acts during the production and injection process. The types of permeability used to model the permeability distribution in Eldfisk are explained in the following paragraphs (COPNO, 2010-2012, p.26).

Matrix Permeability (Kmat)

The matrix permeability is defined as the permeability in the porous system of interconnected pores, without any kind of discontinuity (e.g. fractures) (COPNO, 2010-2012, p.25). The matrix permeability is on average less than 1mD, but it ranges from 0.1 mD to 5 mD (COPNO, 2010-2012, p.12).

Enhanced Matrix Permeability (Kenh)

Due to hair-line fractures (small fractures that have limited lateral extent) the matrix system can have an enhancement. The resulting increase in matrix permeability is minimal (e.g. 0.5 mD), but it is important to note that this implies an increment of 50 % if the initial value was 1mD. Therefore it becomes important to include this enhancement in matrix permeability (COPNO, 2010-2012, p.25).

Fracture Permeability (Kfrac)

Areas of high permeability have developed in both Eldfisk and Ekofisk due to an effective and well connected fracture system. These act as preferential conduits for flow. Studies show that two different systems have been identified to give highways of permeability (COPNO, 2010-2012, p.26):

- Fracture corridors/ fault damage zone: These have been identified with the help of different drilling and flow parameters.
- Thief zones: Well-established fracture networks are known to develop in low porosity chalk formations. These are stratigraphically controlled and are most likely associated with hard grounds. There is a lack of data in Eldfisk to clearly identify the thief zones geologically, but learnings from the Ekofisk field show that the fracture networks can play an important role for fluid flow.

To split the well-test derived permeabilities into matrix/matrix enhanced permeability and fracture system permeability, it was decided to use a cut-off value of 5 mD. As a result, permeability measurements above 5 mD is used to model the fracture network permeability, while measurements below 5 mD is used to model the matrix enhanced permeability (COPNO, 2010-2012, p.58).

There is a continuous effort to update these features in the Eldfisk reservoir model. The use of field data to model fractures is explained in chapter 5.1.

Effective Permeability

In order to determine the resulting permeability of the whole rock system, the effective permeability is used as a measure. It takes the matrix, enhanced matrix and fracture permeability into account. In a simple way the process of determining the effective permeability can be explained by **Fig. 3.2** (COPNO, 2010-2012, p.30).

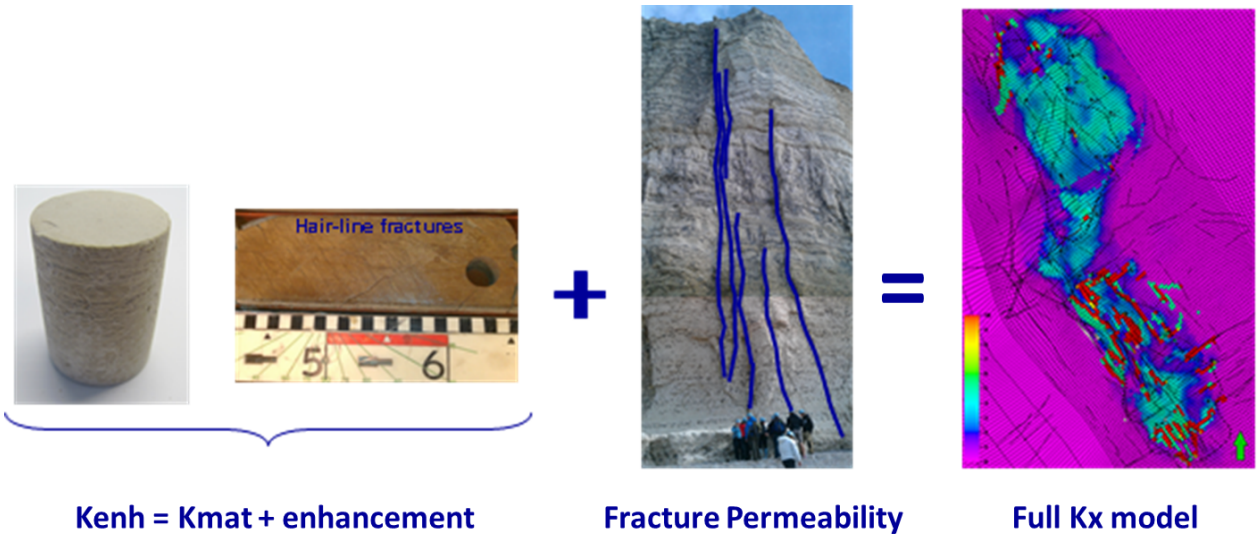

Fig. 3.2 Effective permeability mapping. *Simplified workflow of effective permeability mapping. Enhanced matrix permeability and fracture permeability is combined to estimate the effective permeability throughout the reservoir.*

3.1.2 Relative Permeability in Fractured Reservoirs

A technique to incorporate conductive faults and fractures in a reservoir simulation model is the use of pseudo relative permeability curves. This is key to obtain the rapid water advance in the model when high permeable faults and fractures are present in the reservoir (Lingen et al., 2011). The pseudo relative permeability is dependent on porosity, thickness, residual oil saturation, connate water saturation and the end-point relative permeability of oil and water (Hearn, 1971).

As mentioned in chapter 2.4, the reservoir model is a single porosity model. By the use of pseudo relative permeability functions, the flow coming from both the matrix and the fracture can be modeled more accurately. The pseudo curves are constructed from the fracture system relative permeability and the matrix relative permeability in an oil-water system.

Rock types are used to allocate pseudo relative permeability and the change in permeability with stress in the reservoir. They are derived from the effective permeability and porosity arrays (COPNO, 2010-2012, p.81). Figures showing the definition of the rock-types are given in **Fig. A.9** and **Fig. A.10** in Appendix A. As an example, the construction of k_{ro} and k_{rw} (oil and water pseudo relative permeability) for rock type 5 is given in **Fig. 3.3** (COPNO, 2010-2012, p.87).

Fig. 3.3 shows that the pseudo relative permeability for oil is much higher than for water at low water saturation. This reflects the very favorable imbibition properties of this rock type (this is a trend in high fracture intensity regions). Also, a steep slope exists at water saturation around 0,5 (fraction). This is to reflect the rapid movement of water through the natural fractures when the imbibition process is approaching completion (at residual oil saturation). (Agarwal et al., 2000)

The Eldfisk pseudo relative permeability and the permeability vs stress curves are included in **Fig. A.11** and **Fig. A.12** in Appendix A.

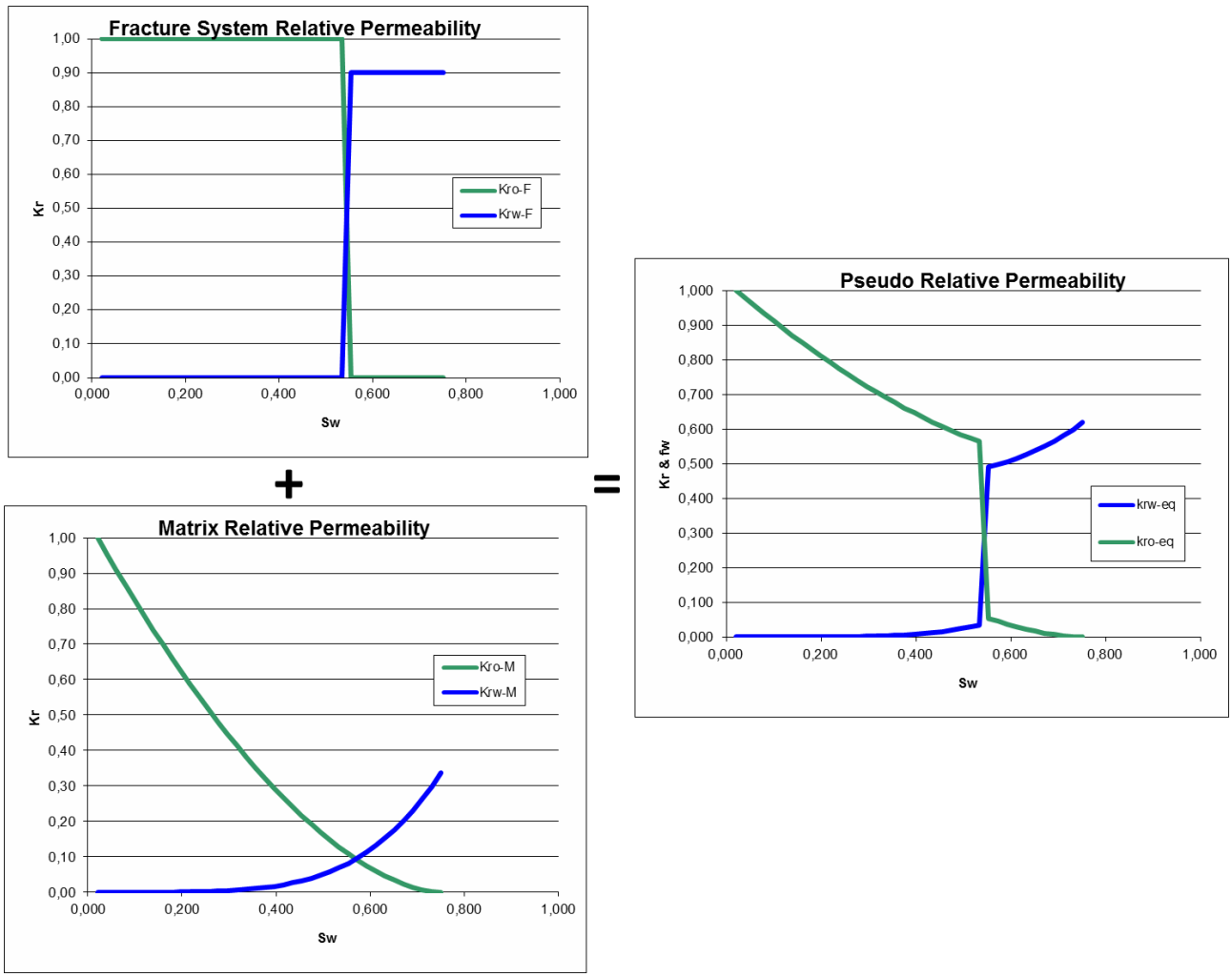

Fig. 3.3 Construction of pseudo relative permeability curves. *Fracture system relative permeability and matrix relative permeability is combined to form the pseudo relative permeability curves. It is visible from the resulting pseudo relative permeability that the fracture system dominates the overall permeability. This is true even though the matrix contains the bulk of the pore volume (Agarwal et al., 2000).*

3.2 Recovery Mechanisms in Fractured Reservoirs

This section focuses on important recovery mechanisms in fractured reservoirs, more specifically on Eldfisk. It includes an introduction to spontaneous imbibition and compaction drive.

3.2.1 Capillary Forces and Spontaneous Imbibition

Capillary pressure is defined as the pressure difference between two immiscible fluids. Denoting the pressure in the nonwetting fluid by P_{nw} and the pressure in the wetting fluid by P_w, the capillary pressure becomes (**Eq. 3.2**)(Ahmed, 2006):

$$P_c = P_{nw} - P_w \qquad \text{..... (3.2)}$$

A study performed on the Eldfisk wettability showed that the reservoir has increasing water-wet characteristics with depth (ranging from neutral to strong water-wet) (Hamon, 2004). With water as wetting phase, Eq. 3.2 then becomes (**Eq. 3.3**):

$$P_{cow} = P_o - P_w \qquad \text{..... (3.3)}$$

The capillary pressure creates a capillary force that displaces fluids in the reservoir. Spontaneous imbibition is defined as water displacing oil from the matrix into the fracture by the capillary forces. Fractures create large surface areas open to imbibition. This can cause highly fractured reservoirs to have economical production rates even if it has low permeability matrix. Spontaneous imbibition of water is a direct function of capillary and gravity forces, but it also depends on the (Haugen, 2010):

- Pore system
- Wettability
- Matrix block sizes and shape
- Interfacial tension
- Boundary conditions
- Initial water saturation

The large contrast in capillary pressure between the matrix and the fractures cause spontaneous imbibition to be an important recovery mechanism in fractured reservoirs (Haugen, 2010). Studies made on the Ekofisk field shows that the injected seawater improves the water wetness of the chalk. The result is an increase in oil recovery by spontaneous imbibition and viscous displacement. The study also showed that the injected water appeared to imbibe efficiently into the matrix in varying wetting conditions, from the Ekofisk Fm and down to the more water-wet Tor Fm (Austad et al., 2008).

The relationship between capillary pressure and spontaneous imbibition can be illustrated by the capillary pressure vs water saturation curves for imbibition and drainage of water (**Fig. 3.4**).

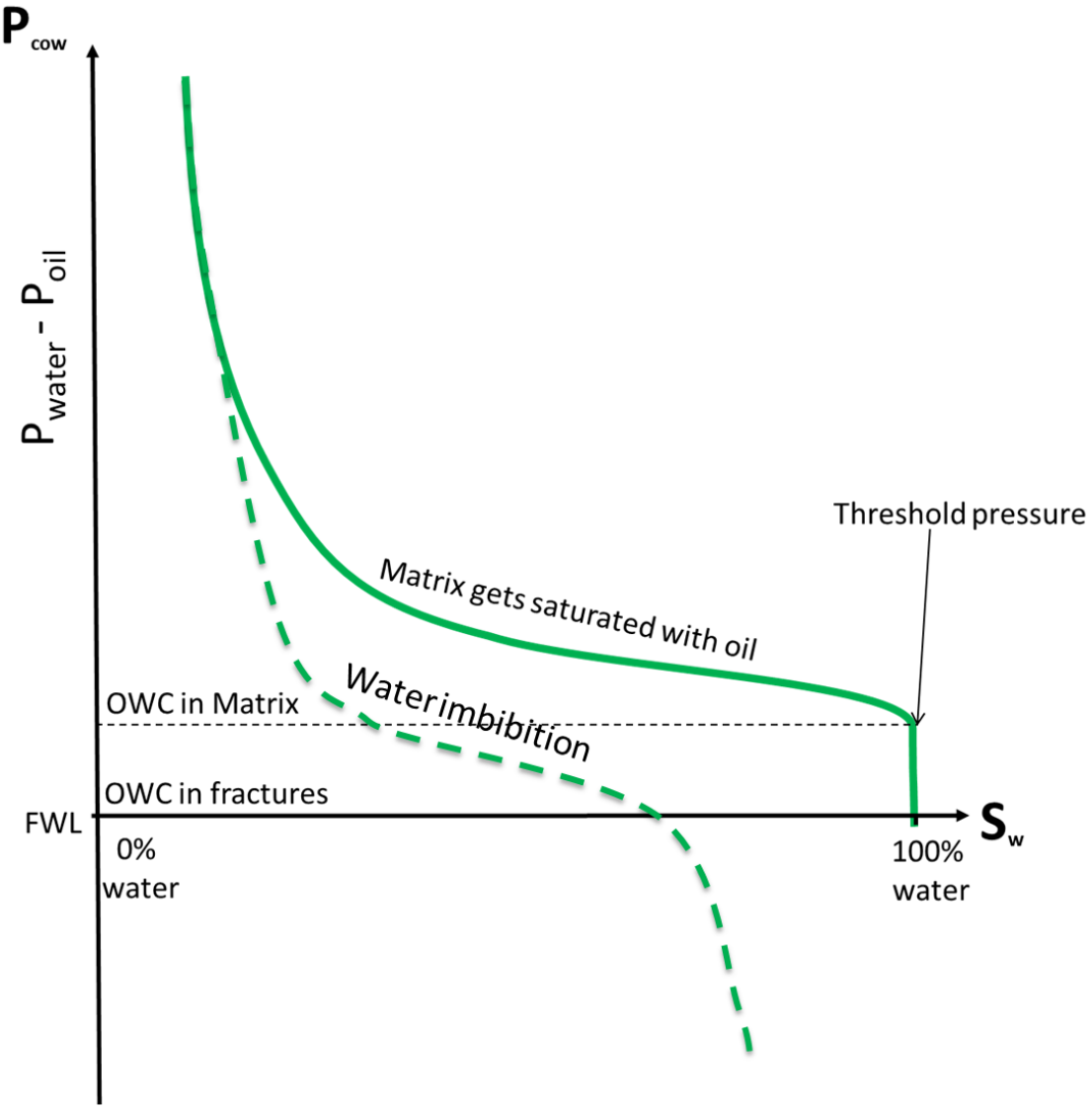

Fig. 3.4 Imbibition and drainage of water. *At start of production, the matrix is saturated with oil and the capillary pressure is high. When a waterflood is introduced to the reservoir, the capillary pressure decreases. This is caused by water spontaneously imbibing the oil (dashed green line with P,cow > 0). With a pressure differential, forced imbibition can occur (increasing water saturation with P,cow < 0 following the dashed green line). This graph is a remake from COPNO (2014c).*

The primary drainage of water, illustrated by the continuous green line, is the process of oil entering into and accumulating in the reservoir. This reduces the water saturation and increases the capillary pressure. The dashed green line describes the scenario of increasing the water saturation. For P,cow > 0, this is the process of spontaneous imbibition. For P,cow < 0, a pressure gradient is necessary to displace the oil by water. This is called forced imbibition (Morrow and Mason, 2001).

The effect of spontaneous imbibition on fluid flow in the reservoir can be illustrated by **Fig. 3.5**.

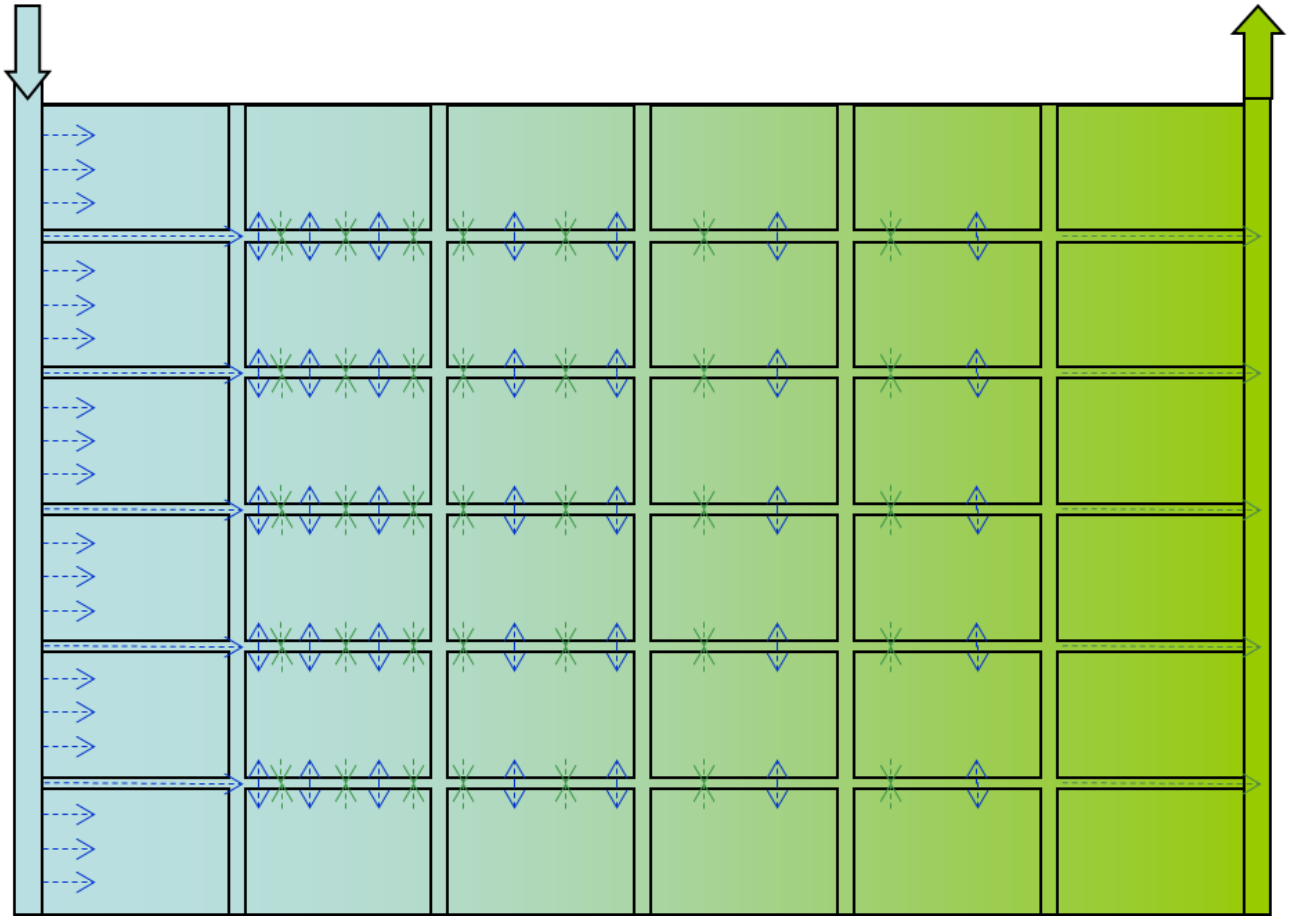

Fig. 3.5 Distribution of injected water with spontaneous imbibition. *The flow of injected water inside the matrix and fractures. Spontaneous imbibition occur throughout the reservoir due to high capillary pressures. Both forced and spontaneous imbibition happens close to the wellbore. The result is a good sweep of the reservoir (COPNO, 2014c).*

The capillary force plays a dominant role in fluid displacement inside a fractured reservoir. During waterflooding, the water is moving inside fractures and is spontaneously imbibing into the matrix. This effect is most dominant at initial conditions (high oil saturation and capillary pressure) and at a distance above the FWL (capillary pressure is proportional to the height above FWL). It results in a good sweep, as can be seen in Fig. 3.5. In a mature waterflood this effect is decreasing because of the increase in water saturation in the matrix, and the resulting decrease in capillary pressure. The injected water is then moving predominantly through the high permeable streaks, and the matrix is mostly bypassed (COPNO, 2014c).

3.2.2 Compaction Drive and Water Induced Compaction

Compaction gives additional drive energy for production. The withdrawal of fluids from the reservoir yields in a decrease in pore pressure and a resulting increase in effective stress. Due to poor rock strength of chalk and the weight of the overburden, this causes reservoir compaction and seabed subsidence (COPNO, 2014b). All reservoirs undergo deformation during exploitation. What differentiate compaction from elastic deformation is the irreducible reduction in porosity and permeability due to pressure depletion. This makes field development much more complex compared to conventional reservoirs (e.g. sandstone reservoirs) (Settari, 2002).

Water injection was implemented in the Eldfisk and Ekofisk fields with the purpose to increase the reservoir pressure and enhance oil recovery. It was expected that this would slow and eventually stop the subsidence at the producing platforms. The result has been an increase in reservoir pressure, while the subsidence has continued. A study of the Ekofisk field performed by Sylte et al. (1999) concluded that when injected seawater is introduced to the chalk, chemical interactions change the grain to grain relationship within the rock. The result is a reduction of yield strength and an increase in compressibility. This phenomenon is called water weakening.

The compression from both pressure depletion (primary recovery) and water weakening resulting from water injection (secondary recovery) have been, and are still, important drainage mechanisms on Eldfisk (COPNO, 2014b). **Fig. 3.6** illustrates the overall process of reservoir compaction.

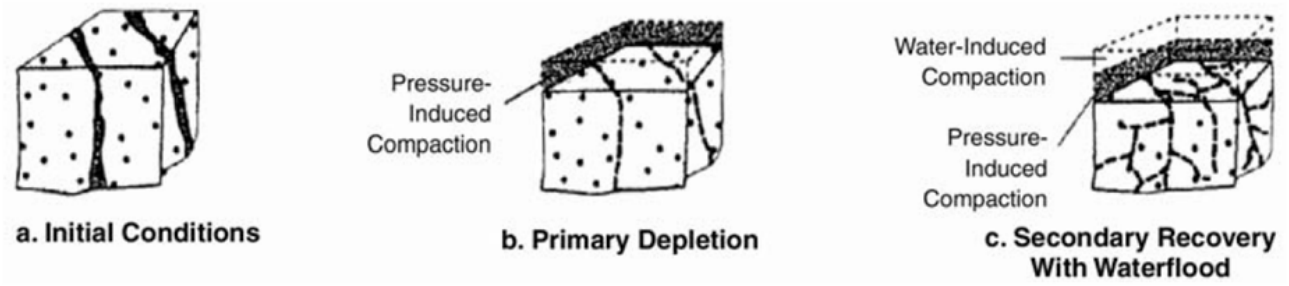

Fig. 3.6 Pressure and water-induced rock compaction. *The figure shows the overall compaction during primary and secondary recovery of a chalk reservoir. During primary recovery by pressure depletion, pore collapse cause reservoir compaction. Water weakening of chalk results in further compaction from secondary recovery with waterflooding (Cook et al., 2001).*

During the primary depletion, temperature remains constant while the pressure decreases. The compression is caused by pore collapse, resulting in plastic deformation. This causes the natural fractures to heal, which then reduces the permeability. During waterflood, the pressure is increased and the temperature is decreased. The average effective stress reduces, which may be compared to a loss in strength of the chalk. The result is further compaction of the rock. Induced fracturing occurs due to the decrease in temperature. This increases the effective permeability (Cook et al., 2001).

A plot of porosity vs effective stress can help explain the water weakening effect further. These are also called compaction curves. **Fig. 3.7** shows the compaction curves for a sample of dry Eldfisk chalk (zero water saturation). It illustrates the reduction in porosity during compaction drive.

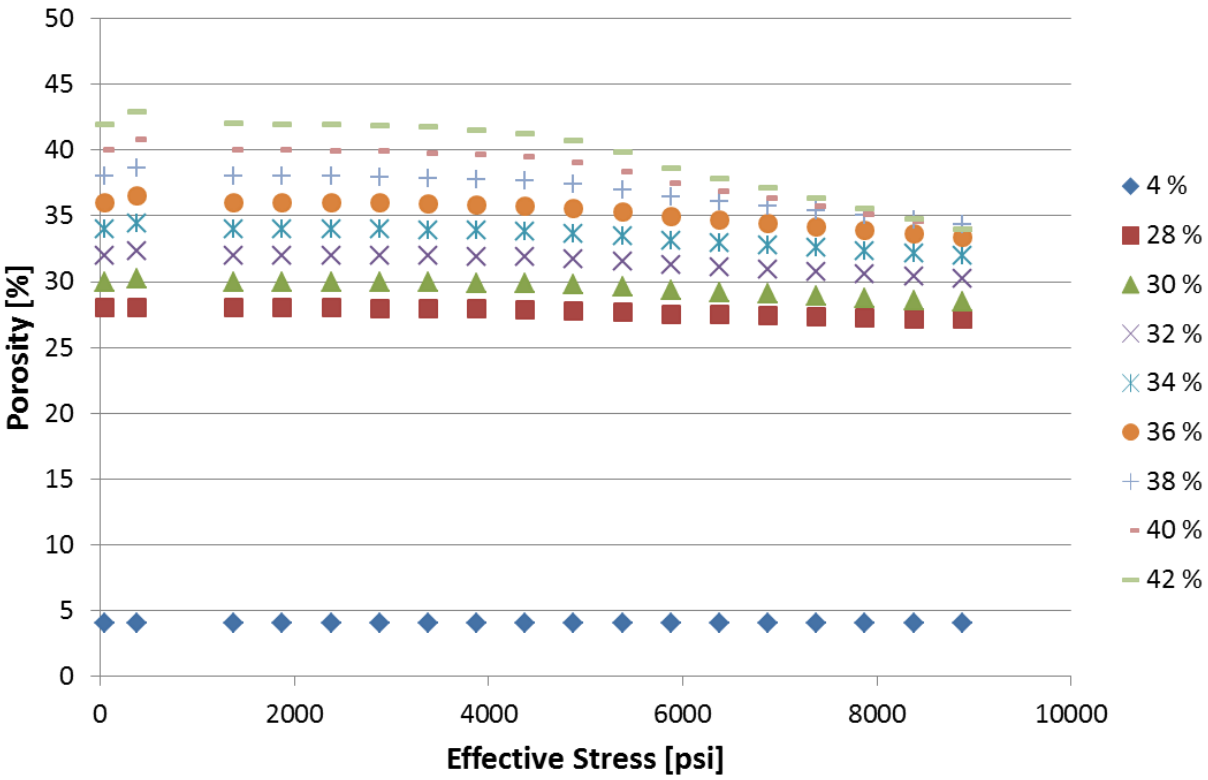

Fig. 3.7 Compaction curves for dry Eldfisk chalk (zero water saturation). *The figure shows the change in porosity with effective stress (COPNO, 2010-2012, p.81). The porosity reduces during primary depletion due to pressure-induced compaction. The curves are labeled with the initial porosity. The compaction is more severe for high values of initial porosity. There is no rebound of porosity, which means that a decrease in its value is irreducible.*

Fig. 3.8 displays the compaction curves for a fully wetted sample (when the matrix is fully water wetted and the chalk is fully water weakened). It shows the change of porosity with effective pressure during waterflooding. From Fig. 3.7 and Fig. 3.8 it becomes visible that compaction (i.e. reduction in porosity) is a function of water saturation, initial porosity and effective stress. It is observed that high porosity chalk is more compressible and that the reduction in porosity during water injection is many times greater compared to the same chalk with zero water saturation.

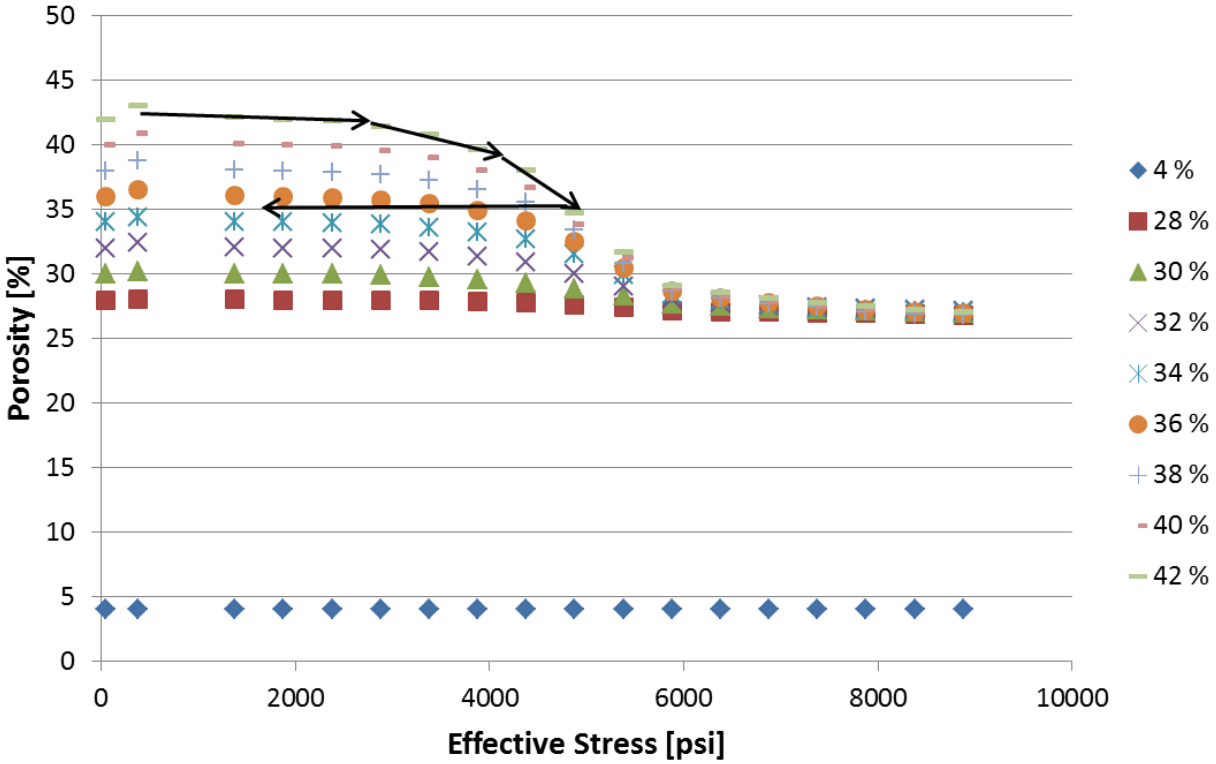

Fig. 3.8 Compaction curves for fully wetted Eldfisk chalk. *The figure shows the situation where the chalk is fully water weakened (COPNO, 2010-2012, p.81). This is the change in porosity with effective stress during waterflooding (secondary depletion). The curves are labeled with the initial porosity. As can be seen, the compaction is more severe due to the water weakening phenomenon (especially for chalks with high initial porosity). There is no rebound of porosity, as described by the black arrows.*

There is no rebound of porosity. Therefore, as mentioned previously, the reduction in porosity is irreducible. This means that even if the reservoir pressure increases due to water injection, there is no increase in porosity (Sylte et al., 1999).

Compaction can be an important drive mechanism, but it also creates changes inside and outside the reservoir that can become problematic. Seabed subsidence is of high importance. This can be challenging for the oilfield structures, seabed pipelines and the environment.

Additional problems can be wellbore failure (due to casing deformation), reactivation of faults, reduction in permeability and the risks associated with deformation of overlaying shales and aquifers (Settari, 2002). On Eldfisk, wellbore failure and platform subsidence are present challenges (COPNO, 2014b). This has the potential to increase development costs and can create barriers to project acceptance. Therefore, detailed analysis of the compaction effect is crucial in the field development of a compacting reservoir (Settari, 2002).

3.3 Ultimate Oil Recovery Factor and Recovery Efficiency

This section is mostly a modification taken from the specialization project written by the author (Kittilsen, 2014).

In the assessment of the profitability of a hydrocarbon reservoir, the oil recovery factor is estimated. This is the fraction of oil assumed to be commercially recoverable from the volume of oil in place, as defined in **Eq. 3.4** (NPD, 2009):

$$Oil\ Recovery\ Factor = \frac{Estimate\ of\ recoverable\ oil\ volume}{Estimate\ of\ oil\ volume\ in\ place} \quad \text{..... (3.4)}$$

The value of the RF changes throughout the lifetime of the field as new technology gets implemented and reservoir properties are updated (NPD, 2009). Commercial concepts, oil price volatility and development and operational costs are also important factors in determining the RF (Schulte, 2005). An example is the change in estimated oil ultimate RF (URF) for Eldfisk with time, shown in **Fig. 3.9.**

The project reaches its economic limit when the net operating cash flow equals zero. This is an important concept, as it will determine the economic lifetime of a field and can significantly affect the value of recoverable oil (PRMS, 2011, p.112).

There are many different recovery mechanisms that can be used to deplete a reservoir. The amount of immobile oil left in the reservoir at the end of production depends on the efficiency of the displacement process. The overall recovery efficiency, E, is the product of the

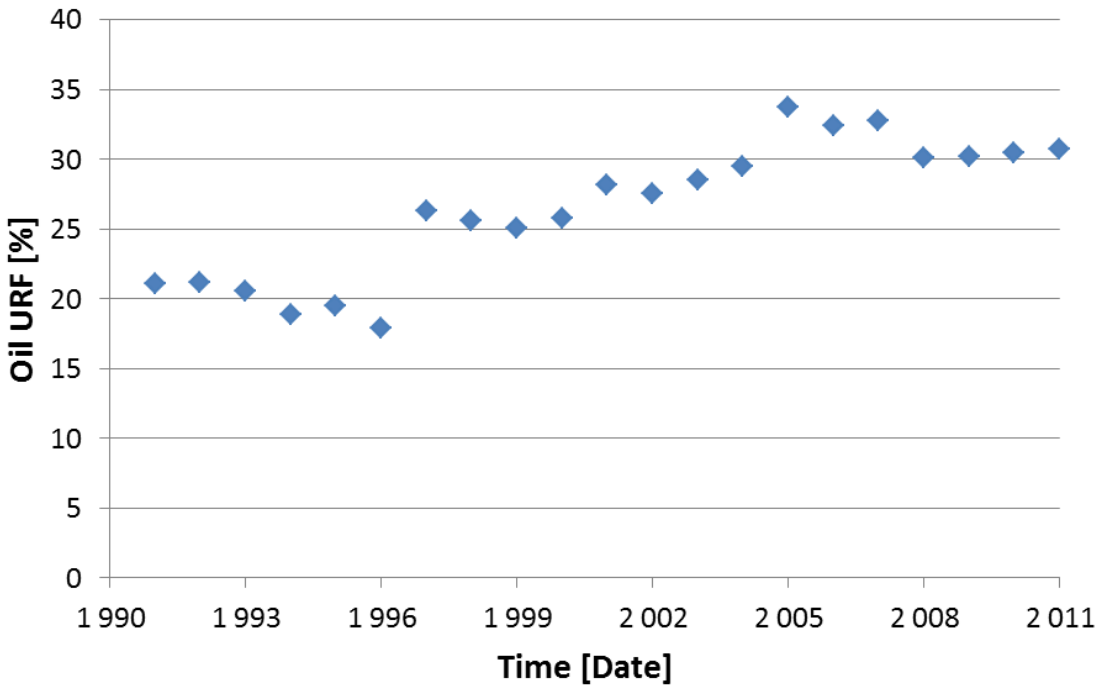

Fig. 3.9 The change in estimated oil URF with time on Eldfisk. *These estimates are calculated in the assessment of updating the reservoir management plan (RMP) (ConocoPhillips, 2012, p.60). It becomes visible how the URF changes throughout the lifetime of the field. This can be caused by technological changes, updates of reservoir properties, commercial concepts, oil price volatility and development and operational costs (NPD, 2009 and Schulte, 2005).*

macroscopic displacement efficiency, E_V, and the microscopic displacement efficiency, E_D, as described by **Eq. 3.5** (Terry, 2001):

$$E = E_V \cdot E_D \qquad \text{..... (3.5)}$$

The amount of oil bearing reservoir rock the displacing fluid comes in contact with, determines the macroscopic displacement efficiency. Once the displacing fluid is in contact with the oil, the microscopic displacement efficiency is a measure of how well it mobilizes the residual oil (Terry, 2001).

The macroscopic (volumetric) displacement efficiency is a function of both horizontal and vertical sweep efficiency of the displacement process. Factors influencing the volumetric displacement efficiency are heterogeneities and anisotropy, lithology, placement of wells and mobility ratio (Terry, 2001). In Eldfisk, the presence of micro and macro fractures causes a lot of heterogeneities and anisotropy. This is especially influencing the horizontal sweep efficiency. During waterflooding, the injected water is inclined to flow through the fractures

because they act as high permeability pathways. As a result, there may be large amount of bypassed oil.

Interfacial and surface tension forces, wettability, capillary pressure and relative permeability influence the microscopic displacement efficiency (Terry, 2001). As mentioned previously, the wettability in Eldfisk varies from neutral to strong water-wet. The interfacial and surface tension forces, capillary pressure and relative permeability are all factors strongly related to the wettability. As a result, there can be large differences in the microscopic displacement efficiency throughout the Eldfisk reservoir.

As a summary, many factors determine the oil URF. The author (Kittilsen, 2014) concluded that the value of planning a project is major. Collection of key data early in the lifetime of a field is important to ensure sustainable reservoir management. It is also necessary to continuously gather and update subsurface information with increasing field maturity in the effort to increase both the microscopic and macroscopic displacement efficiency. This affects the profitability of a project and with that the ultimate recovery of oil (**Fig. 3.10**).

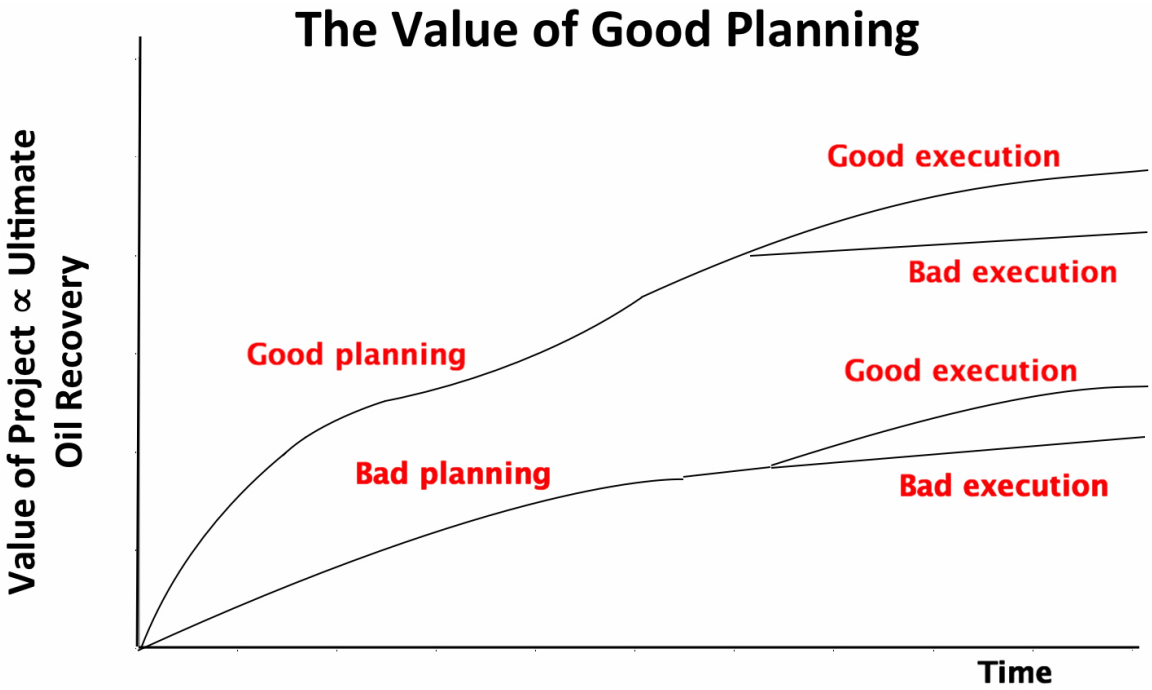

Fig. 3.10 The value of good planning. *It is important to adapt a good drainage strategy from the initialization of a project. As can be seen in this figure, the quality of the planning phase is of significant value for the resulting oil URF. The quality of execution of methods to increase oil recovery (e.g. waterflooding) will also have a substantial impact on the ultimate recovery of oil (Kittilsen, 2014).*

4 Eldfisk Water Injection

Water injection is an important part of the reservoir management on Eldfisk as it is considered to be the dominant recovery mechanism. The status of the waterflood and value of future water injection will be discussed in this chapter.

4.1 Status of Water Injection on Eldfisk

Water injection on Eldfisk has resulted in increased oil recovery. The waterflood has contributed to a sustained oil rate and it has slowed down the subsidence rate. Approximately 75% out of the active producers have been affected by the waterflood. The result has been collapsing GOR, increasing oil production rate, increasing water production rate or a combination of all three (COPNO, 2011, p.39). The current waterflood on Eldfisk can be described as a partial waterflood, with primarily horizontal line drive.

Fig. A.13 - Fig. A.21 in Appendix A shows field performance data related to water injection on Eldfisk. On a field scale it is observed that:

- At start-up of water injection in year 2000, both the oil and liquid production rate increased.
- The water-cut (WC) has increased as a result of the waterflood, but is still at a relatively low value (~40 %).
- The pressure in the reservoir has increased since year 2000 as a result of the pressure support from WI. It is important to note that there exists large pressure differentials on Eldfisk, especially in the Bravo structure, and that **Fig. A.19** only shows the average reservoir pressure. Investigation of the reservoir model, including pressure distribution, is presented in chapter 5.2.

Investigation of the field data shows that Alpha has:

- A relatively stable oil and liquid production rate.
- High water injection rate.
- Increasing WC with decreasing water injection rate since 2008.
- A field VRR with an average of about 1.0. This indicates a good balance in the reservoir in terms of voidage replacement.
- The highest VRR in the Tor Fm.

The field data shows that Bravo has:

- Declining oil and liquid production rate.
- Stable WC (~27%).
- A field VRR with an average of about 1.0.
- A large difference between the Ekofisk Fm and Tor Fm VRR. The Ekofisk Fm is lagging behind in terms of water injection support, and has an average VRR of only ~0.1.

The objective with Eldfisk Phase II is to continue the current waterflood, but also expand it to the rest of the field. The Ekofisk Fm in the Bravo structure will be an important part of this expansion since no significant injection has taken place in this area so far, as can be seen by its low VRR (COPNO, 2011, p.40).

4.2 The Value of Future Water Injection

This chapter presents a study made on the overall value of future WI. One run was made without any WI from 01/01/2015. This was compared to the Base Case, where all injectors (existing and future) are included.

The oil rate and cumulative oil production versus time, with and without WI, are shown in **Fig. 4.1**. From this data it was calculated that 39 % out of the cumulative production from 01/01/2015 is due to WI. This equates to 117 MMSTB of oil. The oil RF in 01/01/2015 is estimated to be 23 %. The oil URF is 30 % without WI and 34 % with WI, according to the Base Case.

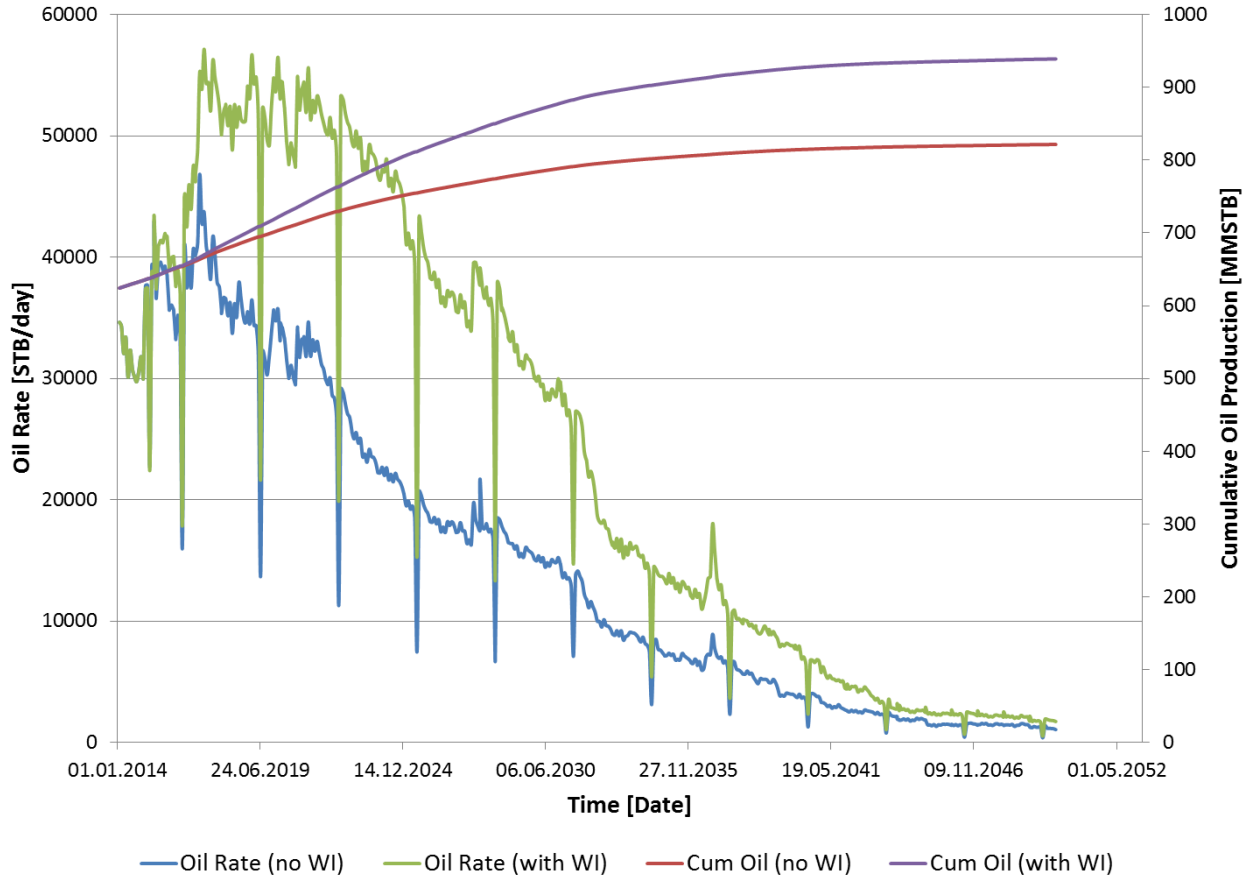

Fig. 4.1 Forecast of oil production with and without WI. *The figure shows the value of future WI. As can be seen, there is a significant drop in the oil rate without WI. This results in a 117 MMSTB reduction in cumulative oil production. MMSTB =10^6 STB.*

As Eldfisk is a mature oil field, WI to re-pressurize the reservoir is crucial for oil production. In the scenario with no water injection, the reservoir pressure will decrease. This has not only a detrimental effect on oil production (as seen on Fig. 4.1), but can also compromise the safety of the operations as pressure maintenance is important in relation to well integrity and platform subsidence. The reservoir pressure versus time, with and without WI, is given in **Fig. 4.2**. It shows the average pressure in hydrocarbon bearing cells (HCP,avg). Water injection pressure limit is based on the overburden seal pressure. The target is not to exceed the initial pressure (initial HCP,avg was 6869 psia) (Ozoglu-Topdemir, 2014).

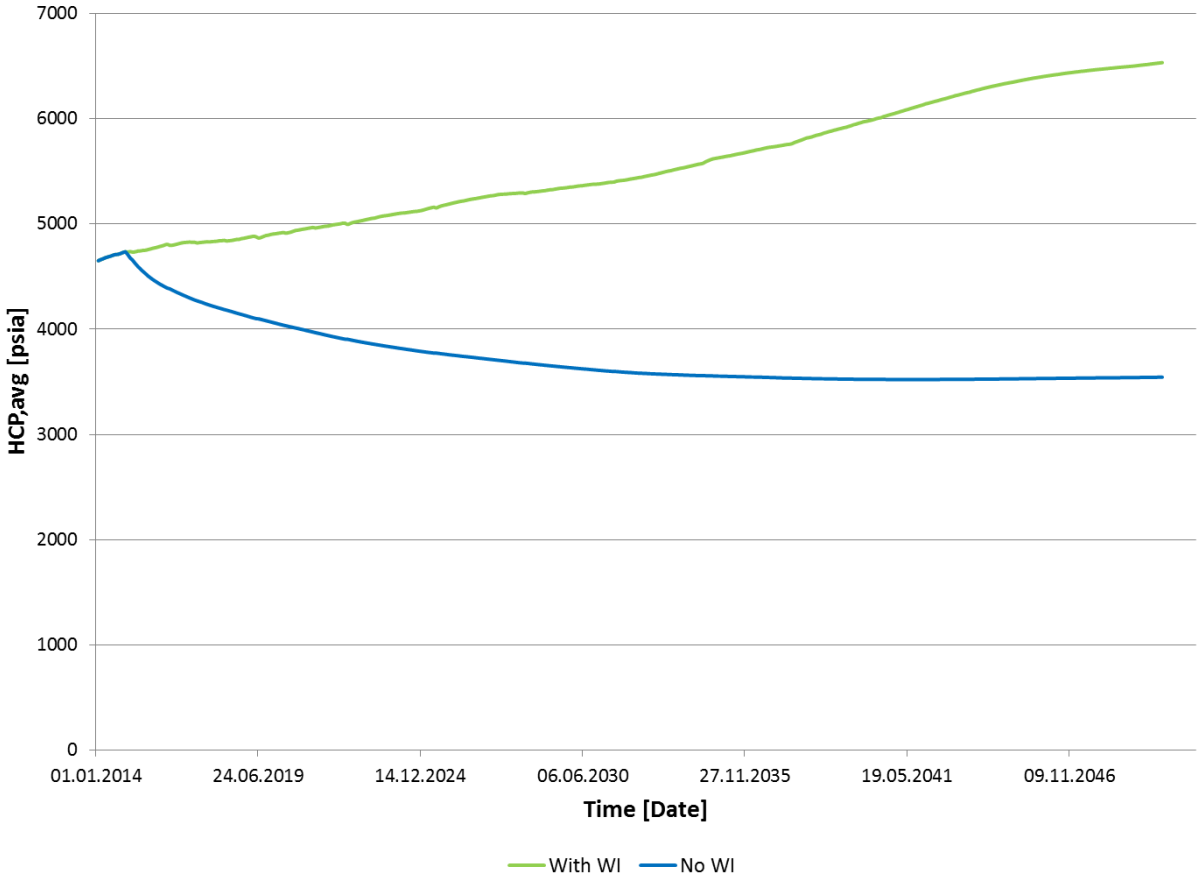

Fig. 4.2 Forecast of average field pressure vs time, with and without WI. *The green line shows the predicted average field pressure with WI, and the blue line shows the predicted average field pressure without WI. It becomes visible that water injection is crucial for pressure support on Eldfisk. Water injection pressure limit is based on the overburden seal pressure. The target is not to exceed the inital pressure (initial HCP,avg was 6869 psia) (Ozoglu-Topdemir, 2014).*

The strategy of waterflood management has become more focused on optimizing sweep (areal and vertical) as the Eldfisk field has matured (ConocoPhillips, 2012, p.24). As mentioned in chapter 2.4, the reservoir model is divided into regions. One output from the simulation runs is the RF by region. This is displayed in **Fig. 4.3**. The green bars show the RF in 2015, while the blue and red bars represent the oil URF.

On Alpha, the future WI has the highest increase in sweep efficiency in the Ekofisk Fm. This can be explained by the addition of three new Ekofisk injectors on Alpha. These wells will add energy to the reservoir and, according to Fig. 4.3, increase the RF significantly in the Ekofisk Fm. **Fig. 4.4** is a graph of the cumulative WI per region in the Base Case. Alpha Ekofisk Fm is represented by the blue line. It is visible from this graph that it has the largest increase in injected volume of water from 2014 (interpreted from the increase in slope).

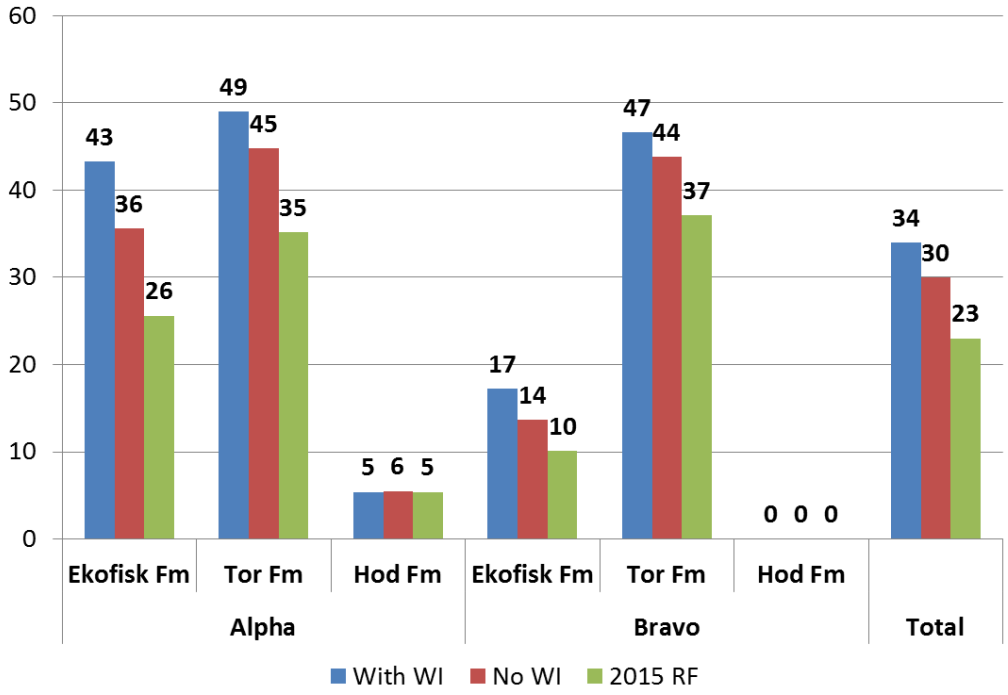

Fig. 4.3 Current and forecasted recovery factor by region, with and without WI. *The Tor Fm has the highest RF in both 2015, but also in 2050. This is the case with and without WI. In Bravo, the permeability constrast between the Ekofisk Fm and the Tor Fm is much higher. This results in a large difference in RF between the two formations in this structure.*

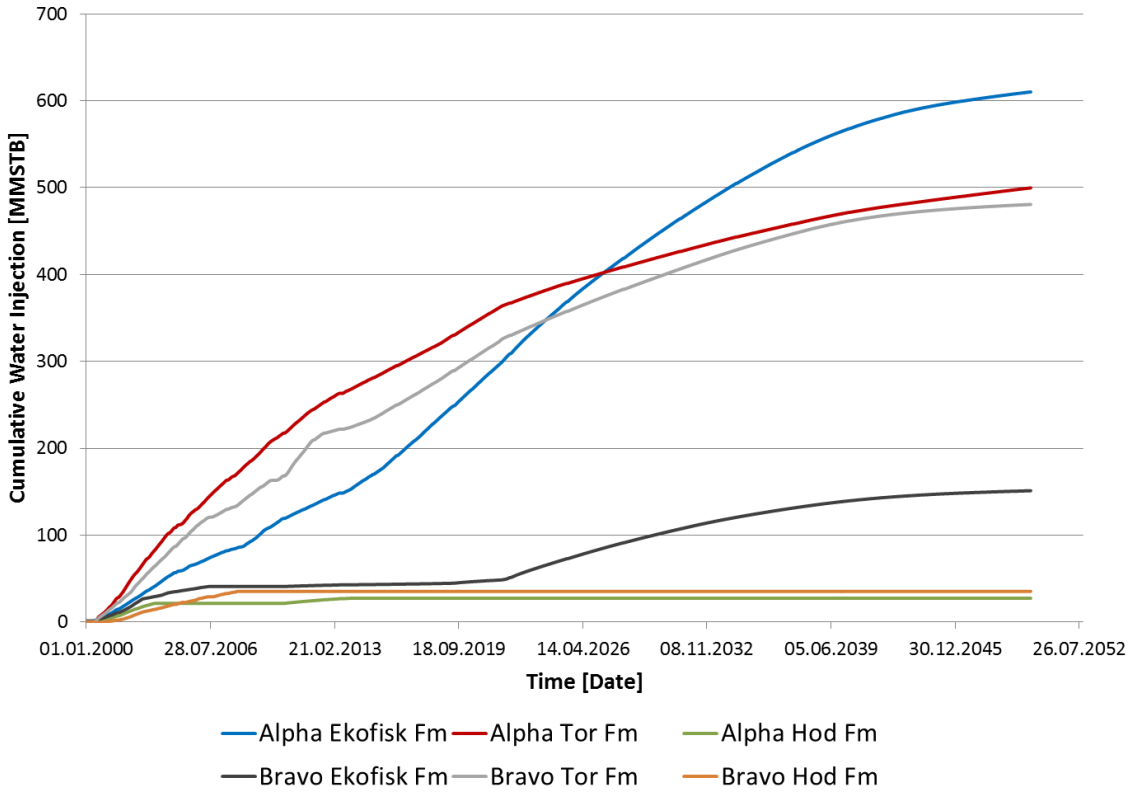

Fig. 4.4 Cumulative water injection by region in the Base Case. *Alpha Ekofisk and Tor Fm, and Bravo Tor Fm have been and will continue to be the targets of WI. These are also the formations with the highest RF.*

The Tor Fm has the highest URF. Because of its relatively good reservoir properties, large amounts of the WI in both the Alpha and Bravo structure have been targeted to the Tor Fm to this date (Fig. 4.4). In both scenarios, the Hod Fm has low RF. Because of its poor reservoir properties this formation has not been the focus of WI (Fig. 4.4). Combining the information from Fig. 4.3 and Fig. 4.4 it becomes visible that the Ekofisk Fm in the Bravo structure still has a lot of potential for optimization by WI.

5 Analysis of Reservoir Flow Dynamics

This chapter gives an analysis of the reservoir flow dynamics based on the reservoir model. First, a discussion about fracture modeling on Eldfisk is given in chapter 5.1. It explains briefly how field data is used to map the permeability distribution in the reservoir model. Then, an investigation of change in saturations and effective permeability in the model with time is presented in chapter 5.2. The method used to model areas with changing permeability is introduced in chapter 5.3.

5.1 Modeling of Fractures

Studies of Eldfisk show that the reservoir has an effective and well developed fracture system. As fractures (including faults) can act as preferential conduits for fluid flow, these high permeability streaks become an important part of modeling Eldfisk. To identify the different types of fractures in the reservoir is also one of the main challenges, due to lack of data in Eldfisk (COPNO, 2010-2012, p. 26).

Since start of production in 1979, more than 135 wells have been drilled during both the depletion and water flooding phase. A deterministic approach was used to map the fracture network based on data collected from these wells. The following dynamic and static data was used in the mapping process (COPNO, 2010-2012, p.5):

- Permeability measurements from well testing.
- Core fracture data.
- Massive water break through events.
- Production, water-cut and water injection data.
- Tracer information.
- Interference test.
- Drilling mud loss measurements.

As mentioned in chapter 3.1.1 about effective permeability in fractured reservoirs, a cut-off value of 5mD is used to identify fracture network contribution when investigating the response from well tests. Core data is used to investigate the amount and orientation of fractures. A massive water break through event indicates that there is a pathway connecting a

producer and an injector (COPNO, 2010-2012, p.39). Tracers are added in the injected water, which can be detected when testing fluids from production wells. This can give an idea of the WI pattern in the reservoir (COPNO, 2010-2012, p.36). An interference test can verify a pressure communication and with the help of other data, as mentioned in the above bullet points, it is possible to map pathways of high permeability (highways) (COPNO, 2010-2012, p.39). Recording of mud losses is performed consistently throughout the drilling operation. A loss of more than 50 bbl per hour can be an indication of a fracture network. The uncertainty with this indicator is that the fracture might not be at bit depth if there is differential pressure along the wellbore (COPNO, 2010-2012, p.41).
In most cases it is necessary to take several indicators into consideration at the same time. An iteration process between the geologist and the reservoir engineer was used to reach a geologically valid history matched permeability model of Eldfisk (COPNO, 2010-2012, p.5).

5.2 Investigation of the Reservoir Model in CView

In order to investigate the reservoir model, a .PVWV file was made for the Base Case. Water saturation (Sw), pressure and effective permeability (k,eff) were evaluated through time in order to analyze flow dynamics in the reservoir model. Only the initial k,eff (named kx in CView) is included in the model. Instead, it uses transmissibility to represent dynamic fracturing and distribute the fluids through time. The option of Cell Math in CView makes it possible to calculate k,eff for all times from transmissibility and initial k,eff. The following procedure was used (where U1, U2 and U3 are user-defined functions):

1. U1 was set to be the difference between the initial transmissibility and the current, for all times: U1 = Tx(1979) - Tx(t)
2. U2 = U1 + Tx(t) = Tx(1979)
3. U3 = (k,eff(1979) * Tx(t)) / U2

The equation in step 3 is given in **Eq.6.1.**

$$k_{eff}(t) = \frac{T_x(t)}{T_x(1979)} \cdot k_{eff}(1979) \qquad \text{.....(6.1)}$$

As a quality check the new function U3=k,eff(t) was visualized with the initial k,eff (named kx) in CView to validate that they were matching.

The initial average matrix permeability on Eldfisk was less than 1 mD, with natural fractures having permeability up to approximately 200 mD (COPNO, 2010-2012, p.25). **Fig. 5.1** and **Fig. 5.2** shows the change in permeability from start of production until 01/01/2014 in the Ekofisk and Tor Fm respectively.

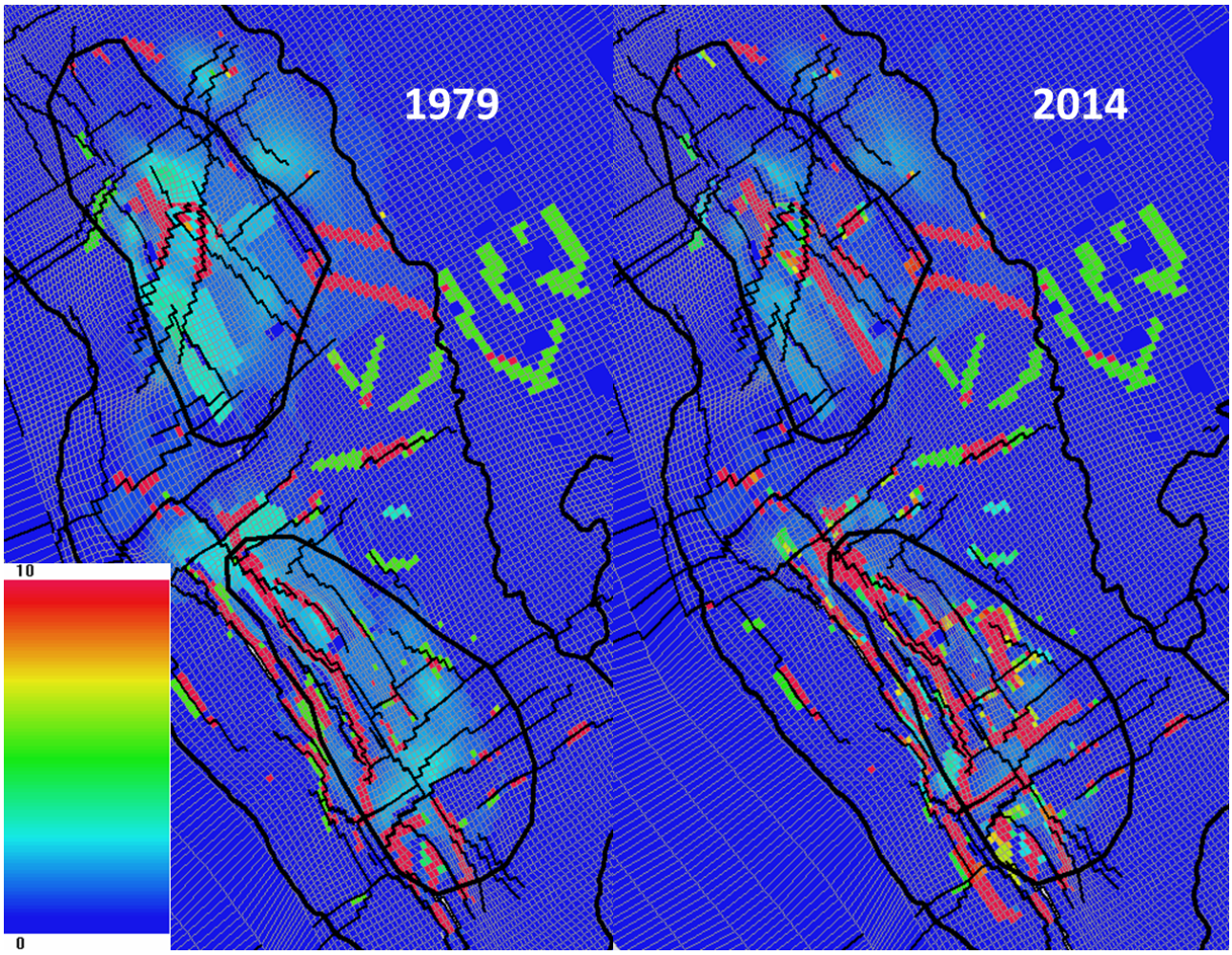

Fig. 5.1 Permeability in the Ekofisk Fm in 1979 and 2014. *The figure shows the change in permeability in the Ekofisk Fm (layer 5) in Alpha from start of production until 01/01/2014. More conductive pathways for flow have developed through time. The permeability distribution has also become more heterogenous with time. The scale is in mD.*

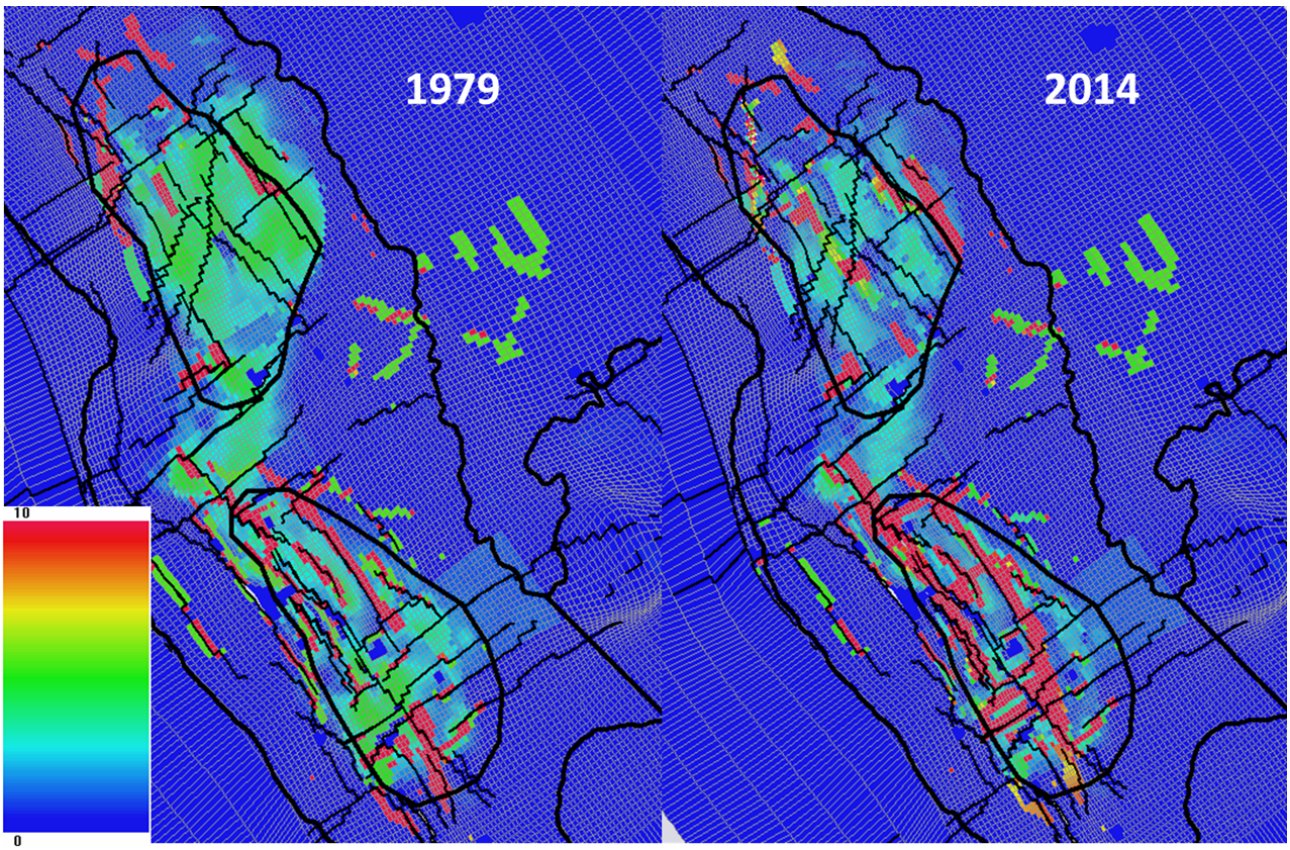

Fig. 5.2 Permeability in the Tor Fm in 1979 and 2014. *The figure shows the change in permeability in the Tor Fm (layer 9) from start of production until 01/01/2014. More conductive pathways for flow have developed through time. The permeability distribution has also become more heterogenous with time. The scale is in mD.*

An increase in pressure around the injectors can cause fractures to develop and propagate a distance away from the wellbore dependent on the local geology. As a result pathways of direct communication can develop between the injectors (bridges), similar to what can be observed on Alpha. It can also be seen that initial fracture corridors in Alpha and Bravo have become more extensive during injection, both vertically and horizontally. Another observation is that the permeability distribution has become more heterogeneous with time. The MODR KVSTR keyword is used to model these areas of higher permeability, as will be explained in chapter 5.3. These fractures can cause communication between the Ekofisk and Tor Fm, resulting in cross flow between the formations (COPNO, 2010-2012, p.135).

The highways have become more conductive with time. Changing the permeability scale in the previous picture makes this visible (**Fig. 5.3**). Investigation of the model shows that some highways are given a very high value of permeability (in the scale of 10^6). This is done to emphasize the fact that they are very conductive and to be able to history match the model (Eremenko, 2014).

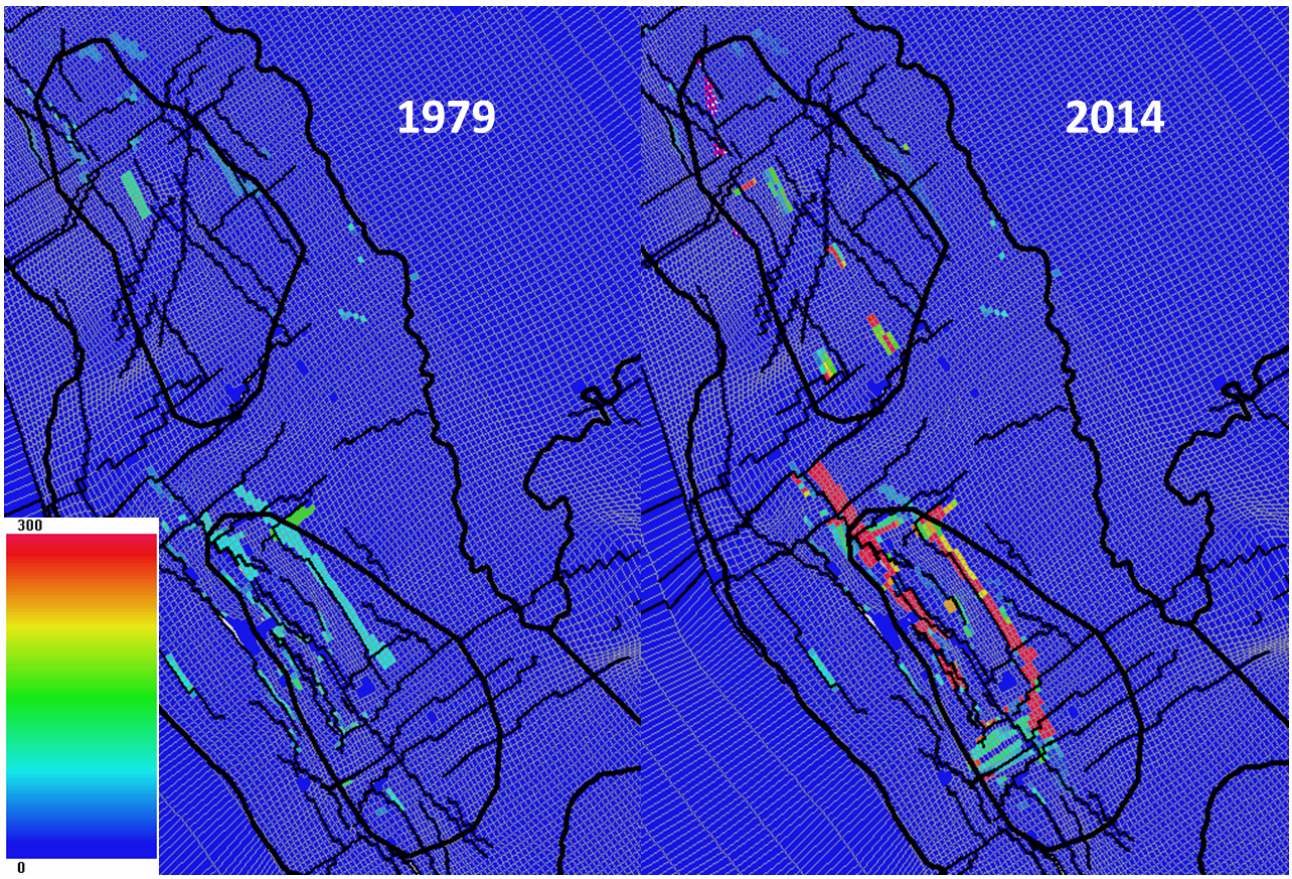

Fig. 5.3 Illustration of more conductive highways with time. *The picture shows permeability in the Tor Fm (layer 9) in 1979 and 2014. Changing the scale maximum from 10 mD to 300 mD, emphasizes the fact that the highways have become more conductive with time.*

Fig. 5.4 shows the permeability in 1979 and 2014 in the Ekofisk Fm (layer 5) in Alpha, and its current injectors. As can be seen, all active injectors on Alpha are connected to both natural and induced fractures. A-5 is an example of how the wells behave in relation to fractures in this structure. This well has induced fractures and has made the natural fractures more conductive and larger in extent. It is mainly perforated in the Ekofisk Fm (layer 5).

The fracture along the heel of A-5 extends vertically, and in the Tor Fm (layer 9) this fracture develops into a bridge connected to A-4 and A-13. This is shown in **Fig. 5.5**. It is visible that Alpha has a well-developed fracture network in general, and that all the injectors are communicating through fractures. To better visualize the injection pattern, pictures showing the development in S_o and pressure with time are included in **Fig. 5.6** and **Fig. 5.7**.

Bravo is a low permeability reservoir, with a less developed fracture network than Alpha (COPNO, 2010-2012, p.131). The crestal area has the most fractures. These are natural fractures and faults that have developed more extensively during water injection (COPNO, 2010-2012, p.137).

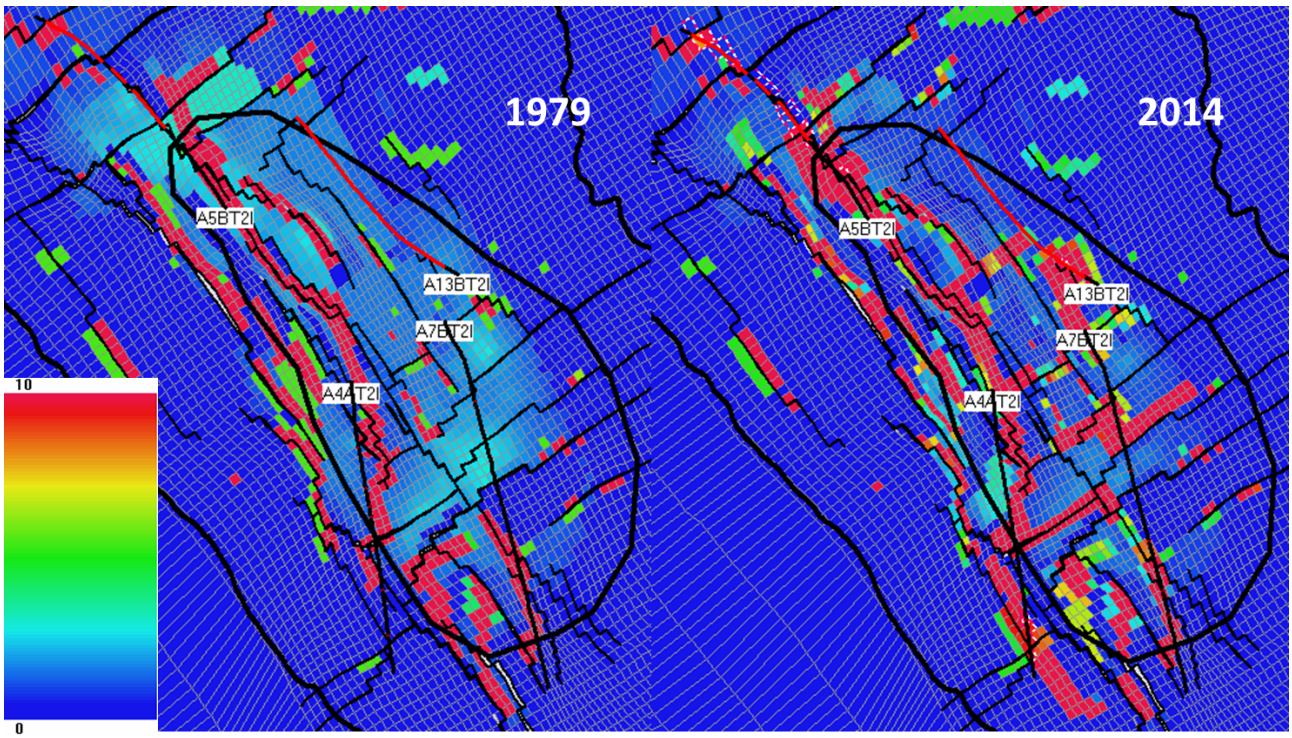

Fig. 5.4 Permeability in Alpha in 1979 and 2014. *The picture shows the change in permeability in the Ekofisk Fm (layer 5) from start of production until 01/01/2014 in Alpha. The location of the highways are close to existing injectors. The red dashed cells are perforated cells in this layer. The scale is in mD.*

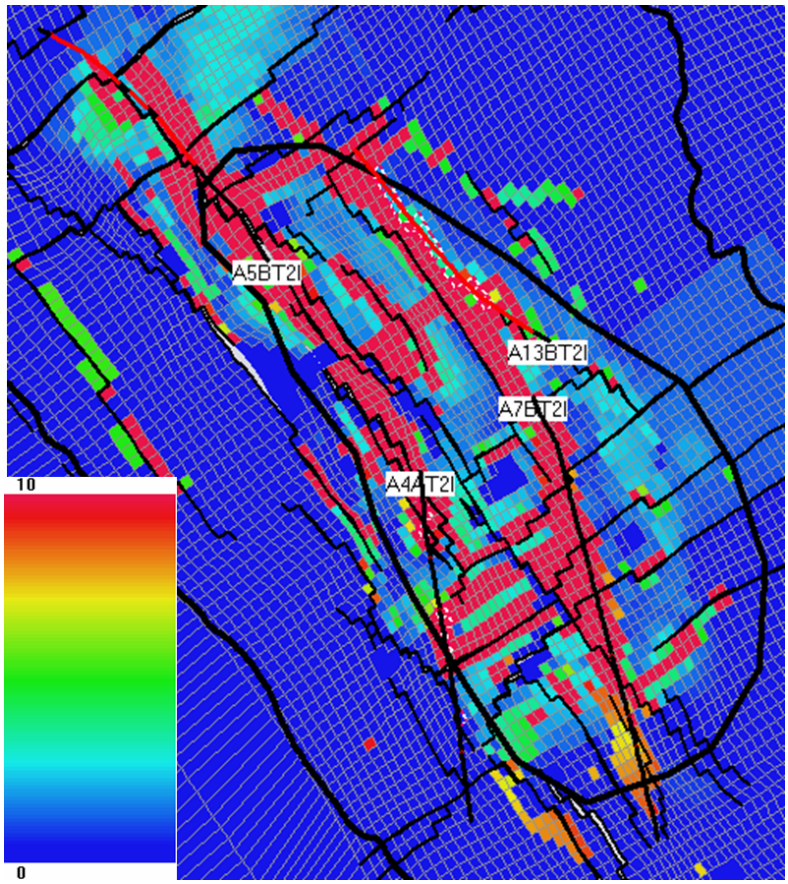

Fig. 5.5 Fracture network in Alpha. *The Tor Fm (layer 9) in 01/01/2014, showing a well-developed fracture network in Alpha. The scale is in mD.*

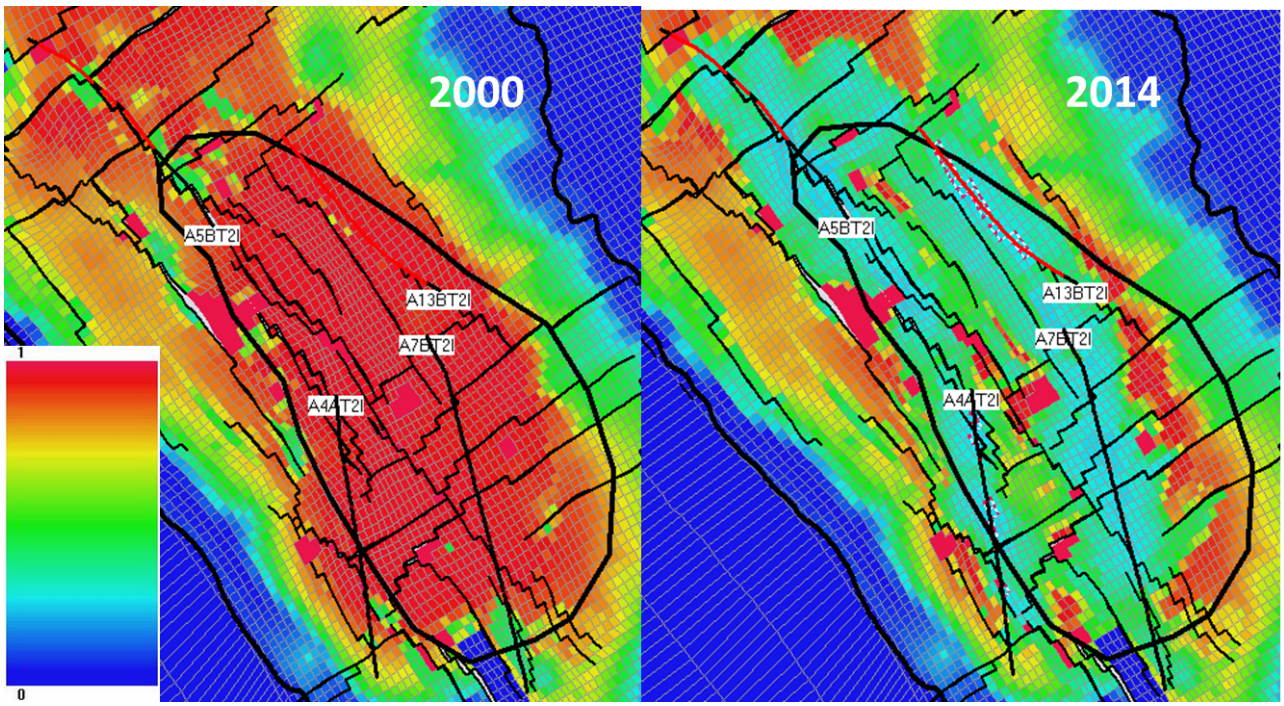

Fig. 5.6 Oil saturation in Alpha (Tor Fm) in 2000 and 2014. *The picture shows the change in oil saturation in the Tor Fm (layer 9) from start of WI to 2014. The oil saturation has decreased in and around the highways. The flank areas still have high oil saturation.*

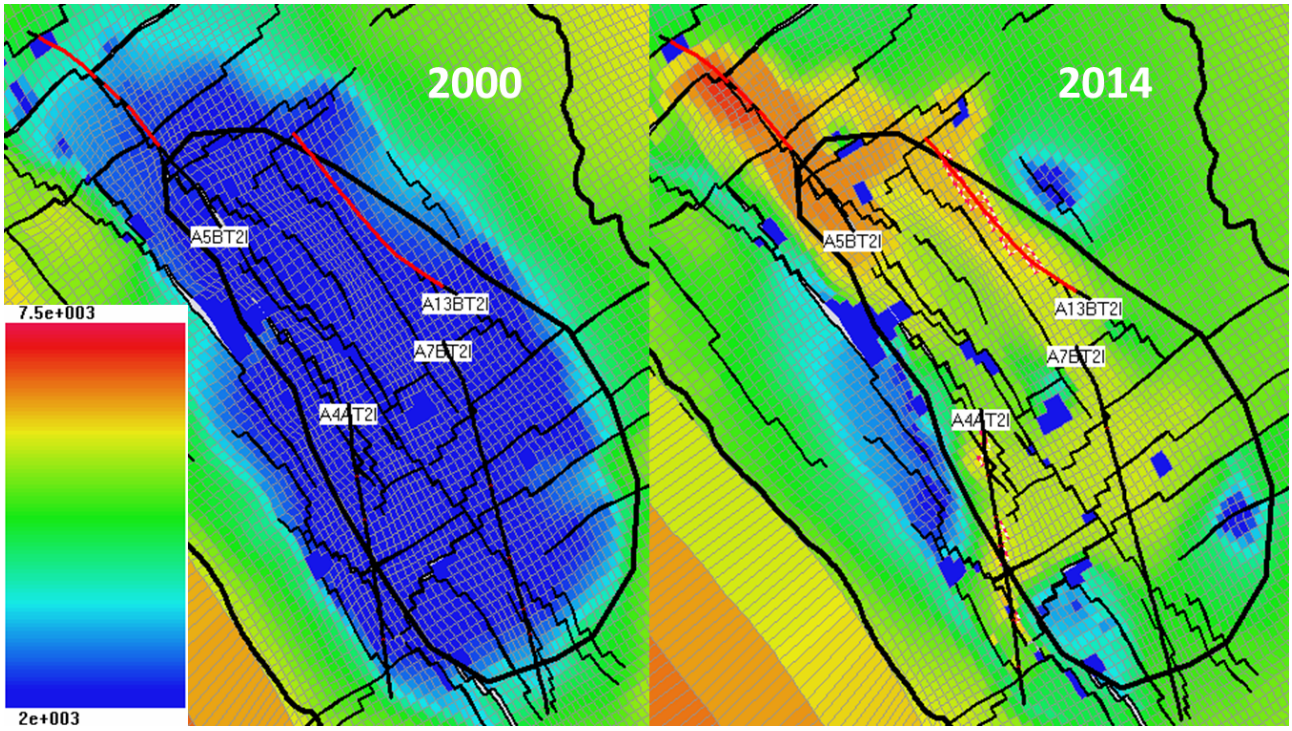

Fig. 5.7 Pressure in Alpha (Tor Fm) in 2000 and 2014. *The picture shows the change in pressure in the Tor Fm (layer 9) from start of WI to 2014 in Alpha. The pressure in the reservoir was at a low level before start up of WI. Except for a few pressure sinks, the pressure has increased by 2014. This is especially true in and around the highways. The scale is in [psia].*

B-8 is an example of an injection well in the Bravo structure that is opening up fractures along naturally occurring faults. It is also connecting two faults by induced fractures. This can be seen in **Fig. 5.8**. The red dashed cells are perforated cells in this layer. B-8 was set on reduced injection in 2012 to prevent a non-matrix water break-through event. The picture to the right in Fig. 5.8 is from 01/01/2012. It shows the fracture system when B-8 had its initial water injection rate constraint.

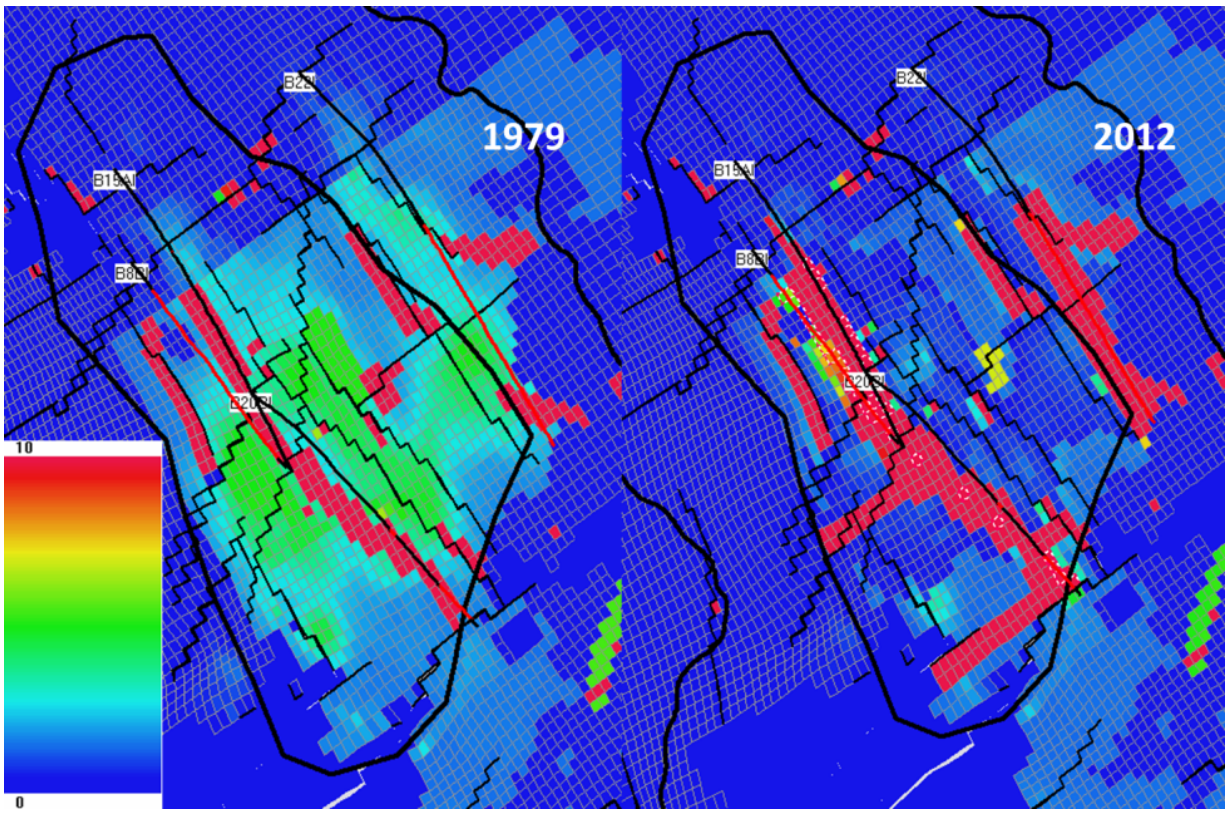

Fig. 5.8 Fracture development in the Bravo structure. *The picture shows the permeability in the Tor Fm (layer 12) in 1979 and 2012. It is visible that the existing Bravo injectors are connected to natural and induced fractures. The scale is in mD.*

There are large areas of low pressure (pressure sinks) in Bravo, which can be observed in **Fig. 5.9**. The pressure decreases during primary depletion, causing a reduction in the permeability in the pressure sinks (Fig. 5.8). It is also observed that the oil saturation is higher in these areas, as they are not sufficiently swept by water injection. This is visualized in **Fig. 5.10.**

Investigation of the reservoir model showed that there is a lack of pressure support in the Ekofisk Fm in the Bravo structure. The pressure sinks are more prevalent in the Ekofisk Fm, as can be seen in **Fig. 5.11**. This is in agreement with the estimates of RF presented in chapter 4.2, which where 10 % for the Ekofisk Fm and 37 % for the Tor Fm in 2015.

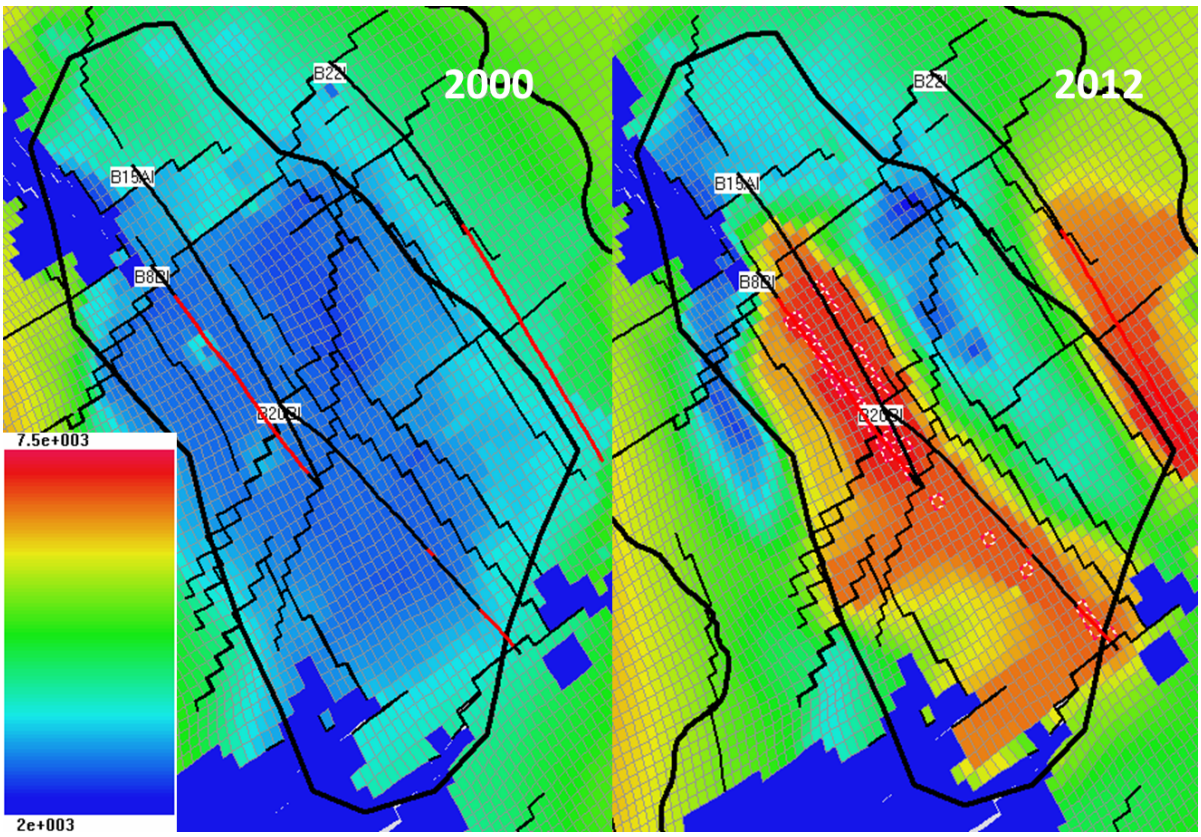

Fig. 5.9 Pressure in Bravo (Tor Fm) in 2000 and 2012. *The figure shows the change in pressure in the Tor Fm (layer 12) from start of WI until 2012. As can be seen, the Bravo structure has large pressure differentials. The scale is in [psia].*

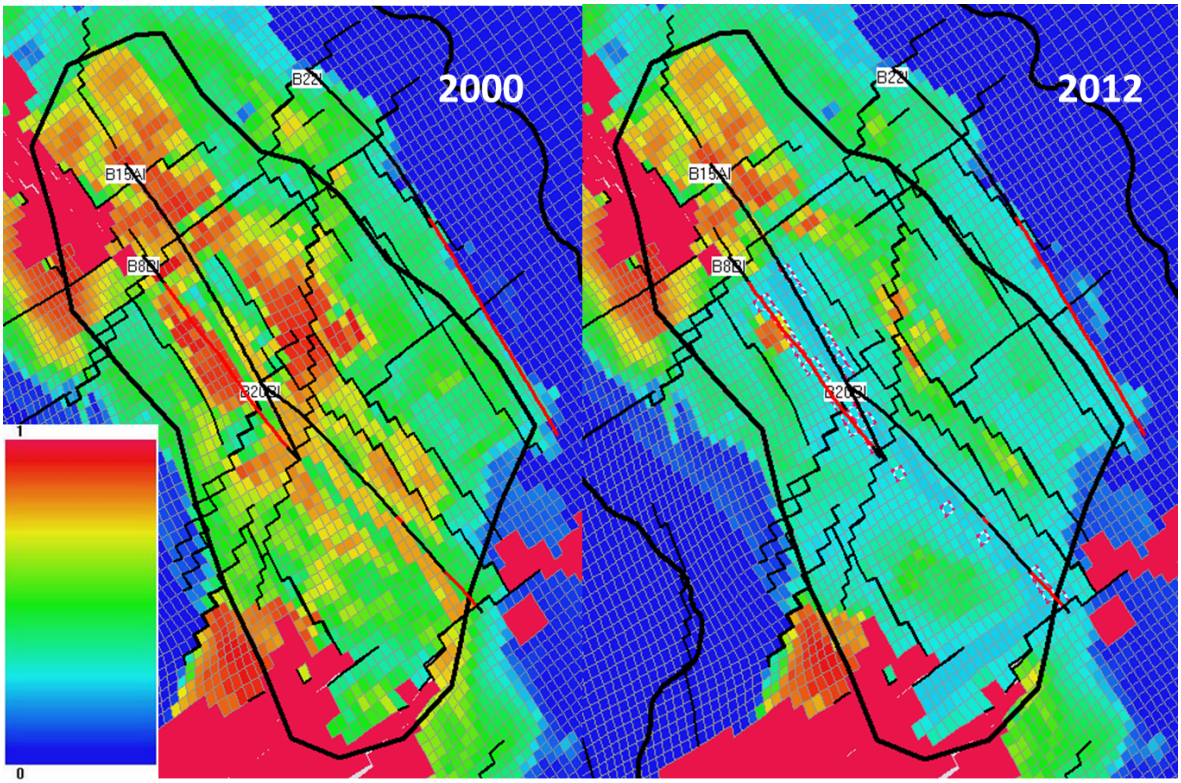

Fig. 5.10 Oil saturation in Bravo (Tor Fm) in 2000 and 2012. *The figure shows that areas with pressure sinks in the Tor Fm (layer 12) have higher oil saturation. These areas are not sufficiently swept by water injection.*

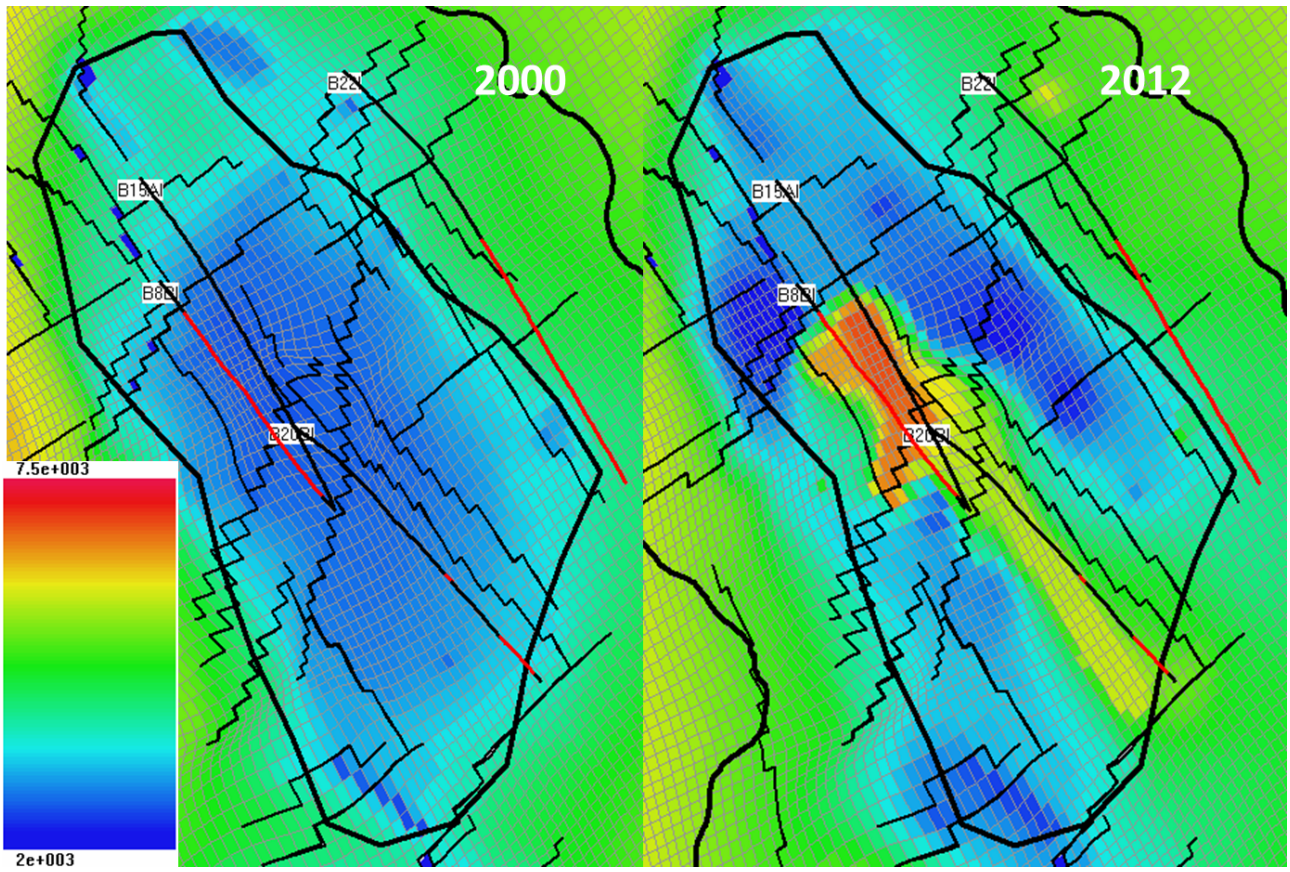

Fig. 5.11 Illustration of lack in pressure support in Bravo (Ekofisk Fm). *The picture shows the change in pressure in the Ekofisk Fm (layer 4) from start of WI to 2012. As can be seen, there is a lack in pressure support in the Bravo Ekofisk Fm. The pressure sinks are areas with blue color. The scale is in [psia].*

The following bullet points summarize the most important findings in the analysis of the simulation model related to flow dynamics:

- There is a lack of pressure support in the Bravo Ekofisk Fm.
- Bravo has lower permeability and a less developed fracture network.
- Alpha has more natural fractures than Bravo.
- Bridges have developed in Alpha, connecting the injectors.
- Initial fracture corridors have developed more extensively during injection in both structures.
- The permeability distribution has become more heterogeneous with time.

5.3 KVSTR keyword

From experience with history matching, the KVSTR keyword is used when an injector is introduced to the reservoir model. This rule was first used in the late 90's in order to be able to model the good injectivity observed at the Ekofisk Field. It was later implemented in the Eldfisk reservoir model (ConocoPhillips, 2012, p.101). KVSTR controls the modification of permeability with the change in pressure and Sw. This creates a permeability field with stronger pressure gradients, which makes it possible to model good injectivity at the injectors (with no need for pseudo perforations) and reduced productivity at the producers (without large skin values) (ConocoPhillips, 2012, p.104). The overall effect in the reservoir is shown in **Fig. 5.12**. The picture shows the development of a more heterogeneous permeability distribution at the Eldfisk field with time, including the wells that have been in the model until 01/01/2015.

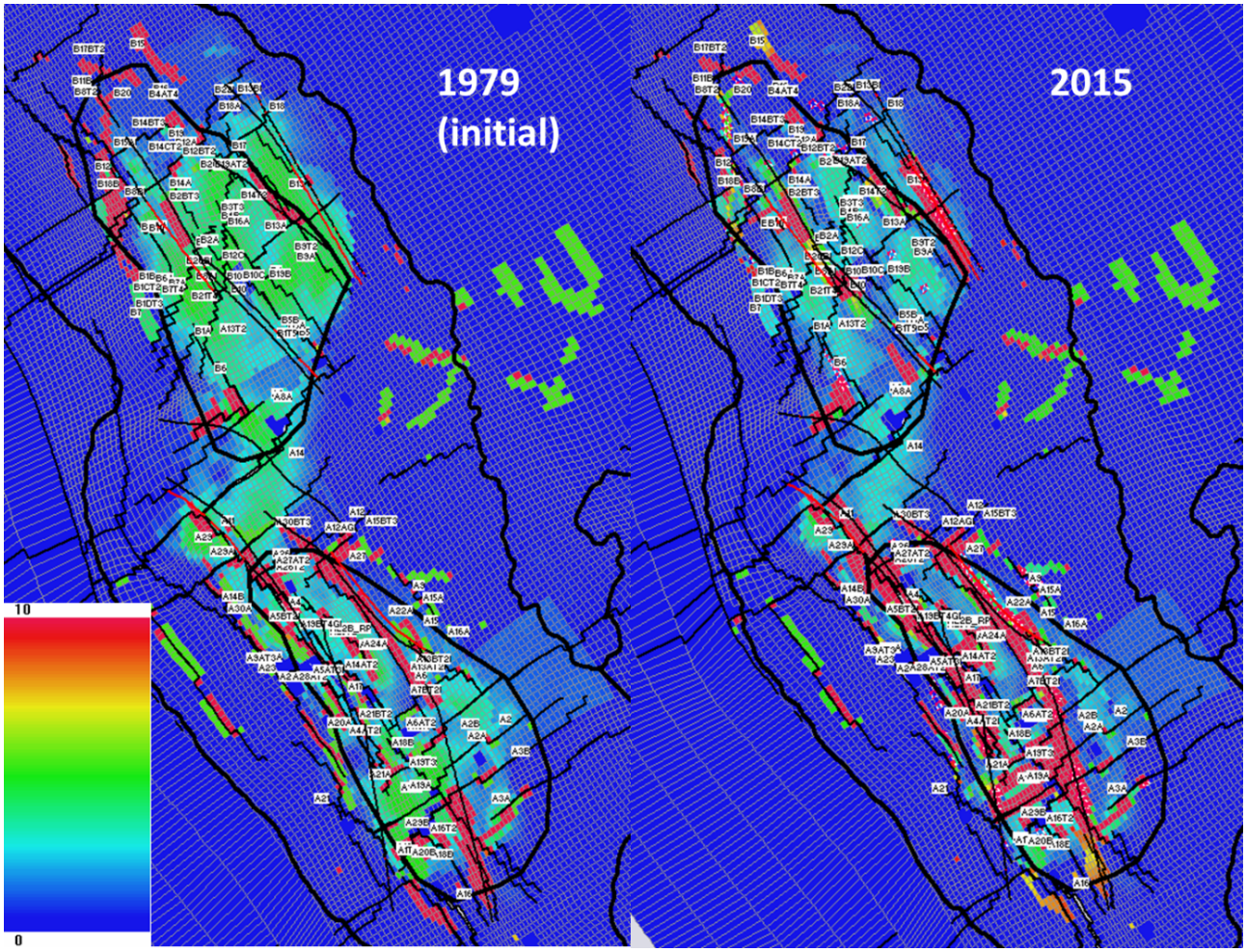

Fig. 5.12 Effect of KVSTR keyword on permeability. *The picture shows the permeability in 1979 and 2015. It illustrates the development of a more heterogenous permeability field with time. The scale is in [mD].*

The KVSTR keyword is inputted as one value which is mapped as an array. This can be modified with time. The value of KVSTR is used in **Eq.6.2** (COPNO, 2010-2012, p.100):

$$factor = \left[table\ factor \cdot \left(1 + \left(\frac{P - P_{min}}{P_i - P_{min}}\right) \cdot KVSTRvalue\right)\right] \quad \text{.....(6.2)}$$

The factor is the actual multiplier to the permeability at a specific time and location. A value of the table factor is generated based on the location/rock type, pressure and water saturation. P, P_{min} and P_i is the current, historical minimum and initial pressures respectively.

Modeling of injection induced fractures is a challenging task. The following observations were made during history matching:

- The injectors generally have pressures of about 7000 psia, which is above minimum shear stress for the reservoir rock (above fracturing pressure). This is most likely the reason for the need to enhance permeability in these areas, and in that way simulate the development of fractures.
- The lower the permeability around the injectors, the longer the fracture length (requires an increased number of cells affected by KVSTR).
- Neighbouring injectors will create high pressure / high permeability bridges connecting them (as shown in the flow dynamics analysis given in chapter 5.2).

PSim uses the MODR keyword to modify properties in certain arrays around a well on a specific date. To invoke permeability versus stress hysteresis, the KVSTR keyword is used with MODR. **Table 5.1** shows values inserted in the MODR section in the Existing Wells worksheet in SplicerXL (in this study).

Table 5.1 MODR section in SplicerXL to control KVSTR keyword. MODR is used in SplicerXL to control the input variables in the KVSTR keyword. It defines what property array to change, which cells that are to be modified, the KVSTR value and which completion to target with these changes.

MODR			
Array	Range	Mod	Completion
KVSTR	1IJ	=2	

KVSTR is the property array name that will be modified. 1IJ is the range of cells that will be modified. In this study the original cell and one cell in the range of (I-1) to (I+1) and (J-1) to (J+1) will be changed. This will amount to 9 cells with modifications in the IJ plane for each original cell. Mod is set to be =2. This means that the KVSTRvalue equals 2. The completion is the name of the completion for the well of interest, defined in the Well Completions worksheet.

An example of the change in permeability around perforated (red dashed) cells is given for B-17 BT2 when it is converted to a water injector. This is shown in **Fig. 5.13**.

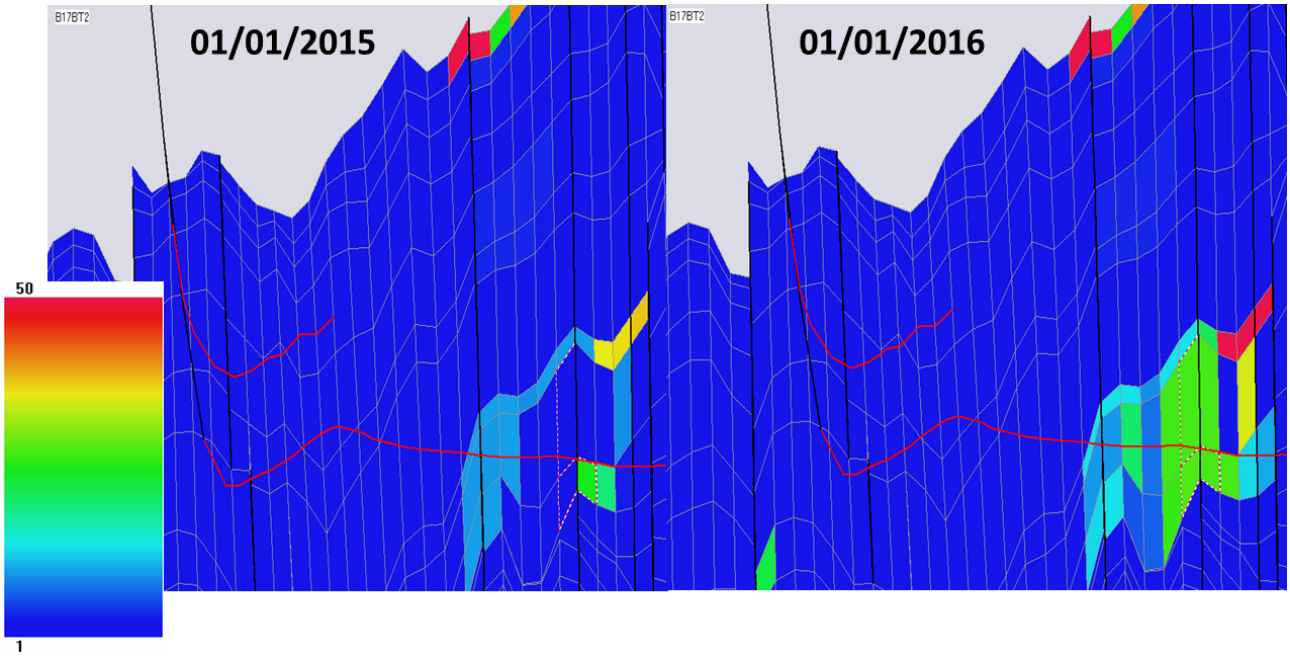

Fig. 5.13 Permeability around B-17 BT2 before and after conversion to water injector. *The picture shows a cross section of the B-17 BT2 wellbore in the JK-plane. The permeability before conversion is shown to the left, while the permeability around B-17 BT2 after conversion is to the right. The permeability change around the perforated cells according to what is stated in the MODR section in SplicerXL. The cells affected by the KVSTR keyword initially have blue color. After conversion they become green because of an increase in permeability. The scale is in [mD].*

6 Injector Performance Analysis

In order to maximize the reservoir recovery potential of Eldfisk, it is important to investigate influencing factors on efficient water injection. This chapter presents a study performed to evaluate the performance of existing and future injectors.

6.1 Sensitivity Runs

To estimate the value of the individual injectors, the following case study was done for the existing injectors:

- A sensitivity analysis was performed, where one of the existing injectors was SI at 01/01/2015 while the others were according to the Base Case. The loss in ultimate oil production was used as an estimate of the value of the injector.
- The future injectors were kept in the model according to the Base Case.

A similar study was done for the future injectors:

- One injector was SI on its start-up date, per run.
- The existing injectors were according to the Base Case.

6.2 Simulation Results and Discussion

The results of the sensitivity analysis are summarized in **Table 6.1**. The cumulative water injected from 2015 until well SI date is also included. A comparison of the results in 2025 for existing injectors is given in **Table 6.2**, which indicates their short-term well value.

The value of cumulative water injected divided by the loss in ultimate oil production (well value) was used to estimate the injectors performance. In practice, this gives an estimate of how much water that needs to be injected to produce one STB of oil. The lower these values are (would be 1 STB/STB in an ideal situation), the better the performance of the injector. These estimates of injector performance are also included in Table 6.1 and Table 6.2.

A plot of the injectors' overall performance by 2050 and 2025, is given in **Fig. 6.1** and **Fig. 6.2**. The results of the value runs of existing and future injectors will be discussed in chapter 6.2.1 and 6.2.2 respectively.

Table 6.1 Injector performance by 2050. The table shows the loss in ultimate oil production realtive to the Base Case in 2050, when one of the existing or future injectors are SI. This is used as an estimate of well value. The table also shows the cumulative injected water and an estimate of the performance of each injector (how much water that needs to be injected to get 1 STB of oil).

Well SI	Cum Injected [MMSTB]	Well Value [MMSTB]	Injector performance [STB/STB]
A4AT2I	61	0,3	214
A5BT2I	154	7,4	21
A7BT2I	180	1,3	144
A13BT2I	51	1,2	43
B8BI	32	3,9	8
B15AI	32	4,4	7
B20BI	40	5,9	7
B22I	40	6,1	7
S-17W	55	11,2	5
NFBE-55W	59	5,5	11
N5AE-32W	24	3,3	7
NFBT-31W	41	5,9	7
N5BE-51W	26	6,0	4
N5AE-02W	8	0,6	14
N5BT-01W	110	4,9	22
N5BE-54W	78	3,9	20
N5BE-81W	47	3,8	12
NFBE-88W	37	5,1	7

Table 6.2 Injector performance by 2025. The table shows the loss in ultimate oil production realtive to the Base Case in 2025, when one of the existing injectors are SI. This is used as an estimate of well value. The table also shows the cumulative injected water and an estimate of the performance of each injector.

Well SI	Cum Injected [MMSTB]	Well Value [MMSTB]	Injector performance [STB/STB]
A4AT2I	42	1,9	23
A5BT2I	68	4,5	15
A7BT2I	58	3,2	18
A13BT2I	35	2,2	16
B8BI	32	4,9	7
B15AI	32	5,5	6
B20BI	40	7,9	5
B22I	40	6,4	6

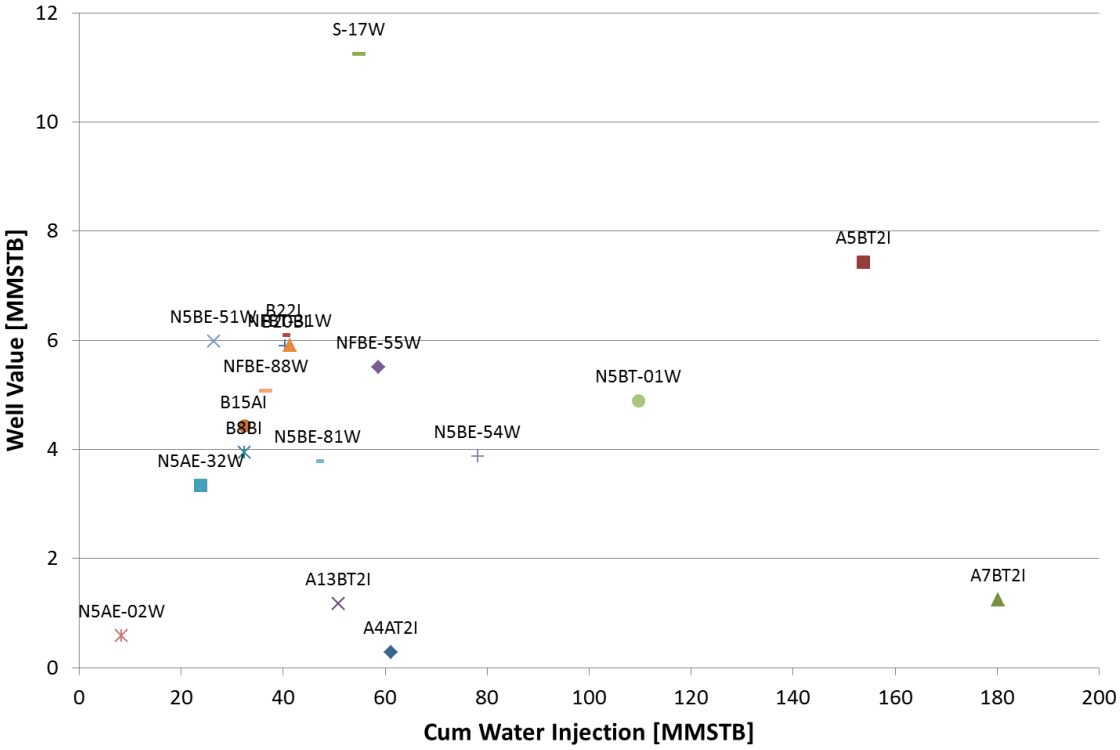

Fig. 6.1 Overall injector performance by 2050. *The plot shows the relationship between the cumulative water injected and the well value by 2050.*

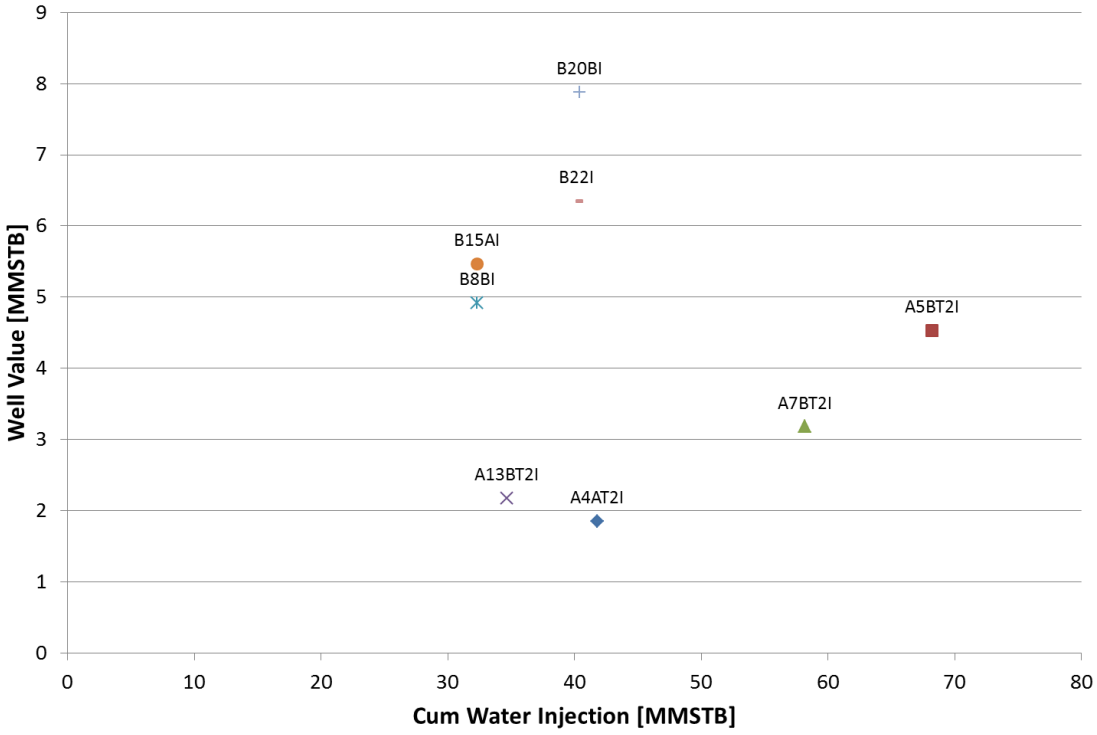

Fig. 6.2 Overall injector performance by 2025. *The plot shows the relationship between the cumulative water injected and well value by 2025.*

6.2.1 Existing Injectors

This chapter evaluates the performance of existing injectors. There is a discussion about both low and high performance injectors.

The injectors performance is evaluated until 01/01/2050. Therefore, it would require a redrill to use the existing injectors locations since the Alpha and Bravo platforms will be SI in 2025 and 2022, respectively. As an economic criteria for justifying a redrill, injectors should have a value higher than 2 MMSTB in the sensitivity runs (Ozoglu-Topdemir, 2014). Therefore, injectors with value less than 2 MMSTB will be referred to as having low performance in this study.

6.2.1.1 Low Performance Injectors

One observation from Table 6.1 and Table 6.2 is that all Alpha injectors, except A-5, lose its value with time. Based on the flow dynamics analysis it can be argued that this is a result of the highways becoming very dominant in their injection pattern with time. This will cause little change in streamlines and the situation were the injectors only are supporting areas that have already been swept. It can also be argued that, in the model, future producers will have a direct communication to these Alpha injectors. This will cause high WC, which is detrimental on production. Therefore, redrilling of the Alpha wells should be planned accordingly.

It was decided to perform further investigation of A-4 because of its low well value and performance. From the WAF output file (generated from streamline simulation) it is possible to find well allocation factor with time for the different injectors. Visual inspection shows that A-4 gives most of its support to A-1 T2, A-28 AT2, NFAE-88 and N5AE-43. All these wells have high WC in the Base Case. When A-4 is SI the WC is reduced in the producers, while the oil rate is not reduced by as much. As an example, the change in oil rate and WC in A-1 T2 is given in **Fig. 6.3**. This figure indicates that a large amount of the water injected by A-4 is cycled in the producers, and that the other injectors take over the support when the well is SI.

Fig. 6.4 can help explain the communication between the injectors on Alpha. Investigation of reservoir pressure distribution reveals that there are large pressure differences within this

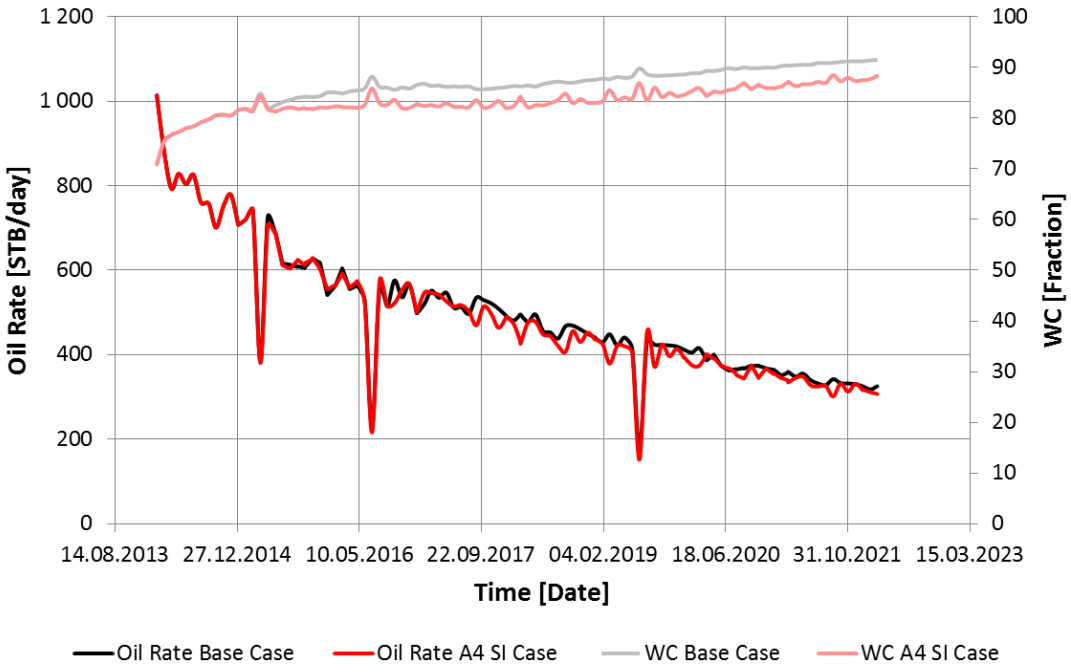

Fig. 6.3 A-4 SI effect on A-1 T2 oil production. *The graph shows the change in oil rate and WC in A-1 T2 as a result of A-4 SI. What can be observed is that the WC is reduced, while the oil rate do not change much. This is an indication that A-4 injection water is cycled in the producers, and that the other injectors make up for the lack in pressure support due to A-4 SI.*

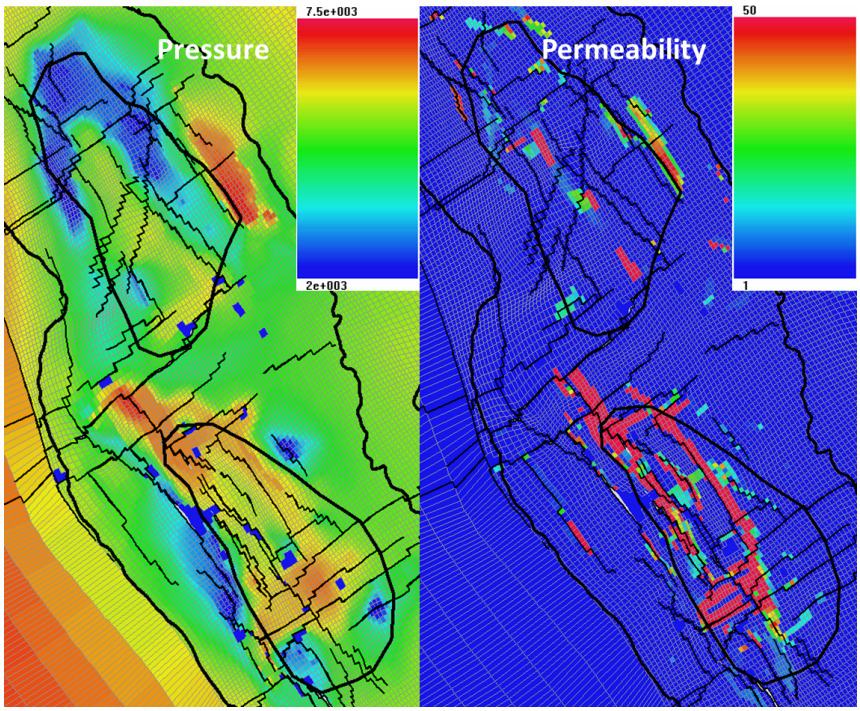

Fig. 6.4 Pressure and permeability indicating communication between Alpha injectors. *The picture shows the pressure and permeability in the Tor Fm (layer 9) in 01/01/2013 in the Base Case. The maximum and minimum values of the scales are chosen to visualize the pressure and permeability distribution more clearly. The actual values of the cells with color equal to maximum or minimum of the scale can be higher or lower. The pressure scale is in psia and the permeability scale is in mD.*

structure. Comparing the location of high pressures to the location of high permeability indicates that the water injection pattern in Alpha is governed by highways. Therefore pressure is high in and around these areas, while areas outside have lower pressures. The other injectors will reach the producers mainly supported by A-4 through these highways when this well is SI. This is also visible from streamline simulation, as shown in **Fig. 6.5**. The figure shows that the streamlines from A-5, A-7 and A-13 are replacing A-4 streamlines.

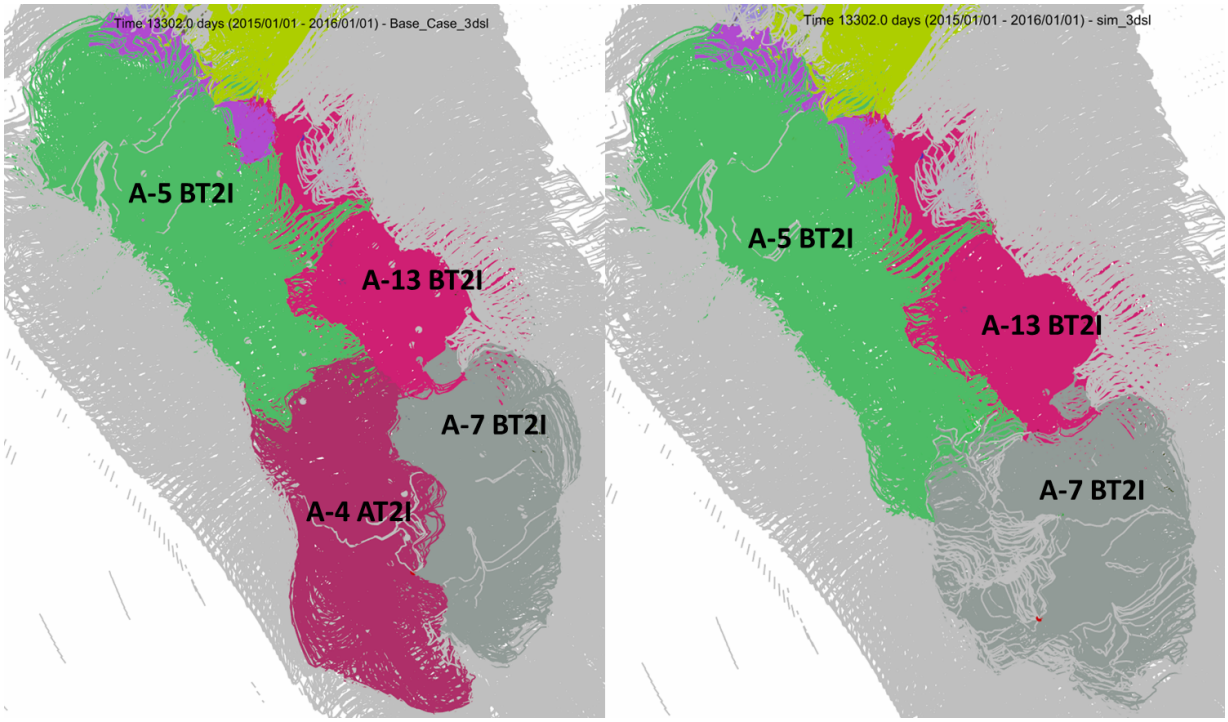

Fig. 6.5 Change in streamlines when A-4 is SI. *The picture shows the change in streamlines one year after A-4 is SI (01/01/2016). It becomes visible that the streamlines from A-5 and A-7 extends into the area where A-4 used to be. The Base Case is displayed to the left.*

6.2.1.2 High Performance Injectors

A-5 is the only dedicated Ekofisk injector in the Alpha structure. It is also supporting Tor with cross flow through fractures, like explained in the flow dynamics analysis. As a result this injector is crucial for Ekofisk support, as shown in **Fig. 6.6**.

A ConocoPhillips developed tool named Run Extract 3.0 makes it is possible to compare production from simulation runs. With the help of this tool and streamline simulation it becomes visible that this injector sweeps a large area and therefore supports many producers. **Fig. 6.7** shows that many wells lose production and **Fig. 6.8** shows that many of the wells produce less water when A-5 is SI. The latter is an indication of water cycling, but A-5 still has high value with regards to oil production.

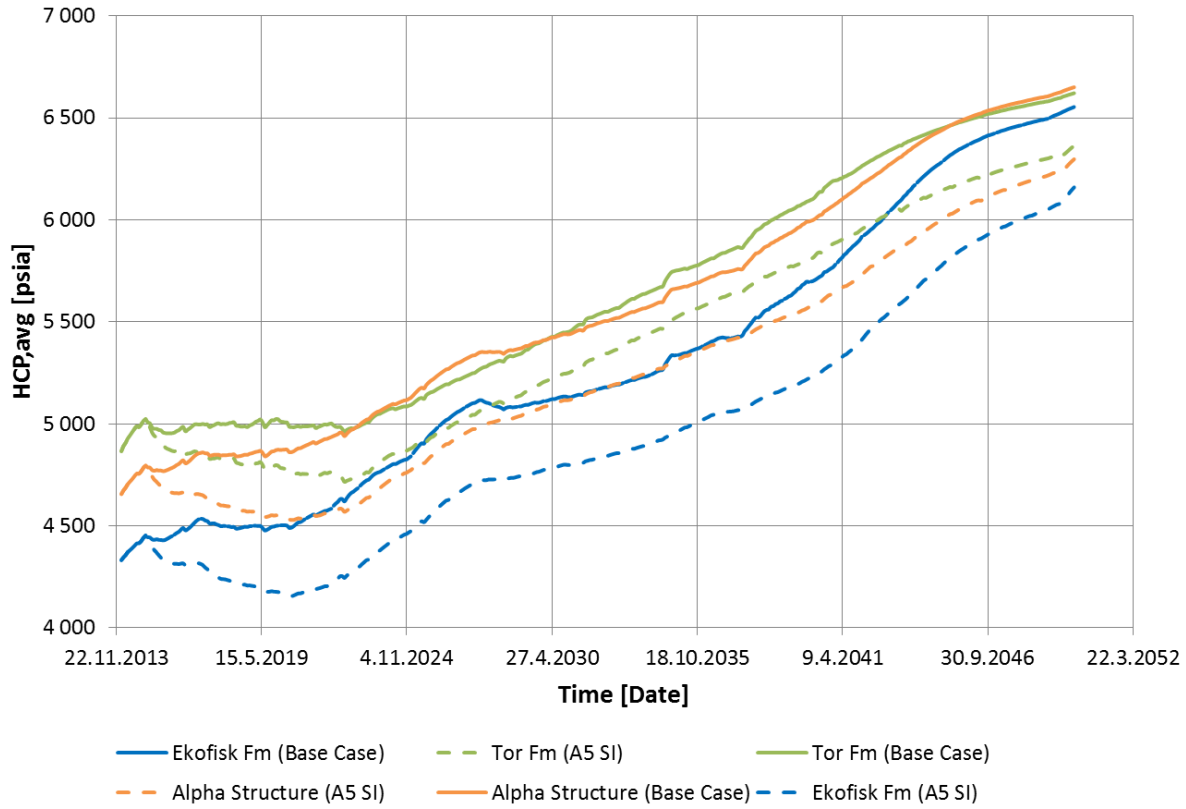

Fig. 6.6 Pressure loss when A-5 is SI. *The graph shows the pressure loss when A-5 is SI in 2015. All of the pressure profiles are in the Alpha structure (Ekofisk Fm, Tor Fm and the whole Alpha structure). It can be observed that the pressure loss in the Ekofisk Fm is severe when A-5 is SI.*

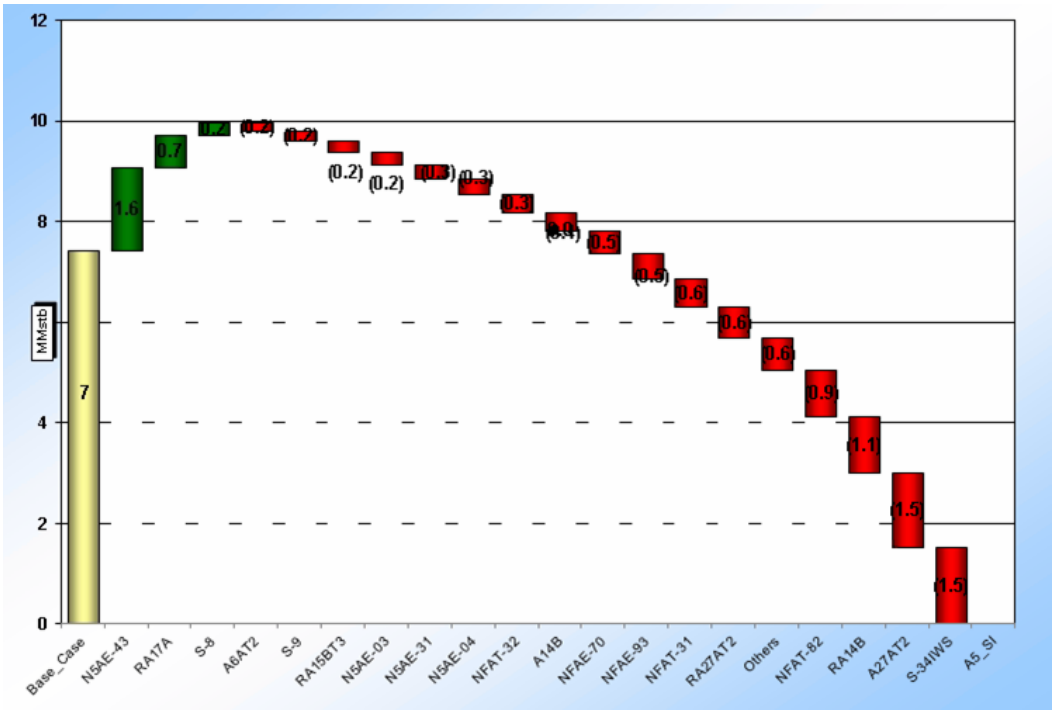

Fig. 6.7 Change in oil production when A-5 is SI. *The picture shows the wells that are the most affected by A-5 SI (change in oil production > 0.2 MMSTB), and their loss or gain in oil production. It becomes visible that A-5 supports many producers. The graph is generated by Run Extract 3.0.*

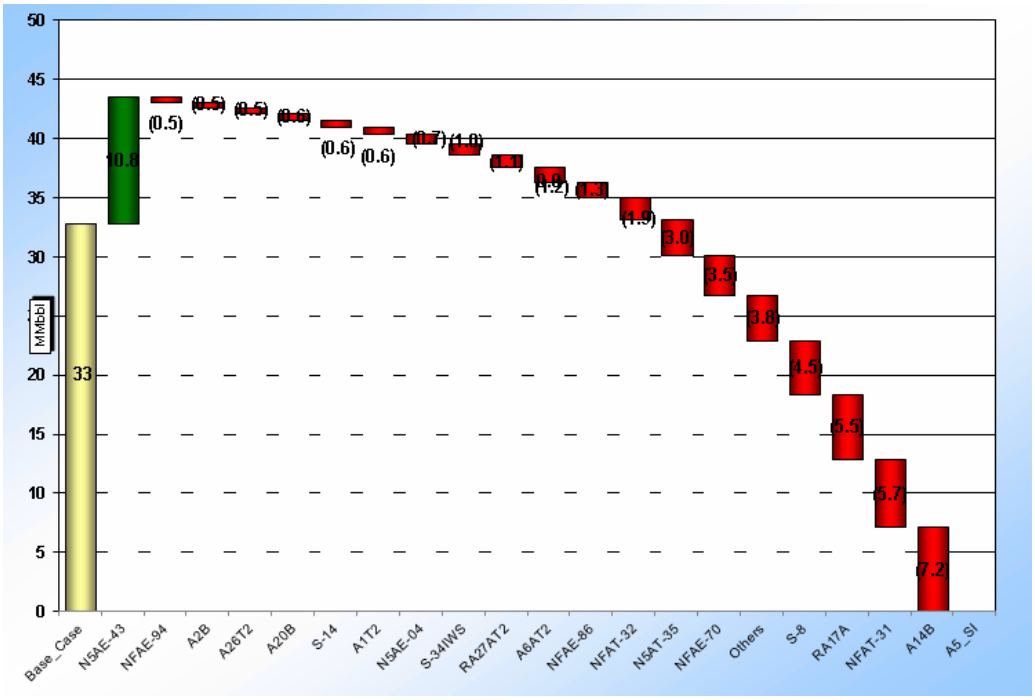

Fig. 6.8 Change in water production when A-5 is SI. *The picture shows the wells that are the most affected in regards to water production by A-5 SI. This shows that many of the wells produce less water when A-5 is SI, which is an indication of water cycling.*

Fig. 6.9 shows the change in streamlines one year after A-5 is SI. It is visible that the other injectors are not capable to cover the same area as A-5 despite of the highways connecting them in the Tor Fm.

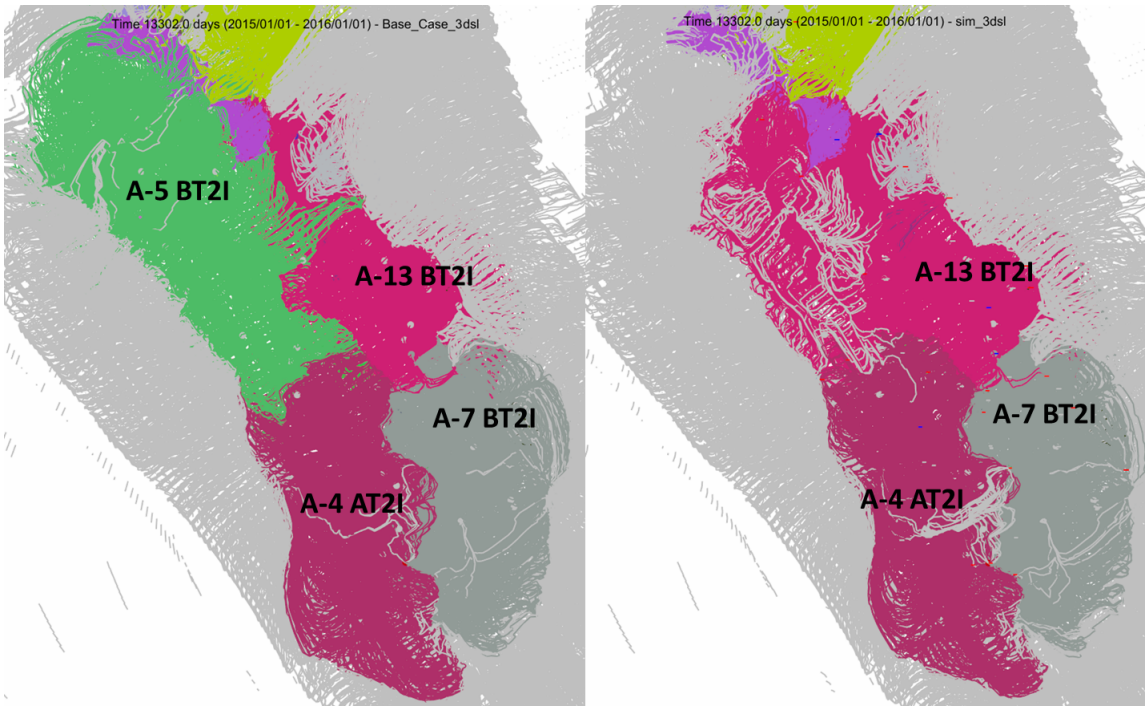

Fig. 6.9 Change in streamlines when A-5 is SI. *The picture shows the change in streamlines one year after A-5 is SI (01/01/2016). It becomes visible that the other Alpha injectors are not capable to cover the same area as A-5. The Base Case is to the left.*

Table 6.1 showed that the loss in ultimate oil production is higher when the Bravo wells are SI (except for A-5). Investigation of field pressure shows that the pressure loss is higher in the value runs of Bravo injectors. A comparison of A-4 (low efficiency) and B-20 (high efficiency) was made to investigate this further. B-20 will be SI in 01/01/2022 in the Base Case, which means that the time of interest is from 01/01/2015 until 01/01/2022. By year 2022, it is evident that the overall pressure loss in the field is higher in the B-20 SI sensitivity run. This is illustrated in **Fig. 6.10**. Since Eldfisk is a mature oil field, pressure support is crucial for oil production. Therefore this agrees with the estimation of a higher well value for B-20, compared to A-4.

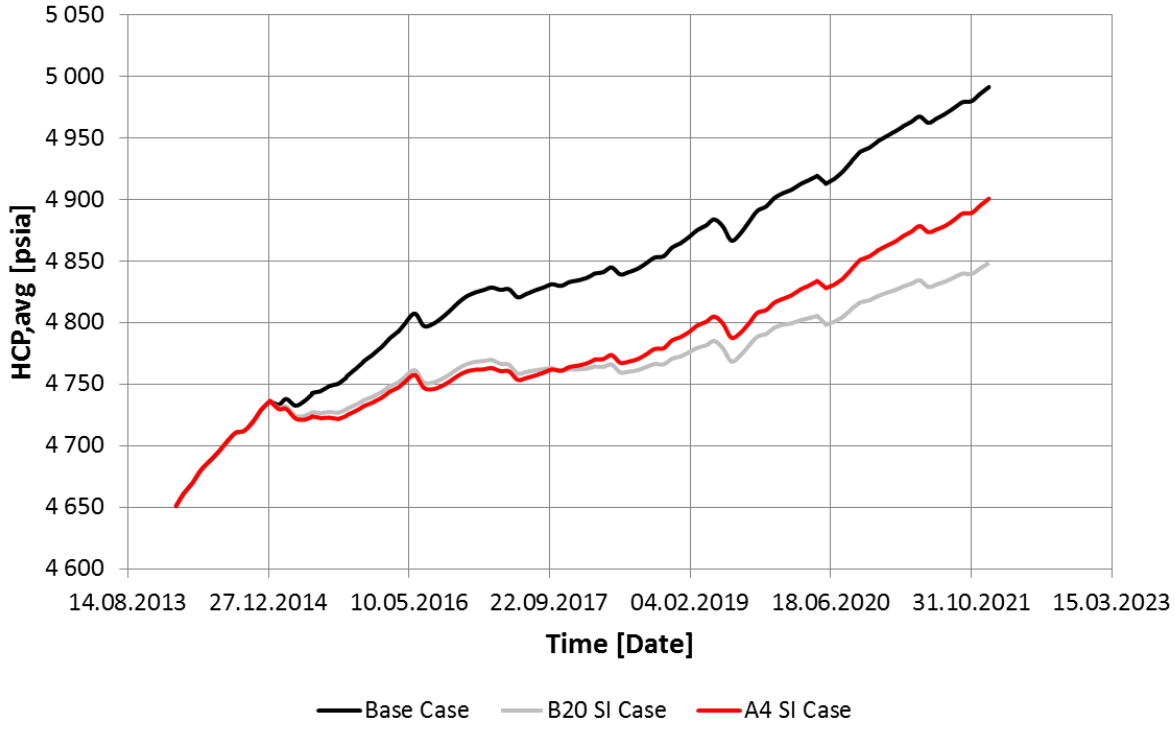

Fig. 6.10 Comparison of loss in field pressure when A-4 and B-20 are SI. *The graph shows the pressure profile in the Base Case, B-20 SI case and A-4 SI case. The loss in pressure is more severe when B-20 is SI, compared to A-4. This agrees with the observation of a more severe oil production loss when B-20 is SI.*

Both the pressure and permeability in Fig. 6.4 showed that the injection wells in Bravo are not as connected through highways as the ones in Alpha. Investigation of the change in streamlines in the Bravo structure as a result of B-20 SI, shows that the other Bravo injectors are not compensating for the loss in pressure support in the same way as when A-4 is SI (**Fig. 6.11**). This agrees with the higher value of B-20 relative to A-4. The aquifer compensates for the loss of B-20, but this is not as strong as the support coming from water injection.

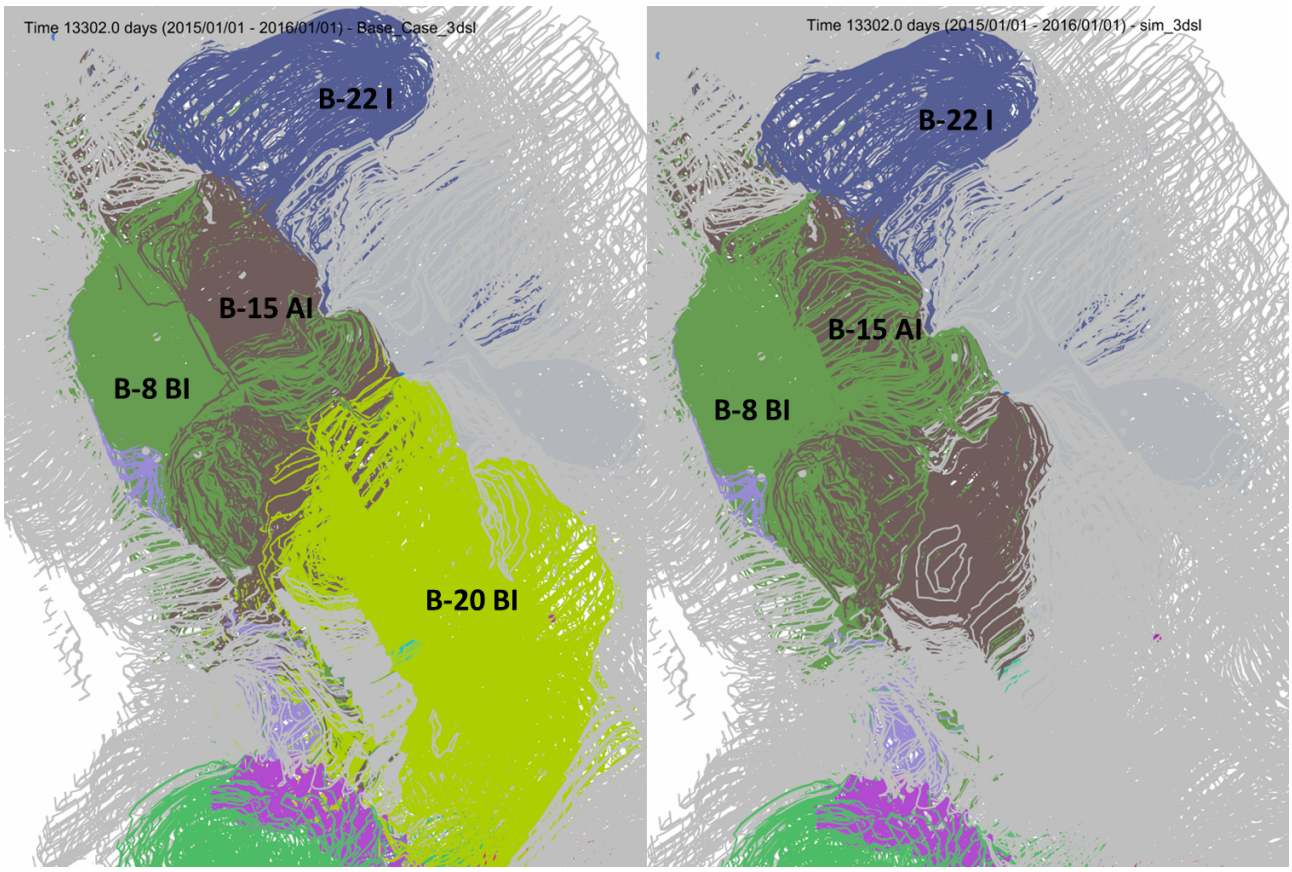

Fig. 6.11 Change in streamlines when B-20 is SI. *The picture shows the change in streamlines one year after B-20 is SI (01/01/2016). It becomes visible that the other Bravo injectors are not able to compensate for the loss in pressure support in the same way as the injectors on Alpha. The Base Case is displayed to the left. The light grey color is representing the aquifer.*

This observation is supported by comparing BHP and WI rate of A-4 and B-20 in the Base Case. It becomes visible that the BHP of A-4 is higher, while the rate is lower (**Fig. 6.12** and **Fig. 6.13**). In the analysis of reservoir flow dynamics it was concluded that the water injection pattern in Alpha is governed by highways. After a long time of injection it becomes problematic to inject into these highways, as can be explained by their high pressures. This can cause the situation that appears when comparing B-20 and A-4, were it is more difficult for A-4 to inject.

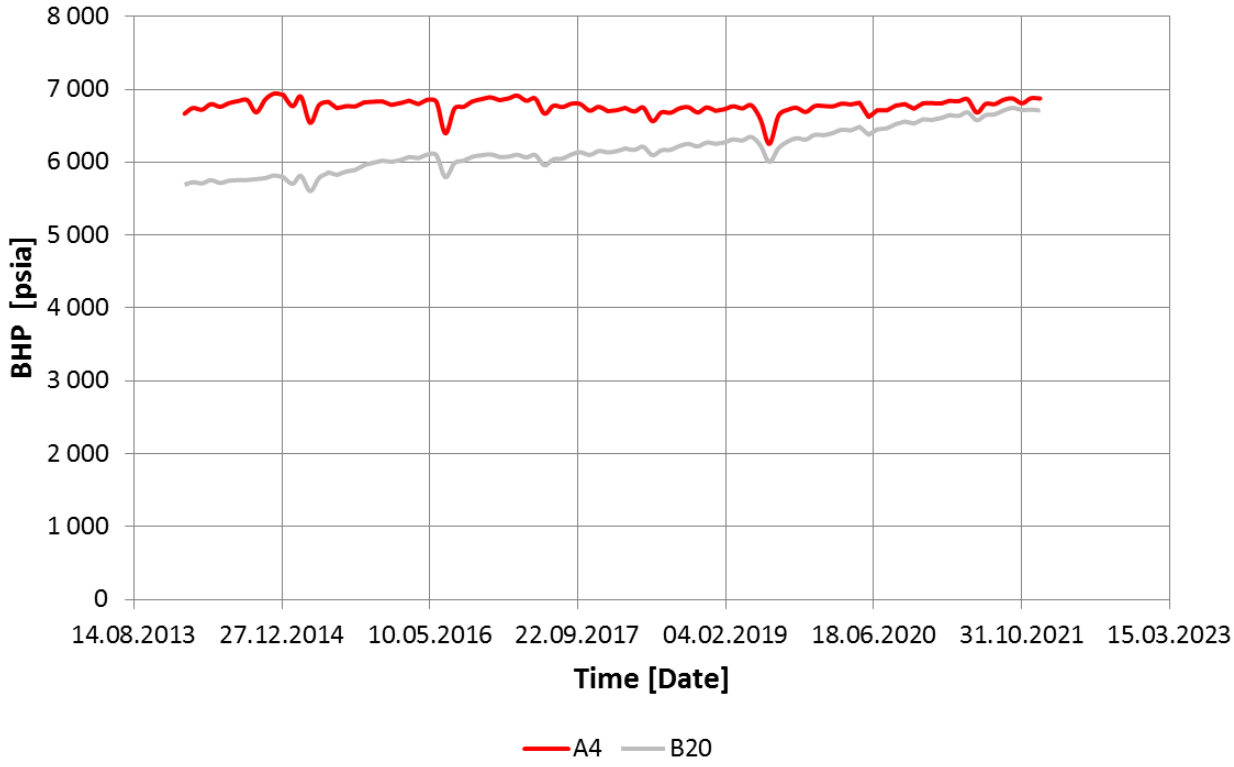

Fig. 6.12 BHP comparison of A-4 and B-20. *The graph shows that A-4 has higher BHP than B-20. This is due to the high pressure inside the highways in the Alpha structure.*

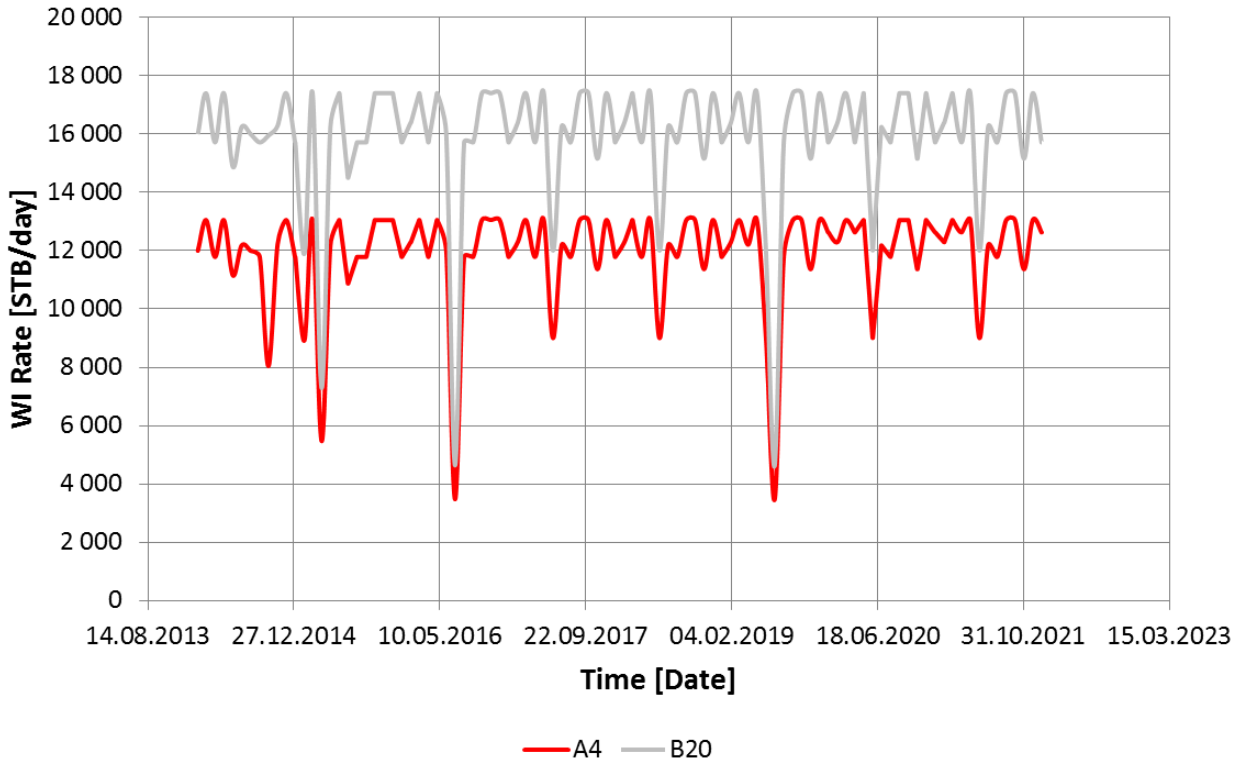

Fig. 6.13 Water injection rate comparison of A-4 and B-20. *Due to the high pressure in the highways in Alpha, A-4 has lower WI rate compared to B-20.*

Table 6.3 shows the percentage loss in field cumulative WI volume in the value runs compared to the Base Case. High well value should result in a significant loss in pressure support in the value runs, and therefore a high percentage loss in WI. In year 2025, all the existing wells have a relatively high well value, and therefore they all contribute with valuable pressure support. By 2050, the future injectors have compensated in areas that had a loss in pressure support when an existing injector was SI. As a result the percentage loss in WI is reduced. Table 6.3 also shows that the loss in WI is more severe when a Bravo injector is SI, which is in agreement with their high performance.

Table 6.3 Percentage loss in field cumulative WI when an existing injector is SI. The table shows values in 2025 and 2050. The loss is less severe in 2050 because the future injectors have compensated in areas that still had a loss in pressure support in 2025.

Well Name	2025 Loss in WI [%]	2050 Loss in WI [%]
A4AT2I	74	28
A5BT2I	83	26
A7BT2I	76	17
A13BT2I	83	39
B8BI	87	66
B15AI	87	66
B20BI	88	69
B22I	91	65

6.2.2 Future Injectors

The well location and completion constraints (rate limit, BHP limit, THP specifications and PI multiplier) of future injectors in Eldfisk are initially developed by the Field Management Team. They are based on the reservoir model, field historic data and field targets. Their values are adjusted to create a balance between the injectors (Jones, 2014). In the next step of planning the injectors, the Well Planning Team updates the specifications of the wells based on a more comprehensive study. The well length and start date (well schedule) is whats most commonly changed. The wells are also assigned a slot on the rig, and with that, a different name (Jones, 2014). Out of the future injectors in the Base Case, S-17 W has been through this process.

The above mentioned process in planning the injectors can of course make changes to the prediction of future performance of the reservoir, but there is another more significant issue with introducing injectors to the model. Compared to the existing injectors, the future wells are not associated with the development of highways. The KVSTR keyword is only used along the wellpath of the injectors in the prediction runs. It is not used to develop fractures and open up faults as the pressure increases around the injectors. This is only done as part of the history matching process. Therefore the existing injectors have high injection potential compared to the future injectors, due to the highways they are surrounded by in the model.

The performance analysis shows that future injectors that replace the existing Bravo injectors all have a relatively high well value. These are inside, or close to, already developed highways. Another observation is that some of the future injectors (f.ex. N5AE-02W) are placed in areas that are tight (close to the flanks). When a chalk formation has low permeability it becomes more brittle, therefore it is likely that these will fracture the formation and develop highways as well. This will increase their injection potential and might increase their well value.

Based on the uncertainty in estimation of well values for future injectors, this data should be treated as a qualitative measure.

6.3 Summary of Observations

As a summary, the most important findings of the injector performance analysis were:

- Highways play a dominant role in fluid flow in Eldfisk, affecting the injectors' performance.
- Existing Alpha injectors (except A-5) have lower value compared to Bravo injectors.
- Based on the fracture analysis this is an indication that the Alpha injectors are communicating through highways: when one injector is SI the others compensate for the lack in pressure support. This effect is less dominant in Bravo.
- Development of highways surrounding future injectors is not included in the model. As a result there is an uncertainty in their well value and injection potential.

7 Producer Conversions

This chapter investigates potential locations for injection through conversion of existing and future producers. The analysis was conducted with the use of reservoir and streamline simulation.

7.1 Sensitivity Runs

To convert a well, a new event was added in the Existing Wells worksheet in SplicerXL. The converted well was completed with well constraint values, which are represented in **Table 7.1**.

Table 7.1 Well constraint values for producer conversions. The BHP constraint is close to the existing injectors BHP, which is estimated to be the maximum pressure allowed to safely inject and not fracture the overburden. The rate is set at a high value, such that the BHP constraint will be the limiting factor. The THP limit and table number is based on historic data.

	Existing Wells	Future Wells
Rate [BBL/day]	25000	25000
BHP [psia]	7200	7200
THP limit [psia]	3800	7000
THP Table #	-50	-44

SPARK was programmed to update the following parameters in SplicerXL: conversion date, well number and MOD (KVSTRvalue). From a lookup table, SplicerXL could locate the appropriate well name from the well number. The lookup table is included in Appendix B (**Table B.5**). In addition, KVSTR was entered in the MODR section as explained in chapter 5.3 about the KVSTR keyword.

The producers have a well life constraint in the Base Case. When a well was converted from a producer to an injector this well life constraint was taken out to be able to investigate the well locations complete potential for successful future WI. The existing producers were converted on 01/01/2015, while the future producers were converted on their start-up date.

The sensitivity study converted all of the existing and future producers to injectors. The post-processor in SPARK was used to find the ultimate oil production (UOP) in each of the cases. From this data it was possible to calculate the difference in UOP compared to the Base Case, in order to reveal the viable cases. The lower limit for the difference in UOP was set to be 2 MMSTB to allow comparison to injector performance analysis. However, it should be noted that a conversion can become economically viable at much lower incremental recovery.

7.2 Simulation Results and Discussion

This chapter presents the results and analysis of the existing and future producer conversions.

7.2.1 Existing Producer Conversions

Conversion of existing producers to injectors yielded both successful and unsuccessful results, both of which will be presented in this chapter.

7.2.1.1 Results

The results of the existing producer conversions are given in **Table B.6** in Appendix B. The difference in UOP relative to the Base Case is shown in **Fig. 7.1.** A positive value means that the conversion run gave a higher UOP. Out of the conversions, three wells have a value higher than 2 MMSTB (B-2 BT3, B-17 BT2 and B-21 T4). These will be discussed in chapter 7.2.1.2, while chapter 7.2.1.3 will present an analysis of unsuccessful conversion runs.

A comparison of the well value as producer and as injector is given in **Table 7.2** and **Table 7.3**. The value of the producers where calculated in the same way as for the injectors. The peach rows are the conversions with value greater than 2 MMSTB, while the green rows are conversions with a higher well value as an injector than as a producer. This was used to identify wells that perform better as injectors compared to producers, but still have a conversion value of less than 2 MMSTB. These wells do not rank high compared to existing and future injectors, but conversions are expected to have lower cost and can therefore be justified at lower incremental recovery as mentioned previously. The amount of wells that have zero or actually negative well value as producers shows that there is a lot of interference between producers on Eldfisk. The observation that many of the wells do better as injectors (26% of the Alpha and 56% of the Bravo producers), indicates a need to increase the pressure support by a higher injector-producer ratio.

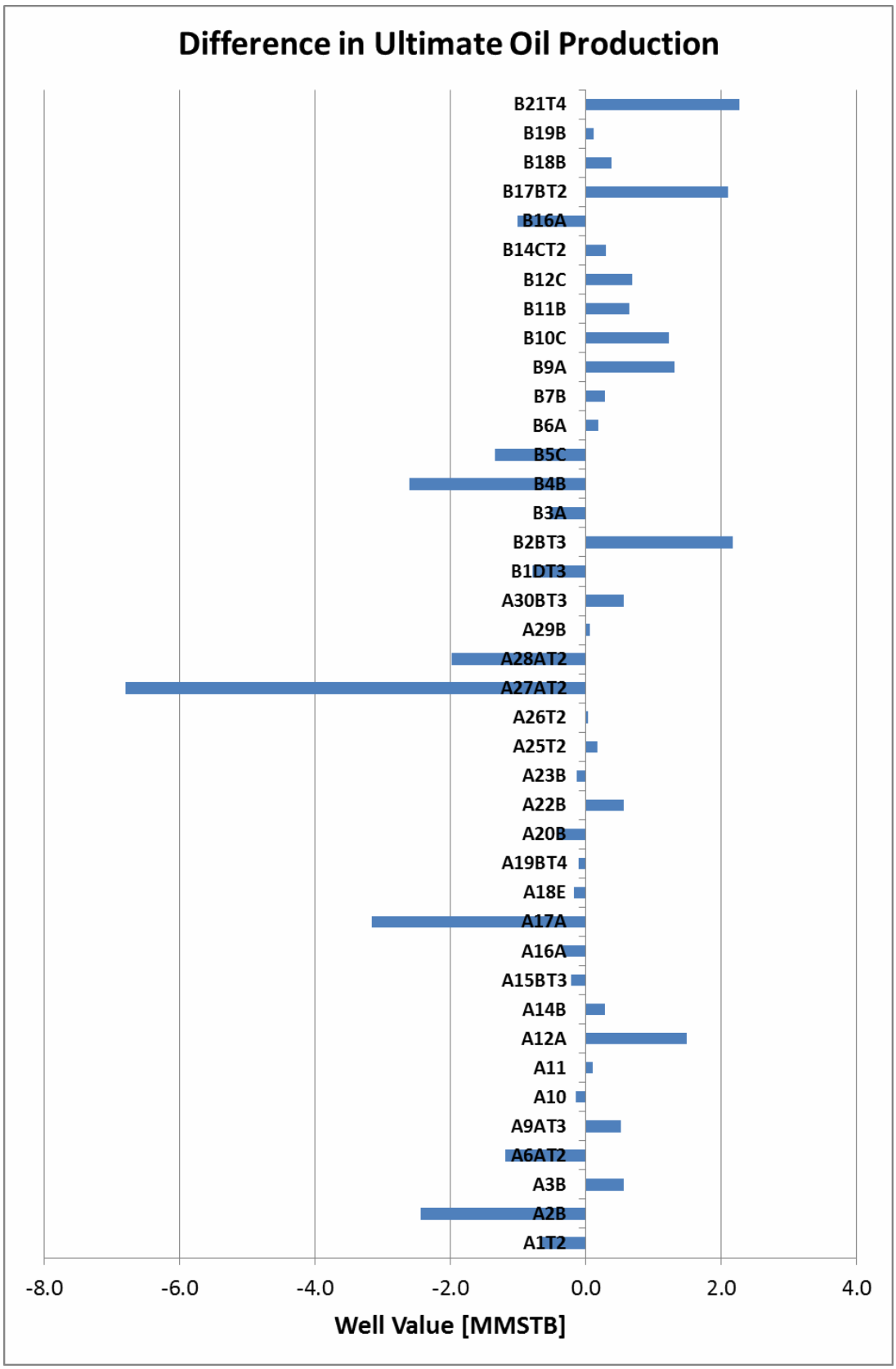

Fig. 7.1 Value of existing producer conversions. *The figure shows the difference in oil production in 01/01/2050 when the individual wells are converted. The lower limit in difference in UOP is 2 MMSTB for the conversion run to be considered as successful. Therefore there are three viable conversions according to this analysis: B-2 BT3, B-17 BT2 and B-21 T4.*

Table 7.2 Alpha producers well value and their value as injectors. The well value is closely related to the well life. The well life of injectors is until 01/01/2050 (or until pressure is too high to inject), and the well life of producers is listed in the table. The green rows are wells that perform better as injecetors than as producers.

Well Name	Value as Producer [MMSTB]	Well Life as Producer [months]	Value as Injector [MMSTB]
A1T2	0.4	98	-0.7
A2B	1.2	99	-2.4
A3B	0.1	50	0.6
A6AT2	0.5	77	-1.2
A9AT3	0	0	0.5
A10	0.1	90	-0.2
A11	0	0	0.1
A12A	-0.2	118	1.5
A14B	0.3	130	0.3
A15BT3	-0.2	160	-0.2
A16A	0.4	36	-0.3
A17A	0	0	-3.2
A18E	0.7	146	-0.2
A19BT4	0.3	50	-0.1
A20B	0.5	112	-0.4
A22B	0	7	0.6
A23B	0	139	-0.1
A25T2	0	0	0.2
A26T2	0.2	83	0
A27AT2	1.2	178	-6.8
A28AT2	0.1	25	-2
A29B	0	65	0.1
A30BT3	0	18	0.6

Table 7.3 Bravo producers well value and their value as injectors. The well value is closely related to the well life. The well life of injectors is until 01/01/2050 (or until pressure is too high to inject), and the well life of producers is listed in the table. The peach rows are the conversions with value greater than 2 MMSTB, while the green rows are wells that perform better as injecetors than as producers.

Well Name	Value as Producer [MMSTB]	Well Life as Producer [months]	Value as Injector [MMSTB]
B1DT3	1.1	84	-0.8
B2BT3	0	0	2.2
B3A	0	0	-0.5
B4B	0.7	85	-2.6
B5C	0	0	-1.3
B6A	0	0	0.2
B7B	0	0	0.3
B9A	0	0	1.3
B10C	-0.4	40	1.2
B11B	0	24	0.6
B12C	0	0	0.7
B14CT2	0.8	66	0.3
B16A	0.5	77	-1
B17BT2	0	12	2.1
B18B	0	0	0.4
B19B	-0.6	40	0.1
B21T4	-0.3	66	2.3

7.2.1.2 Successful Conversions

This chapter presents a study of successful producer conversions. The analysis found that these wells are in areas that do not have an injector in the schedule. Also, they are on the edge or inside pressure sinks and oil pockets. A discussion about injection potential in the saddle area and in the short term perspective is also included in this chapter.

B-21 T4

The location of B-21 T4 (hereafter called B-21) interferes with future producers in the model and therefore has a negative well value as a producer. The future producers perform better when B-21 is SI or converted to an injector, as can be seen by their increase in production in **Fig. 7.2** and **Fig. 7.3**. This can be explained by B-21 producing a lot of the injected water that could have been used to sweep areas of high S_o instead.

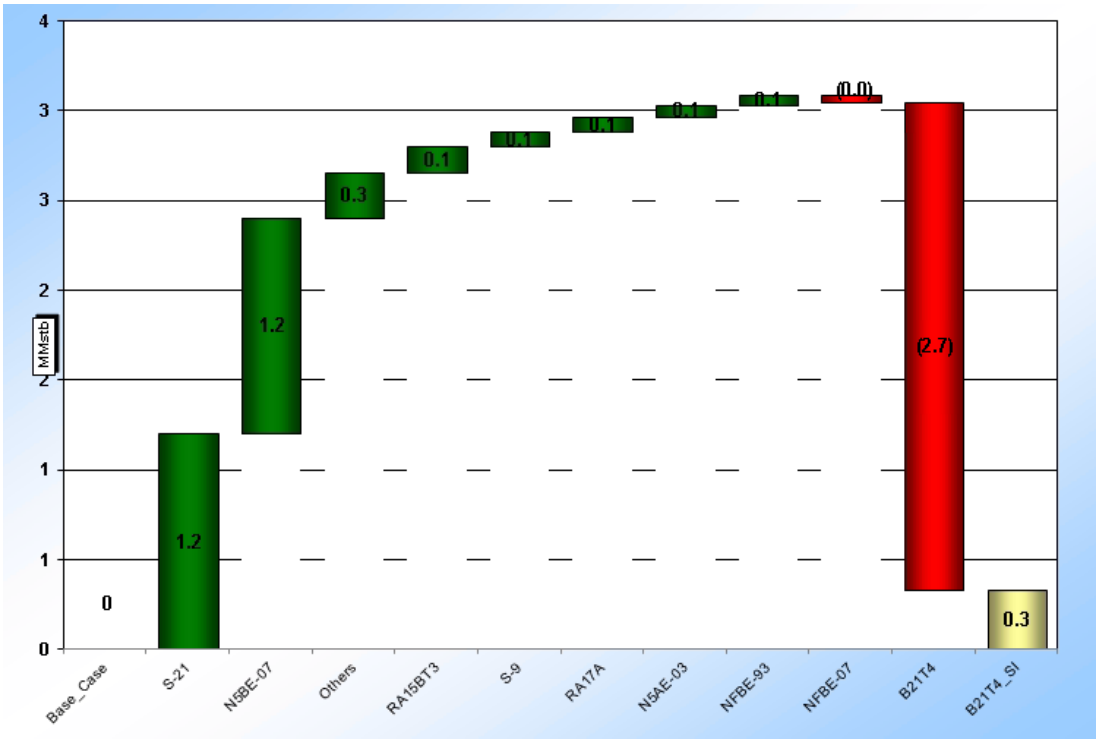

Fig. 7.2 The change in oil production when B-21 is SI. *It becomes visible that many wells have an increase in production when B-21 is SI. This can be the result of B-21 producing a lot of the injected water, which could be used to sweep areas of high oil saturation instead.*

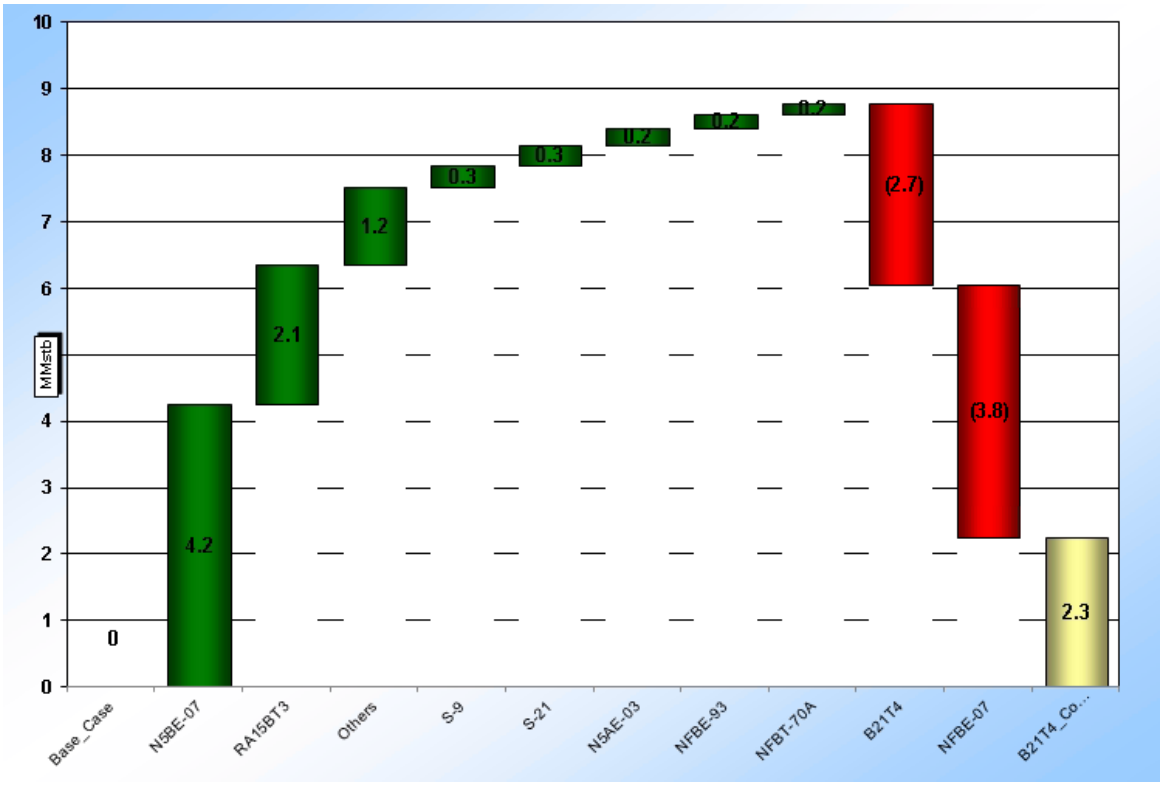

Fig. 7.3 The change in oil production when B-21 is converted to an injector. *Conversion of B-21 yields an even higher increase in oil production in surrounding producers. Now it gives support to the same wells, and other wells in the area. The loss in oil production in NFBE-07 is due to a water breakthrough (WC from an average of 40% to 90%).*

B-21 is in an area that does not have an injector in the schedule, and the pressure support from its injection results in an increase in oil production. From Fig. 7.3 it can be seen that B-21 gives support to the same wells that do better when it is SI, and other wells in the area. One example is that N5BE-07 has a 1,2 MMSTB increase in production when B-21 is SI, but an increase of 4,2 MMSTB when B-21 is converted to an injector.

As can be seen in **Fig. 7.4**, the well is at the edge of an oil pocket and inside a pressure sink in 2015.

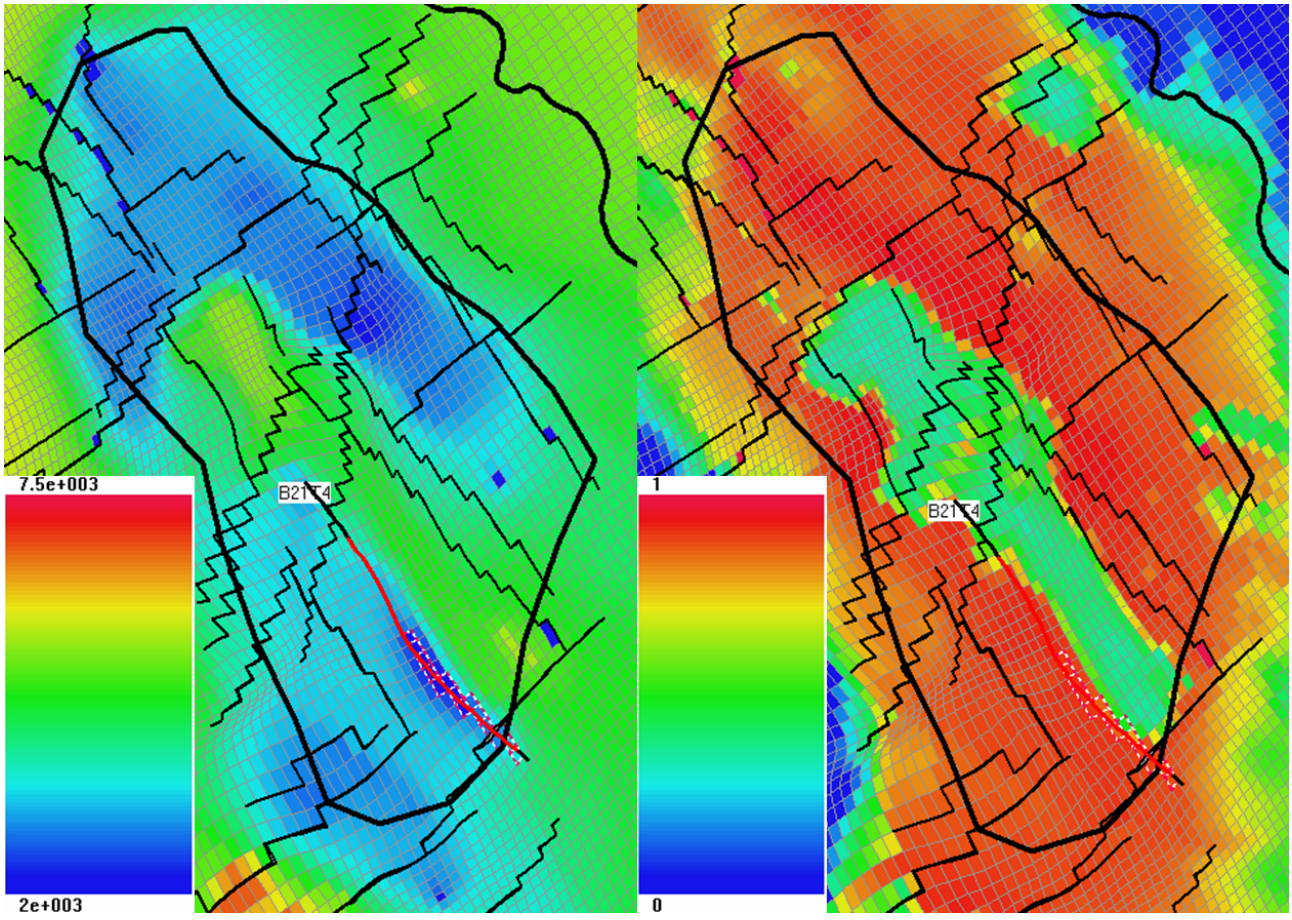

Fig. 7.4 Pressure and oil saturation around B-21 in 2015. *The pressure (to the left) and the oil saturation (to the right) in the Ekofisk Fm (layer 3) in 2015. It can be seen that the well is inside a pressure sink and at the edge of an oil pocket at start of injection. The pressure scale is in psia.*

B-17 BT2

B-17 BT2 (hereafter called B-17) is a good producer, but it is constrained by a well life limit of 12 months. The conversion run still shows that there is potential for injection in this area, and that this well would be a successful injector.

B-17 manages to change sweep as an injector. It covers a new area on top of Bravo, shown in **Fig. 7.5**. It also re-pressurizes a large area of the flanks (**Fig. 7.6**).

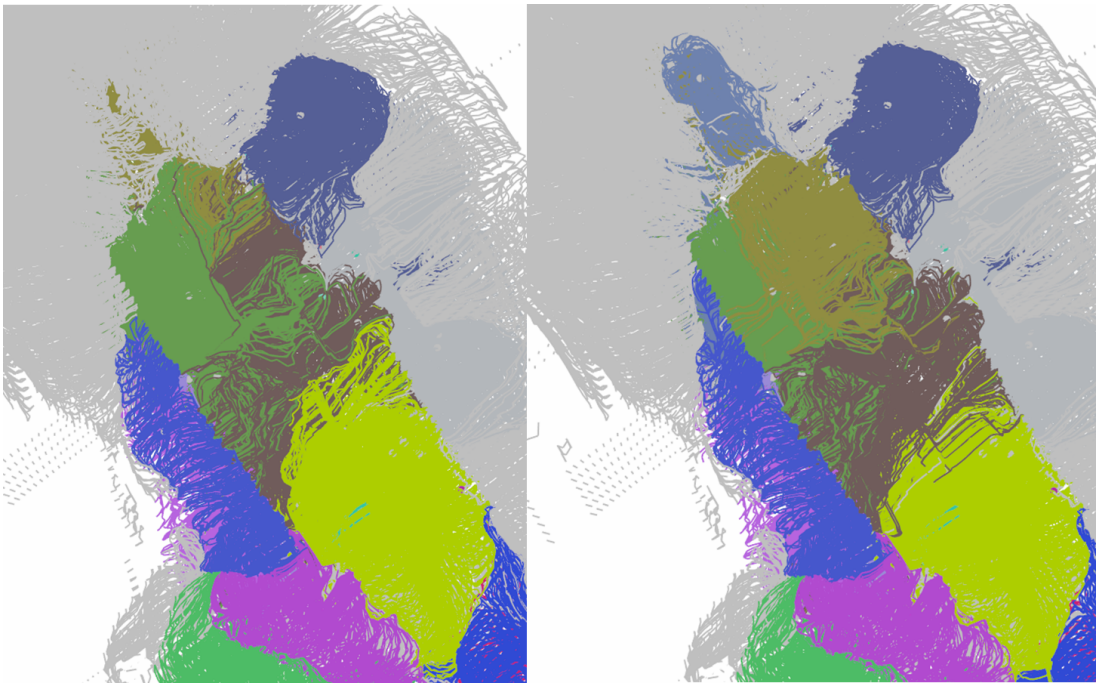

Fig. 7.5 Change in streamlines when B-17 is converted to a water injector. *Streamlines in 2022 shown in the Base Case (to the left) and B-17 conversion run (to the right). The injection from B-17 creates streamlines in a new area, which is an indication of change in sweep. This can be seen by comparing the upper left area in the Base Case to the conversion run.*

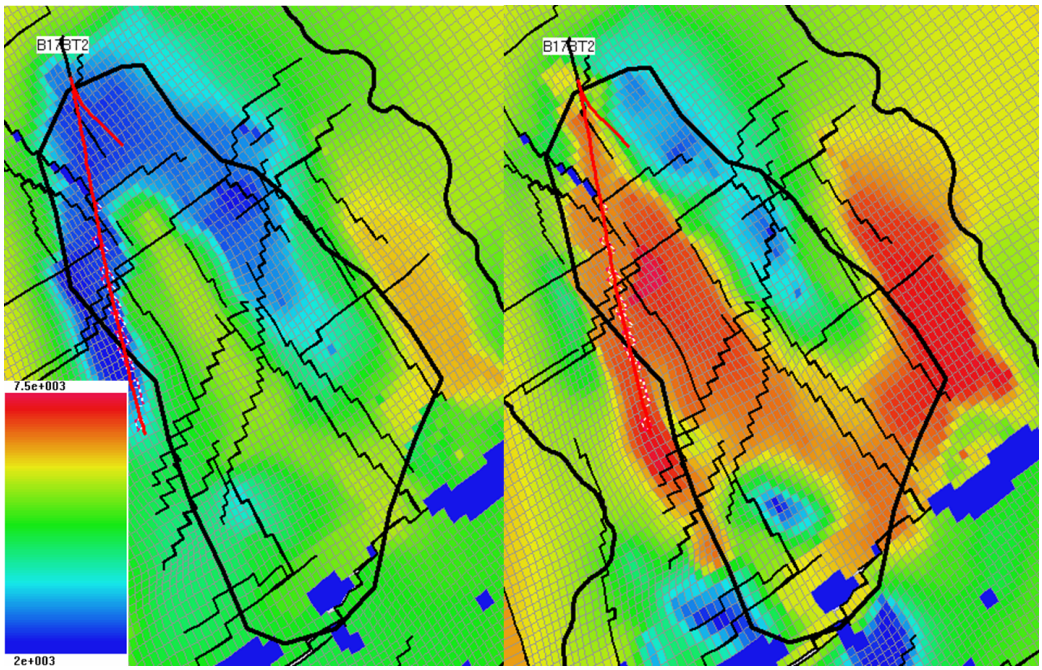

Fig. 7.6 Reservoir re-pressurization due to B-17 WI. *Pressure in the Tor Fm (layer 10) in 2015 to the left and 2022 to the right. B-17 has managed to repressurize zones that were pressure sinks (blue color) in 2015. The scale is in psia.*

Fig. 7.7 shows that B-17 is inside or on the edge of areas with high oil saturation in 2015. It also shows the change in oil saturation in 2022, which underpins B-17's ability to sweep the area.

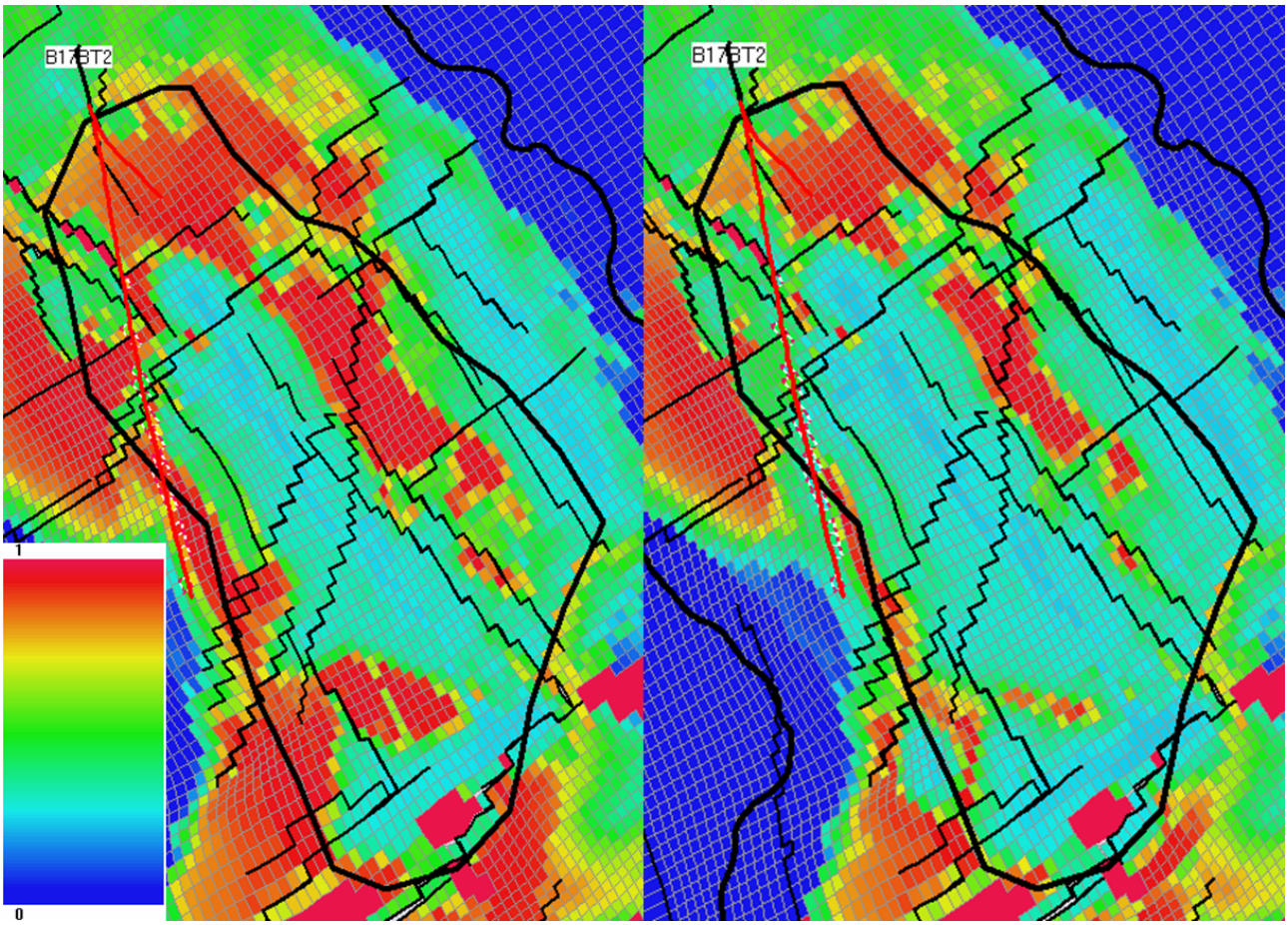

Fig. 7.7 Change in oil saturation in Tor Fm when B-17 is converted to a water injector. *Oil saturation in the Tor Fm (layer 10) in 2015 to the left and 2022 to the right (taken from the conversion run of B-17). Due to the decrease in oil saturation along the wellpath, it becomes visible that B-17 has the ability to sweep its surrounding area with water injection.*

B-2 BT3

Conversion of B-2 BT3 (hereafter called B-2) shows a potential for this location to be used for water injection. This well is SI in the Base Case.

Conversion of B-10 C, which is situated next to B-2, also shows the potential for WI in this area. B-10 C has a shorter wellpath (less perforations) and is therefore not as successful. This is reflected in its contribution to the cumulative injected volume, which is much lower compared to B-2 (Table B.6 in Appendix B).

This area does not have an injector in the schedule. As can be seen in **Fig. 7.8**, B-2 is at the edge of an oil pocket and a pressure sink in 2015.

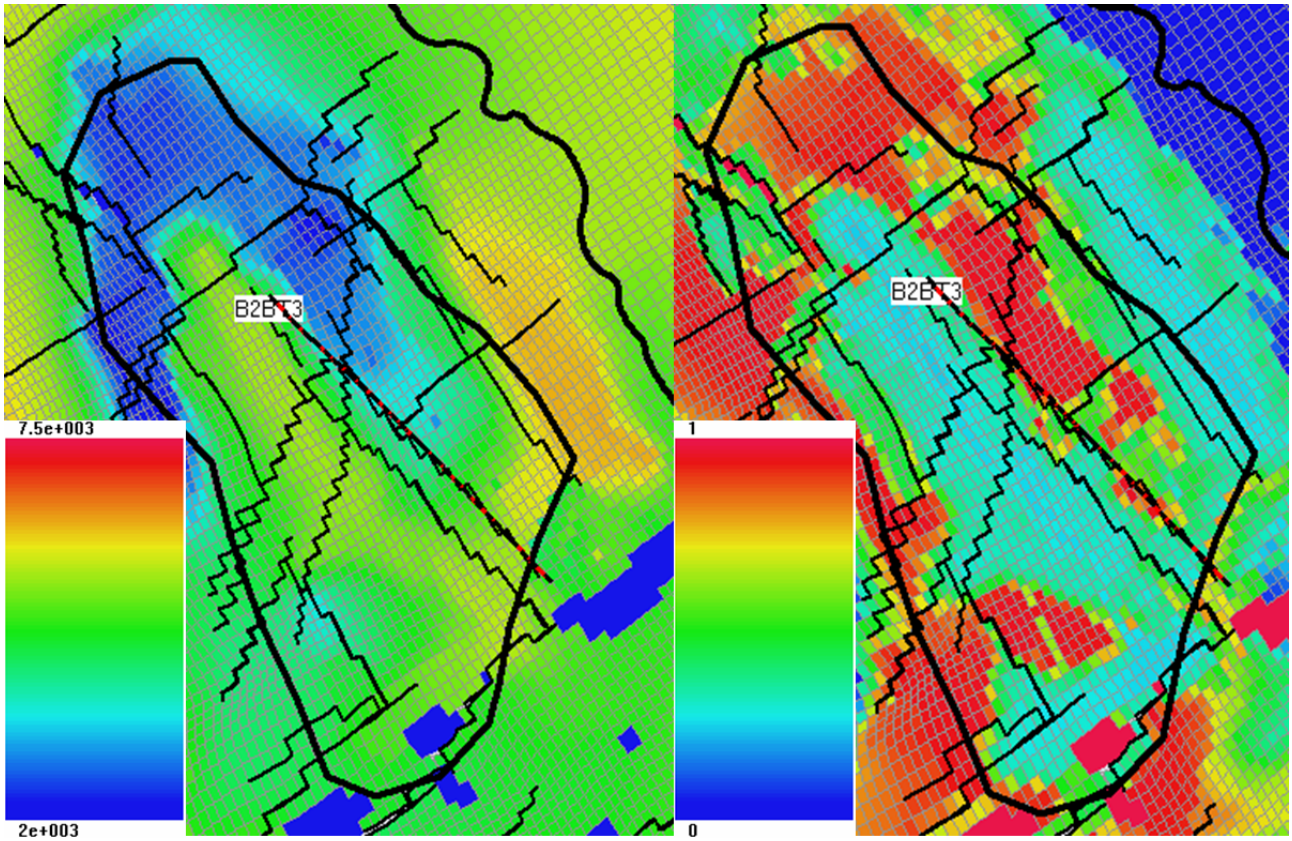

Fig. 7.8 Pressure and oil saturation around B-2 in 2015. *The picture shows pressure and oil saturation in the Tor Fm (layer 10) in 2015. As can be seen, B-2 is on the edge of a pressure sink and an oil pocket. The pressure scale is in psia.*

Saddle area

From Table 7.2 it can be seen that A-12 A has the potential to increase water injection in the saddle area (value of -0.2 MMSTB as producer and +1.5 MMSTB as injector). Investigation of the model shows that this is a region with high oil saturation and low pressure, especially in the Ekofisk Fm. Well A-12 A has perforations mainly in layer 4 and layer 5, which is the Ekofisk Fm.

Successful conversions in the short term perspective

Two Bravo producer locations have potential for successful water injection in the short term perspective; B-2 (also viable in a long term perspective) and B-5 C. **Table 7.4** shows the increment in cumulative production from 2016 to 2022 (the Bravo platform is planned to SI in 01/01/2022).

Table 7.4 Successful conversions in the short term perspective. An overview of the increment in cumulative oil production per year from 2016 until 2022. One observation is that B-2 has a higher conversion value in 2022 than in 2050 (2.8 vs 2.2 MMSTB). Both conversions give a benefit within one year, which then increases to more than 2 MMSTB before platform SI in 2022.

Well Name	Diff cum 2016 MMSTB	Diff cum 2017 MMSTB	Diff cum 2018 MMSTB	Diff cum 2019 MMSTB	Diff cum 2020 MMSTB	Diff cum 2021 MMSTB	Diff cum 2022 MMSTB
B2BT3	0,3	0,9	1,5	2,0	2,3	2,4	2,8
B5C	0,2	0,6	1,2	1,8	2,2	2,3	1,8

7.2.1.3 Unsuccessful Conversions

Investigation of the unsuccessful conversions (value less than 2 MMSTB) revealed two reasons for why the locations were not viable for injection based on the Base Case of this study:

- A lot of the injected water was produced - water cycling.
- The injection rate was very low - low injectivity.

These observations will be explained with examples in the following paragraphs. There will also be given a summary of observations regarding conversion of vertical wells.

Cause 1: Water cycling

When A-3 B (hereafter called A-3) is converted to an injector there is an increase in water production in many wells as it is situated close to several producers. This causes the situation were the injected water is produced directly, instead of sweeping the oil towards the producers. **Fig. 7.9** and **Fig. 7.10** shows the change in water and oil production when A-3 is converted to an injector. It also becomes visible that few wells have an increase in oil production, but many wells have an increase in water production.

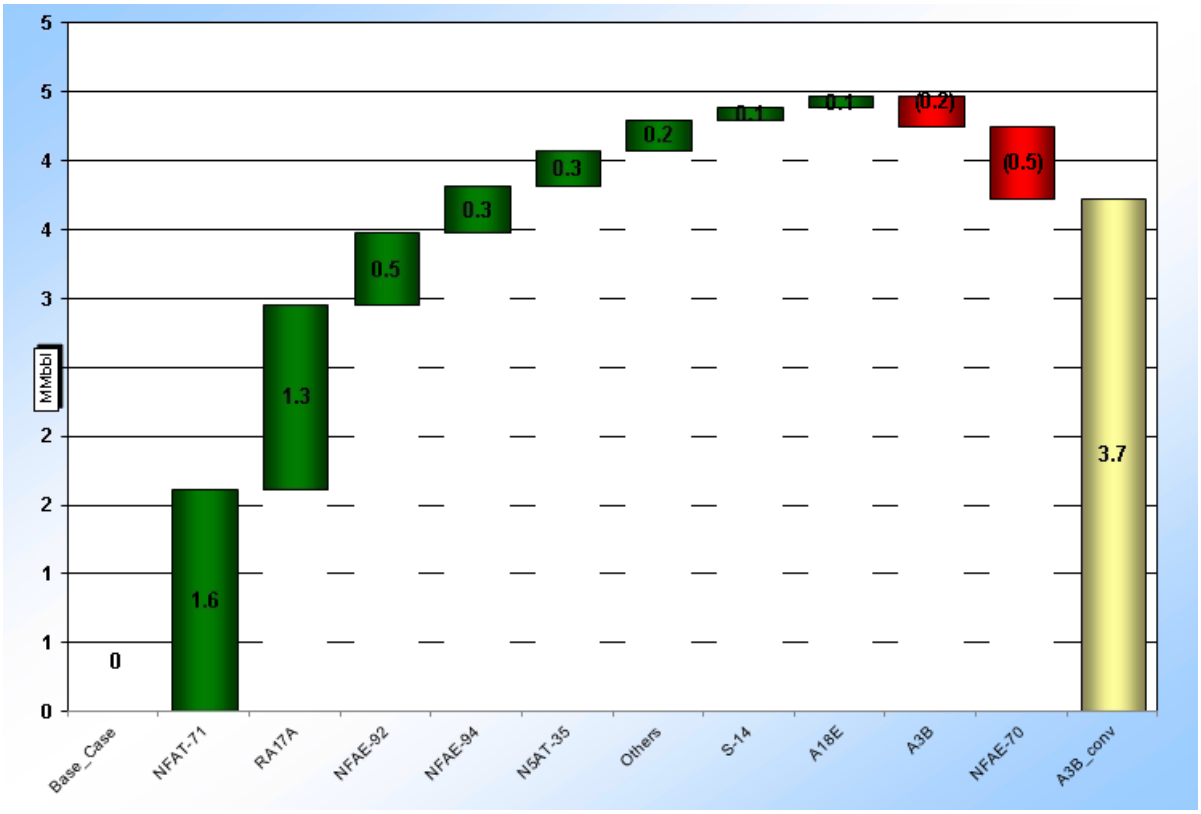

Fig. 7.9 Change in water production when A-3 is converted to a water injector. *The figure shows that many wells have an increase in water production, which is an indication of water cycling.*

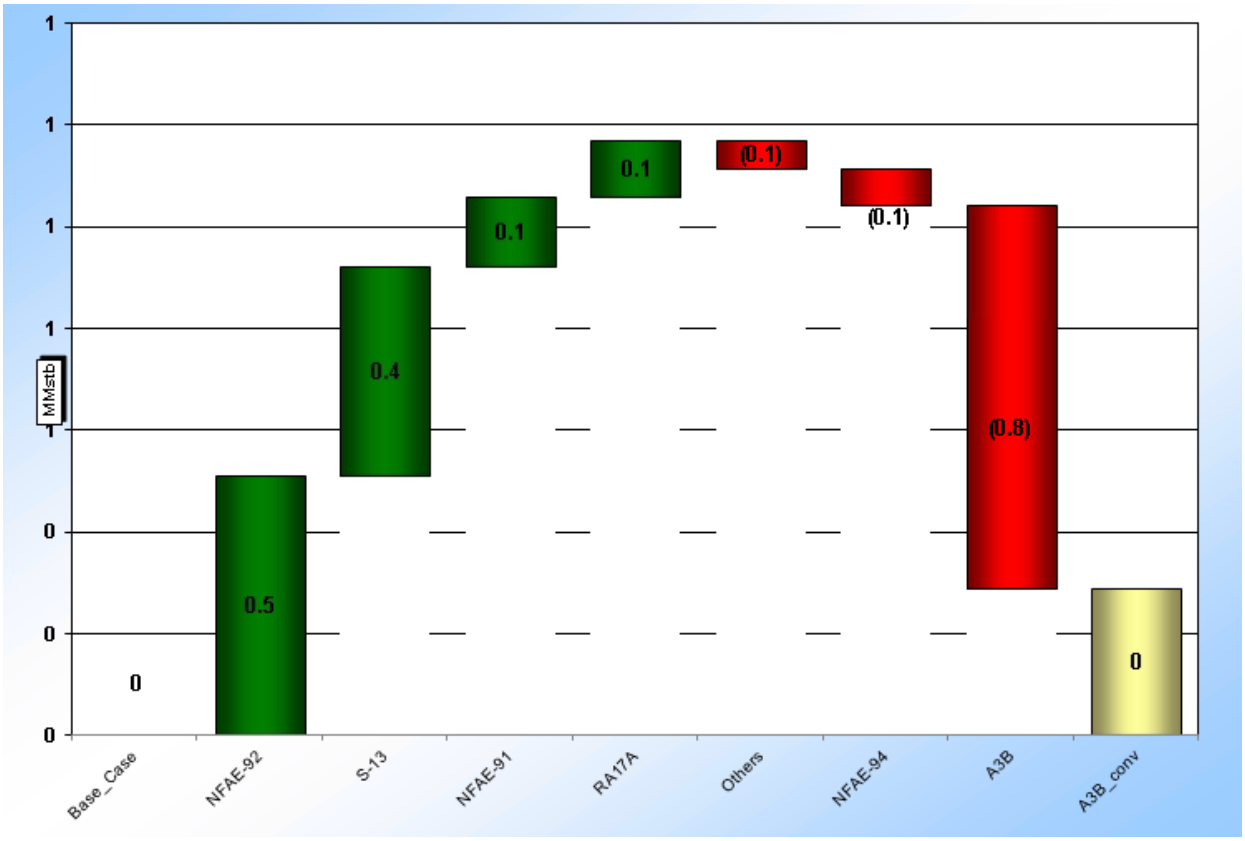

Fig. 7.10 Change in oil production when A-3 is converted to a water injector. *The figure shows that few wells have an increase in oil production.*

Cause 2: Low injectivity

The second observation in the unsuccessful conversion runs was that the injection rates of many of the wells were low. A-26 T2 (hereafter called A-26) is an example of that (average injection rate of 300 bbl/day). This well is located in the area were the highways are connecting the existing injectors on Alpha. As explained in chapter 6.2.1.2 this is an area with high pressures, making it problematic to inject. This can explain the low injection rate from A-26.

With this low rate, A-26 is not able to give pressure support to many producers. From **Fig. 7.11** it is visible that there is a small change in oil production when A-26 is converted, and that few wells are affected.

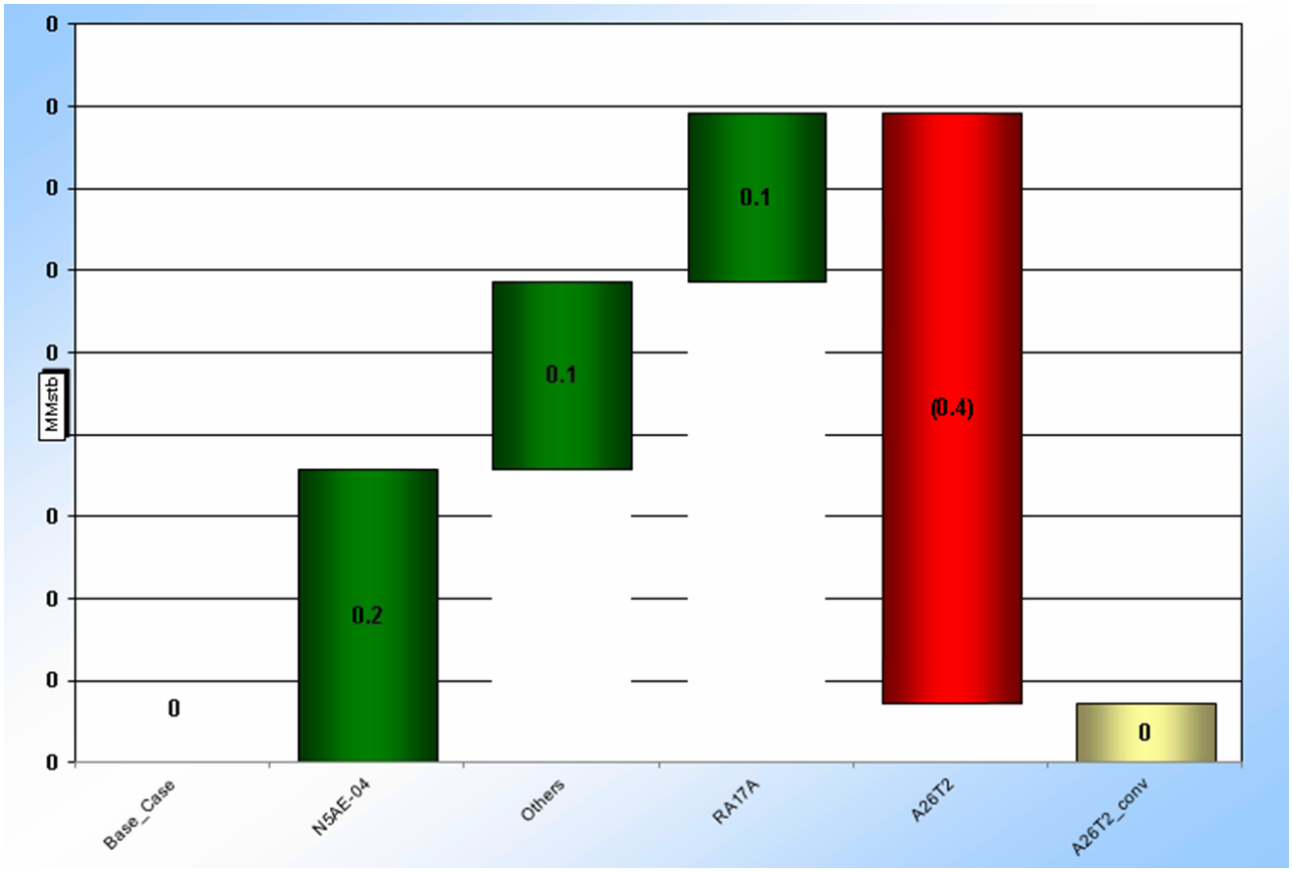

Fig. 7.11 Change in oil production when A-26 is converted to a water injector. *As can be seen, there is not much increase in oil production and few wells are affected by the pressure support from A-26 because of its low rate.*

Investigation of the model shows that other wells, located outside the highways, are situated in areas that are tight (low permeability). In chapter 6.2.2 about the performance of future injectors, it was explained that the KVSTR keyword only was used along the wellpath when

an injector was introduced to the model. All injectors are likely to develop fractures, including the ones that are located in tight zones. Therefore, it is important to keep in mind that some of the conversions might not result in as low injection rate as they do in these sensitivity runs.

Vertical wells

A-26 is a vertical well, but not all the vertical wells perform in the same way. Investigation of the results from the producer conversions showed that vertical wells can:

- Have low or high injection rate.
- Support many or few wells.

As a result, there is no clear trend that vertical wells perform worse than horizontal wells, other than the fact that all the wells with high value are not vertical.

7.2.2 Future Producer Conversions

The conversion runs of future producers were unsuccessful. The results from the study and interpretations of what caused the conversions to not be viable are given in this chapter.

7.2.2.1 Results

Conversion of future producers gave no increase in production larger than 2 MMSTB. The results from the future producer conversions are given in **Table B.7** in Appendix B. A comparison of the well value as producer and as injector is given in **Table 7.5**.

Table 7.5 Future producers well value and their value as injectors. The table shows that none of the future producer locations are viable WI targets. The well value is closely related to the well life. The well life of injectors is until 01/01/2050 (or until pressure is too high to inject), and the well life of producers is listed in the table.

Well Name	Value as Producer [MMSTB]	Well Life as Producer [months]	Value as Injector [MMSTB]
S-14	2,4	192	-1,7
S-8	1,1	96	-1,6
S-13	2,5	192	-3,3
S-9	1,4	192	-1,0
S-4	1,6	192	-0,7
S-34IWS	1,2	277	-0,9
S-21	1,0	264	0,4
S-6	1,6	349	-3,4
NFBT-70A	0,2	132	-1,6
NFBT-70C	6,8	264	-5,8
NFAT-81	1,7	192	-2,4
NFAE-92	3,3	384	-3,8
NFAE-88	5,4	247	-4,7
NFBV-33	4,7	264	-2,8
NFBV-34	2,3	264	-2,0
N5AE-43	4,4	384	-4,8
N5AE-04	0,8	192	0,1
NFAE-93	3,8	192	-3,6
NFAT-79	3,0	192	-2,7
NFAT-32	3,4	384	-1,9
N5AT-35	1,9	277	-1,1
NFBE-93	5,4	264	-9,1
N5BE-07	2,7	217	-2,2
NFET-41	3,6	364	-3,2
NFAT-31	1,5	192	-0,4
NFAE-94	7,0	384	-6,0
NFAT-33	1,8	110	-1,8
N5AE-03	2,4	277	-1,1
NFAE-91	0,6	192	-0,3
NFAT-71	2,3	192	-2,2
NFAT-82	4,7	384	-2,4
NFBE-83	2,9	132	-3,0
NFBV-31	5,5	132	-4,8
N5BE-10	4,6	132	-3,3
NFBV-32	2,1	163	-1,9
NFBT-50	7,6	132	-6,8
NFBE-89	2,0	132	-1,0
N5BE-12	2,4	132	-1,8
N5BE-08	2,9	132	-2,6
NFAE-86	0,8	192	-0,8
N5AE-31	0,5	192	0,7
NFBE-07	2,5	132	-1,7
N5AT-72	1,5	55	-1,3
NFAE-70	2,6	192	-2,9

7.2.2.2 Discussion

As can be seen in Table 7.5, all but three conversions result in a reduction in ultimate oil production compared to the Base Case. This can be explained by the fact that future producers are placed in areas that have relatively high values of both oil saturation (S_o) and pressure. These locations are not connected to highways, since this would result in production of mostly water (Jones, 2014). With both low permeability and high pressures, the injectivity becomes poor.

As a conclusion, the analysis of this study showed that the location of the future producers are not successful injection targets because they have high S_o, high pressure and low permeability. Also, many of the future producers have a high well value. This means that there is a significant loss in production from the well itself when it is converted. Plotting the value as producer vs the value as injector reveals a trend that high value producers are low value injectors (**Fig. 7.12**).

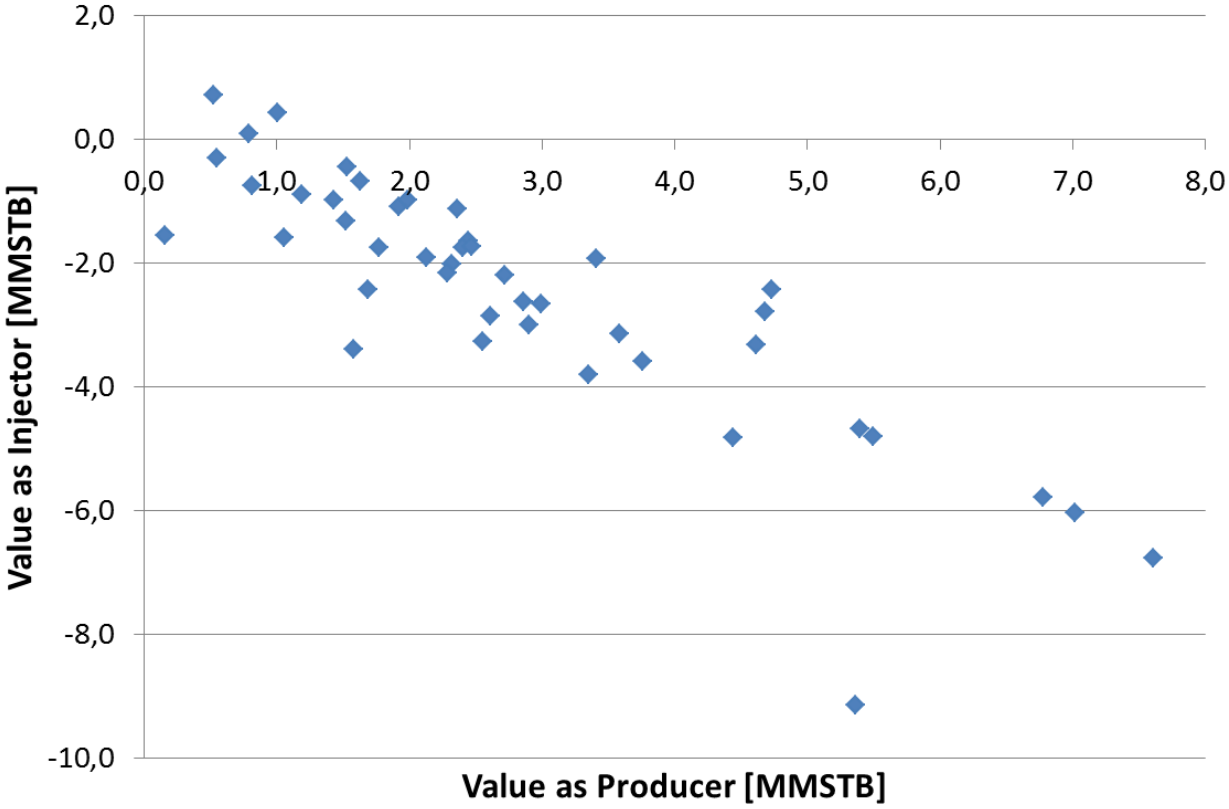

Fig. 7.12 Trend of future producer conversions. *A plot of the well value as producer vs the value as injector reveals a trend - the better the producer, the lower value of converting it.*

7.3 Optimization of Future Water Injection

There are many possible ways of approaching to effort of trying to improve water injection on Eldfisk. The objective of this thesis has been to investigate the possibility of infill injection targets through conversion of existing and future producer locations. Another, and more current, strategy of improving the waterflood would be to increase the injection from current and planned injectors by increasing their BHP and rate constraints.

As mentioned in chapter 2.3.1 about waterflood management, the waterflood was initially managed to maximize injection in order to re-pressurize the reservoir. Currently, there is an effort to inject water to maintain reservoir energy and attain regional reservoir pressure targets. A comparison study was performed to evaluate the impact of increasing injection from the existing and future injectors versus the strategy of adding additional injection targets through producer conversions.

To evaluate the impact of increased injection rate of current and planned wells on the future oil production on Eldfisk, a run was made to utilize their injection potential in the reservoir model. The run had an injection rate constraint of 50 000 bbl/day and a BHP constraint of 10 000 psia. It was observed that the BHP was the limiting factor. The run gave an incremental oil production of 12 MMSTB and an increase in water injection of 535 MMSTB. This means that this specific injection strategy requires 45 STB of injected water to produce 1 STB of oil.

To compare the approach of increasing water injection of existing and planned injectors to the strategy of adding additional injection targets, a run was made were all the three successful producer conversions (B-2, B-17 and B-21) were included in the model as injectors from 01/01/2015. This gave a 6 MMSTB incremental oil production and an increase of 35 MMSTB in water injection. This means that 6 STB of water needs to be injected to get 1 STB of oil. Compared to the case with high BHP and injection rate constraints, this is much more efficient. From this it is concluded that, based on the reservoir model, the addition of water injection targets would be a more effective way of optimizing the waterflood, than to increase water injection of all existing and future injectors. Also this analysis was limited to producer locations, and further investigation of the reservoir model could reveal additional water injection targets which would result in higher incremental oil production.

7.4 Summary of Observations

Infill injection targets investigated through producer conversions showed that:

- Conversion of B-2, B-17 or B-21 to an injector gives an increment in ultimate oil production larger than 2 MMSTB.
- The conversion runs showed a potential to optimize injection in the saddle area.
- Many of the existing wells do better as injectors (26% of the Alpha and 56% of the Bravo producers), which can be explained by interference between the existing producers on Eldfisk. This indicates a need to increase pressure support by a higher injector-producer ratio.
- Alpha area:
    - Conversions inside the well-established injection pattern give low well value due to high pressures.
    - Conversions outside the well-established injection pattern give low well value due to low permeability.
- Water cycling and low injection rates cause unsuccessful conversion of existing producers.
- None of the conversion runs of future producers gave a successful result. This is most likely caused by a combination of high oil saturation, high pressures and low permeability in the well locations. Also, many of the producers cause a significant loss in production when it is used for injection instead.
- The development of fractures propagating away from the wellpath as a result of introducing injectors is not included in the model, even though it is likely for highways to develop due to the high pressures surrounding the injectors. This would increase the injection rates, and by that increase the injection potential and impact area of the individual wells. This gives an uncertainty in the results.
- The strategy of adding additional injection targets was shown to be a more efficient way to improve the waterflood, than to increase injection rate of all current and planned injectors.

A comparison of producer conversions with value greater than 2 MMSTB to the existing and future injectors are given in **Fig. 7.13**. An overview of performance data is given in **Table B.8**

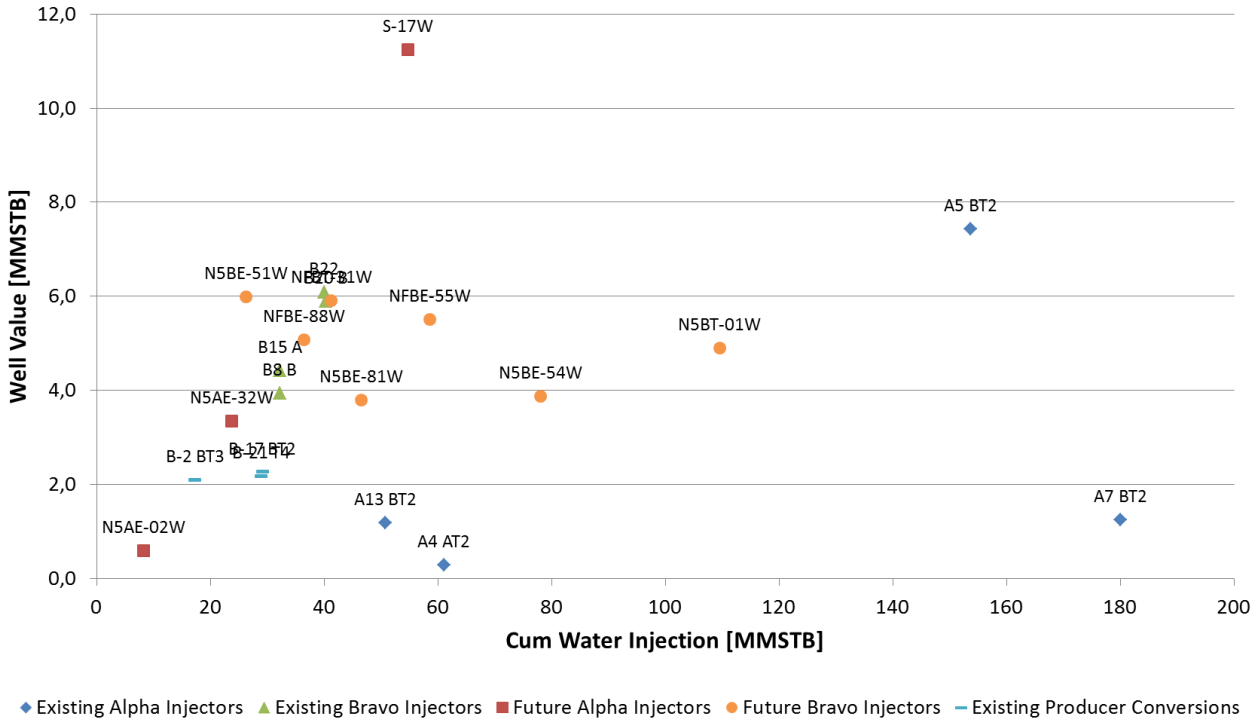

Fig. 7.13 Performance of injectors (including successful producer conversions). *The figure shows the overall performance of existing, future and successful producer conversions in 2050. It can be seen that the producer conversions have the same trend as the existing Bravo injectors. As these are located in the Bravo structure it is highly likely that they develop fractures in the same way as the Bravo injectors. This can result in a performance closer to the current Bravo injectors, which increases the locations injection value.*

in Appendix B. The performance of the producer conversions have the same trend as the Bravo injectors. As these wells are located in the Bravo structure, it is highly likely that they will develop highways in the same way as the existing Bravo injectors. Therefore, these conversions might have the potential to end up with a performance closer to the current Bravo injectors, and as a result increase the locations injection value.

A map showing the location of the successful conversions, and the existing and future injectors, is shown in **Fig. 7.14**. The location of A-12 A, B-5 C and B-10 C is also included.

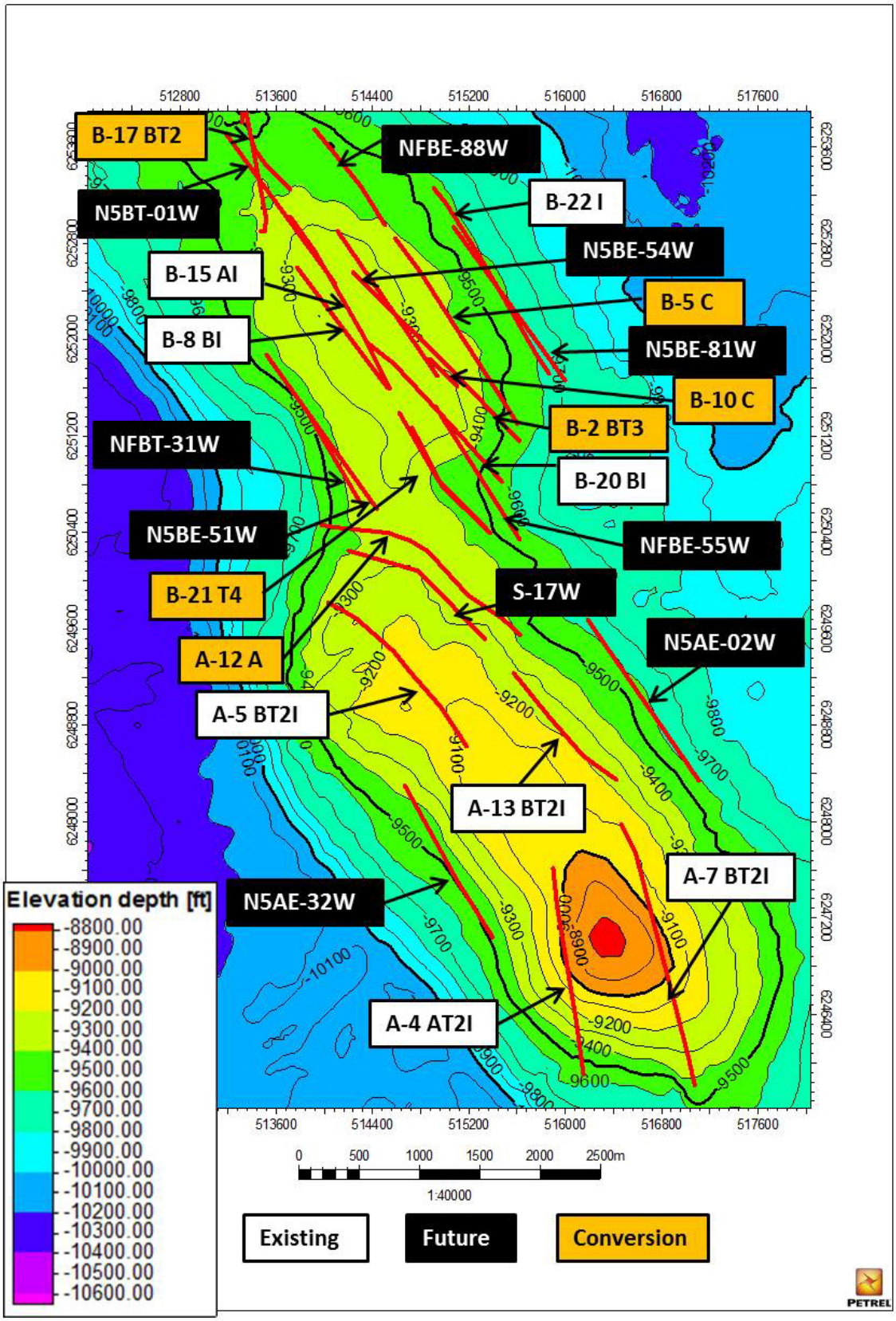

Fig. 7.14 Map of injector locations (including successful producer conversions). *The map shows the location of existing, future and successful producer conversions. The location of A-12 A, B-5 C and B-10 C is also included since they are a part the discussion.*

8 Uncertainty Study - The Impact of Fractures

Investigation of the reservoir model revealed that the fractures dominate the fluid flow and affect the injectors' performance on Eldfisk. Also, the development of highways surrounding future injectors is not included in the forecasts of future reservoir performance. The uncertainty in the location, size and conductivity of the high permeability pathways influence the predictive capacity of the reservoir model.

To evaluate the reservoir model further, it was decided to perform a study where highways are introduced or removed to better understand their impact on fluid flow. An analysis was also made to evaluate the overall impact of injection induced fractures.

8.1 Injectors Connected to Faults

Experience from the Eldfisk field has shown that injectors can open up faults connected to them because of the increase in pressure in the vicinity of the wellbore. One run was made where a highway was added along a fault crossing the proposed well trajectory of injector S-17 W. This was done by introducing a KVSTR value of 500 to a range of cells surrounding the fault (a value commonly used to introduce highways). This resulted in the permeability inside this conduit to increase with time, ranging from 150-500 mD. The permeability distribution surrounding S-17 W in the Ekofisk Fm is depicted in **Fig. 8.1**.

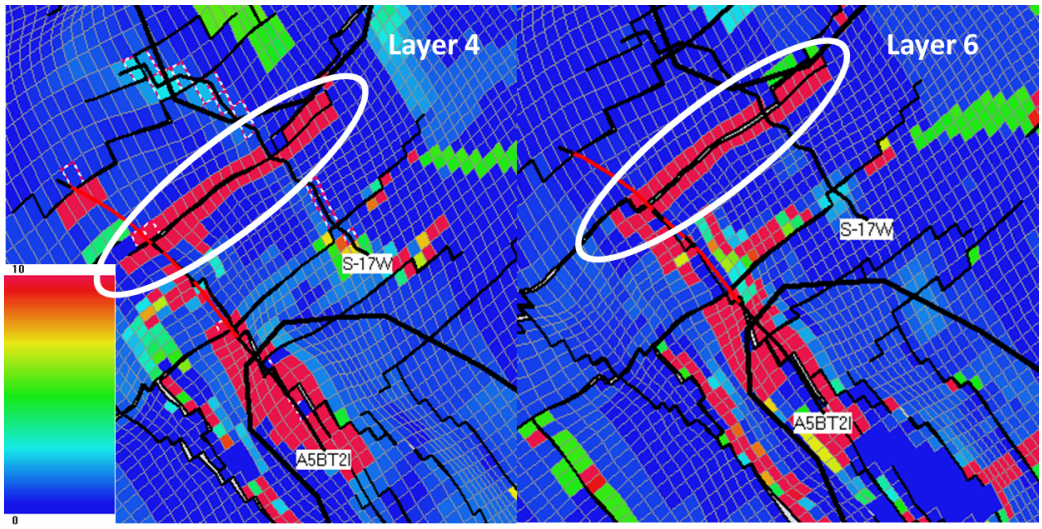

Fig. 8.1 Introduction of a highway connected to injector S-17 W. *The figure shows the permeability distribution in 2017 with the addition of a highway along a fault connected to S-17 W. The highway extends through three layers in the Ekofisk Fm. The permeability increases with time inside the highway, ranging from 150-500 mD. The scale is in mD.*

The change in sweep from the introduction of the highway is shown in **Fig. 8.2**. It shows the oil saturation in layer 4 (Ekofisk Fm) in the Base Case compared to the run with the additional highway. The area affected by the water injected from S-17 W has increased, following the extension of the highway.

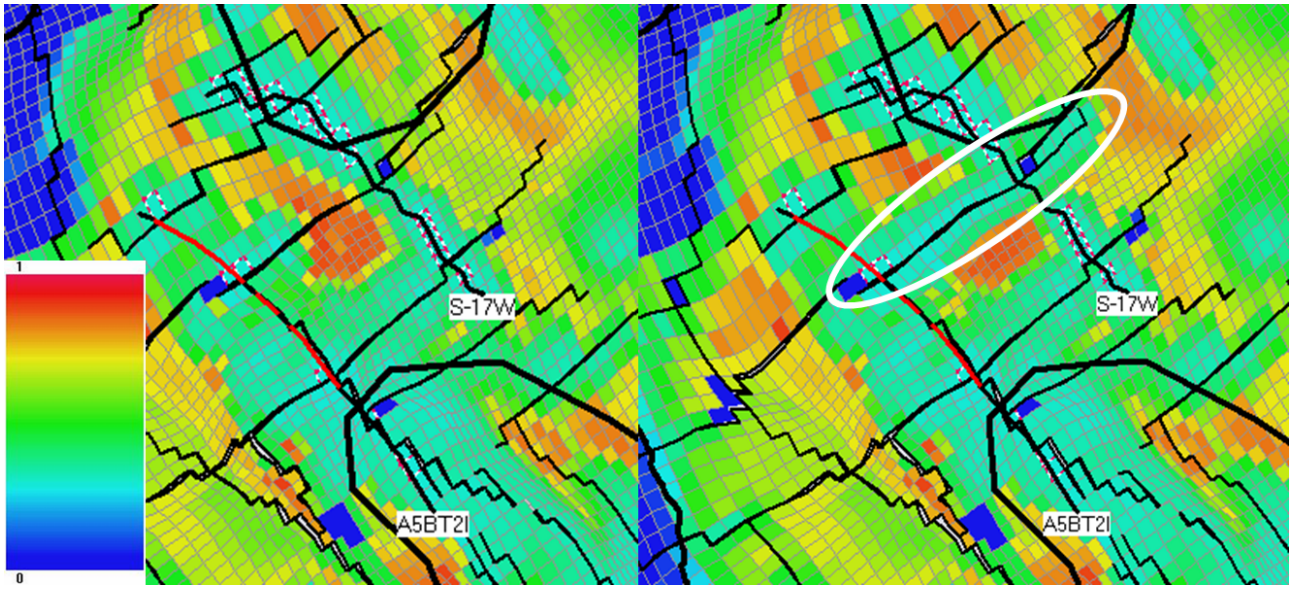

Fig. 8.2 Change in sweep with introduction of highway connected to S-17 W. *Oil saturation in the Ekofisk Fm (layer 4) in 2025 in the Base Case is shown to the left and in the run with the additional highway to the right. There is a visible change in sweep from S-17 W, extending along the highway.*

Analysis of the result also showed that S-17 W injected more water and that the incremental oil recovery was 1.7 MMSTB. As a conclusion, the addition of the high permeability conduit connected to S-17 W showed that a fault crossing an injectors wellpath can be of importance for the performance of the injector. It also showed that this can give additional oil production which is vital information for reservoir management decisions.

8.2 Removal of the Largest Induced Fractures in Alpha

One run was made where the largest induced fractures on Alpha were removed. This study was done in an effort to understand the impact of the well-developed fracture network in Alpha on fluid flow distribution, and the resulting oil production. **Fig. 8.3** shows the initial permeability distribution in the Tor Fm, the distribution without the largest induced fractures in 2024 and the distribution in the Base Case in 2024. It is visible that the highways connecting the injectors have been eliminated.

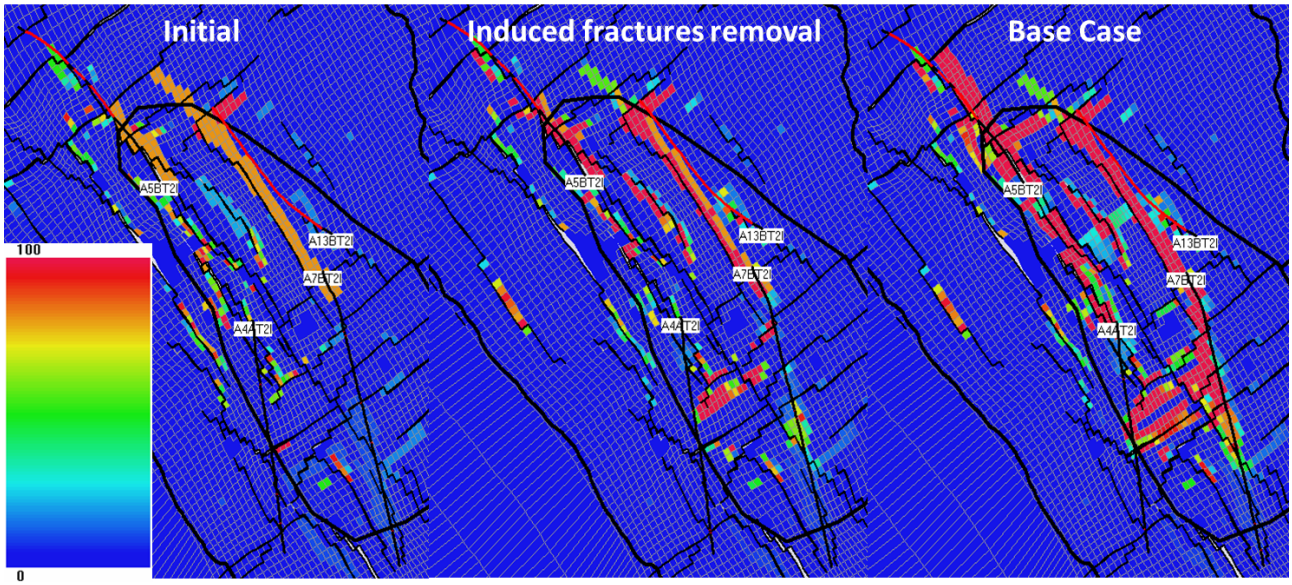

Fig. 8.3 Removal of the largest induced fractures in Alpha. *The initial permeability distribution in the Alpha structure is shown to the left. In the middle is a picture of the structure in 2024 without the large induced fractures that connected the injectors. It was created by eliminating the connection of cells to the KVSTR keyword that created large induced fractures. The picture to the right shows the permeability distribution in the Base Case in 2024. The scale is in mD.*

Investigation of the results revealed a large decrease in water injection of 87 MMSTB and a small increase in oil production of 0.6 MMSTB. This is an indication that the fracture network in Alpha has become inefficient, and that a lot of the water is circulating. This should be looked into further, with the option of water shut-off.

8.3 Impact of Injection Induced Fractures

To evaluate the impact of injection induced fractures, one run was made where KVSTRvalue = 0 for all cells in the model from 01/01/2015. This means that all the injection induced fractures and faults were eliminated from the model, which is depicted in **Fig. 8.4**.

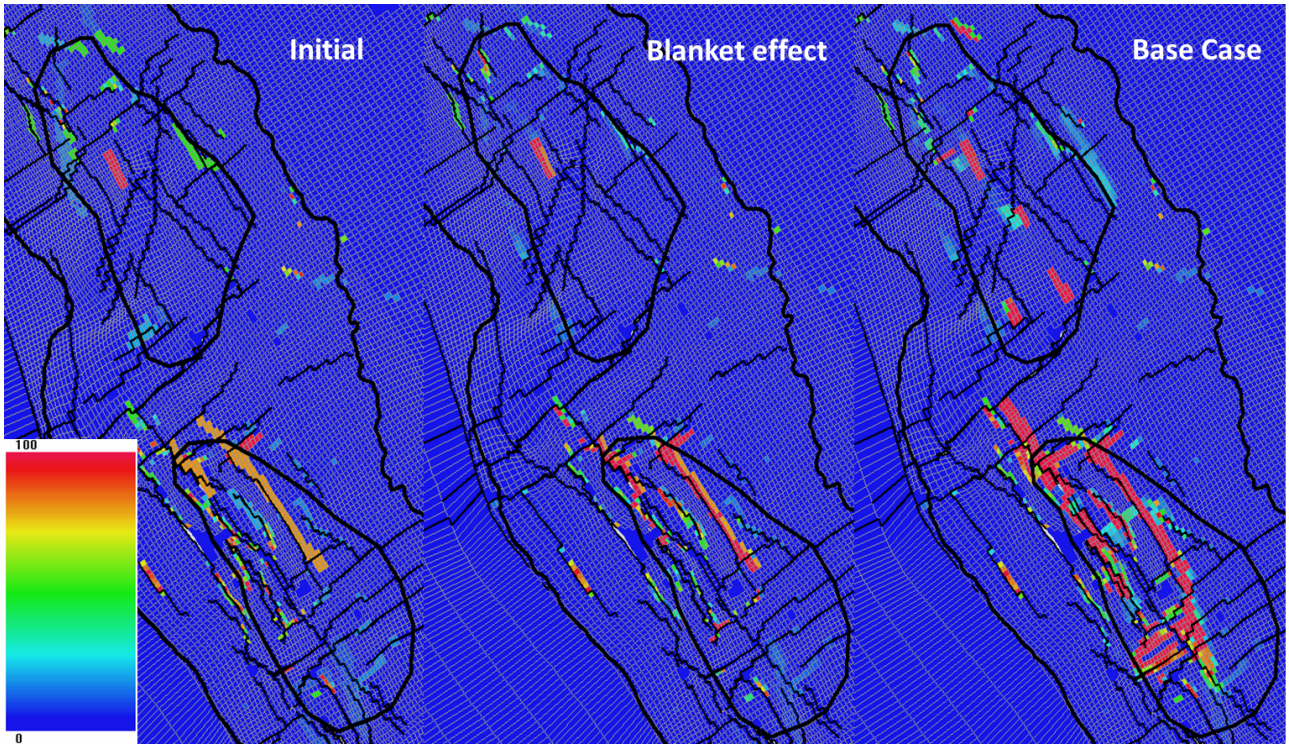

Fig. 8.4 The impact of KVSTRvalue = 0 in the Tor Fm (layer 9). *To the left is the initial permeability distribution in Eldfisk, revealing all the natural fractures. A "blanket effect" was used in the sensitivity run where all the induced fractures were eliminated by having a KVSTRvalue = 0 for all cells in the model. The effect of this is shown in the middle picture in year 2024. The Base Case in 2024 is displayed to the right. The scale is in mD.*

The result was a 19 MMSTB reduction in oil production and a 250 MMSTB decrease in water injection. This indicates that the injection induced fractures and faults play an important role in future oil production and water injection. Including the observations made in the run where many of the Alpha highways were eliminated, it is concluded that induced fractures are beneficial for water injection, but that when fractures connecting injectors become too dominant it can have a detrimental effect on oil production.

9 Summary of Results

The studies performed in this thesis were based on a history matched model - The Base Case. The water injection performance and potential on Eldfisk has been investigated through a combination of technologies, creating a new angle of approach compared to current practice.

The performance of the injectors were analyzed by multiple software that enabled investigation of the fluid distribution and related change in pressure, streamlines and production. It resulted in valuable observations, important for reservoir management decisions.

The potential for water injection in Eldfisk was evaluated using existing and future producer locations as infill injection targets. Since these wellbores were already in the model, it enabled the evaluation of a wide variety of reservoir locations within a limited time frame. Also, it created a new approach compared to current practice.

9.1 Conclusions

The conclusions based on the studies presented in this thesis are the following:

Model based conclusions:

The waterflood plays a significant role in future oil production and repressurization of the reservoir. Investigation of the model showed that:

- Induced fractures are beneficial for water injection, but when fractures connecting injectors become too dominant it can have a detrimental effect on oil production.
- The permeability distribution has become more heterogeneous with time.
- The natural fractures and faults have become more extensive, with increased conductivity over time. These high permeability conduits extend both vertically and horizontally, causing inter-formation flow.
- It has developed pathways of direct communication between the injectors, especially in the Alpha structure.
- The highways play a dominant role in fluid flow, affecting the injectors' performance.

- The individual Alpha injectors (except for A-5) have low well value compared to the Bravo injectors. It was concluded that when one Alpha injector is SI the other injectors have the ability to compensate for the loss in pressure support through the highways connecting them.

Injection strategy conclusions:

Based on this analysis of Eldfisk, the use of infill injection targets is a more efficient strategy to improve the waterflood, compared to increasing injection rate on all existing and future injectors. Reservoir simulation showed that:

- Investigation of producer locations as injection targets resulted in three conversions with a substantial increment in ultimate oil production: B-2, B-17 and B-21.
- There is a potential for infill injection in the saddle area.
- In the Alpha structure, conversions inside the well-established injection pattern gave low well value due to high pressures. Outside the well-established injection pattern, the conversions were unsuccessful due to low permeability.
- In general, water cycling and low injection rates cause unsuccessful conversion of existing producers.
- Conversion of future producers were not viable, which may be explained by their location being in areas of high oil saturation, high pressure and low permeability. This causes poor injectivity, and also the producers have high well value.
- Since the development of highways surrounding future injectors and producer conversions is not included in the model, their well value and injection potential is uncertain. This results in a reduction in the model's predictive capacity.

9.2 Recommendations for Future Work

Based on the work performed in this thesis, the following is recommended for future studies:

Field application:

- Investigate further the opportunities to optimize the waterflood presented in this study and create development plans for the viable options:
  - Successful producer conversions.
  - Injection in saddle area.

- Analyze the opportunity to optimize perforations on injectors:
  - Removal of perforations: shut off water zones or highly conductive paths (fractures) to decrease oil by-pass events.
  - Addition of perforations to improve pressure support.
- The results from the run presented in chapter 8.2 indicated that to shut in large induced fractures connecting the injectors in Alpha could be beneficial for oil production. It is recommended to investigate this further and to look into possibilities of closing these large fractures in the Alpha structure.

Simulation model updates and studies:

- The producer conversions were only converted on 01/01/2015 or on their start-up date. It recommended to investigate the time effect on producer conversions (especially the future producer conversions).
- The focus of this study has been injector based. It could be of interest to investigate the producers' performance to further understand the efficiency of the waterflood.
- The injectors' location in the reservoir has been the focus in the analysis of their performance. It could be of interest to study the impact of well design in the model (PI etc.) on the injectors performance and resulting oil production.
- Investigate opportunities to predict the development of high permeability pathways as a function of pressure and geological properties in the current model.

Other studies:

- Include VRR analysis on a formation or pattern level to investigate the potential for waterflood optimization further.
- Perform a comparison study of the current model and a dual porosity model of Eldfisk.

10 Nomenclature

BHP	Bottom hole pressure
Fm	Formation
HCP,avg	Average hydrocarbon pressure (average pressure in hydrocarbon bearing cells)
k,eff	Effective permeability
LTF	Long term forecast
MSTB	10^3 STB
MMSTB	10^6 STB
RF	Recovery factor
So	Oil saturation
Sw	Water saturation
Tx	Transmissibility in x-direction
URF	Ultimate recovery factor
VRR	Voidage replacement ratio
WC	Water cut
WI	Water injection

11 Glossaries

Anisotropy	Variation of a property of a material with the direction in which it is measured.
Connate water	Water trapped in the pores of a rock during formation of the rock.
Drainage	The process of forcing a nonwetting fluid into a porous rock (increasing saturation of nonwetting fluid).
Effective stress	The portion of the external load of total stress that is carried by the rock itself.
Free water level (FWL)	The highest elevation at which the pressure of the hydrocarbon phase is the same as that of water (zero capillary pressure).
Gravitational forces	The force of gravity that affects the fluid distribution in a reservoir.
Heterogeneity	The quality of variation in rock properties with location in a reservoir or formation.
Imbibition	The process of absorbing a wetting fluid into a porous rock (increasing saturation of wetting fluid).
Interfacial tension	The force per unit length at the fluid-fluid and rock-fluid interfaces.
Mobility ratio	A relative measure of the ability of the displacing fluid to that of the displaced fluid to move through a porous medium.
Plastic deformation	Permanent physical or mechanical alteration that does not include rupture.
Pore pressure	The pressure of fluids within the pores of a reservoir.
Residual oil	Oil that does not move when fluids are flowing through the rock in normal conditions (e.g. primary and secondary recovery).
Saturation	The relative amount of a fluid in a porous rock, usually expressed as a percentage of the total fluid volume.
Scale deposit	Occurs when the solution equilibrium of the water is disturbed by pressure and temperature changes, dissolved gases or incompatibility between mixing waters. It is a coating on the surface of metal, rock or other material.

Transmissibility	A parameter used in reservoir simulation that measure how easily fluids flow between adjacent gridblocks.
Viscous displacement	The displacement of a less viscous fluid by a more viscous fluid.
Voidage replacement ratio (VRR)	The reservoir volume of injected fluids divided by the reservoir volume of produced fluids.
Wettability	The preference of a solid to contact one fluid (wetting phase) rather than another.
Yield strength	The failure criterion of a rock. If the load exceed this threshold, the rock will start to develop fractures.

12 References

Agarwal, B., Hermansen, H., Sylte, J.E. et al. 2000. *Reservoir Characterization of Ekofisk Field: A Giant, Fractured Chalk Reservoir in the Norwegian North Sea - History Match*. SPE Reservoir Eval. & Eng. 3 (6): 534-543. Paper SPE-51893-MS. http://dx.doi.org/10.2118/51893-MS.

Ahmed, T. 2006. *Reservoir Engineering Handbook*, Elsevier.

Austad, T., Strand, S., Madland, M. V. et al. 2008. *Seawater in chalk: An EOR and Compaction Fluid*. Paper IPTC 11370/ SPE 118431 presented at the 2007 International Petroleum Technology Conference, Dubai, 4-6 December.

ConocoPhillips. 2013a. *CSim/CView Reference and Technical Manual*.

ConocoPhillips. 2013b. *PSim Technical Manual*.

ConocoPhillips. 2014a. OneWiki. SPARK, 26.09.14 revision, https://onewiki.conocophillips.net/wiki/SPARK (accessed 30 September 2014).

ConocoPhillips. 2014b. OneWiki. SplicerXL, 27.05.14 revision, https://onewiki.conocophillips.net/wiki/SplicerXL (accessed 30 September 2014).

ConocoPhillips Norwegian Business Unit (COPNO). 2010-2012. *SET II Report for the Eldfisk Field (Part 2), Effective Permeability Mapping and Flow Simulation*.

ConocoPhillips Norwegian Business Unit (COPNO). 2011. *Plan for Development and Operation - Eldfisk II (Part 1)*.

ConocoPhillips Norwegian Business Unit (COPNO). 2014a. *Annual Status Report 2014 for Eldfisk Field, by Fevang, L.*

ConocoPhillips Norwegian Business Unit (COPNO). 2014b. *GEA reservoir overview*. Knowledge share, Tananger, Norway, February 4th.

ConocoPhillips Norwegian Business Unit (COPNO). 2014c. *Spontaneous Imbibition fractures/matrix and simulation modelling issues, by Rolfsvåg, T.* Lunch and Learn, Tananger, Norway, November 21st.

ConocoPhillips Norwegian Subsurface Organization. 2012. *Reservoir Management Plan (RMP).*

Cook, C. C., Andersen, M. A., Halle, G. et al. 2001. *An Approach to Simulating the Effects of Water-Induced Compaction in a North Sea Reservoir*. SPE Res Eval & Eng **4** (2): 121-127. Paper SPE 71301. http://dx.doi.org/10.2118/71301-PA.

Dake, L. P. 1985. *Fundamentals of reservoir engineering*, first edition. Elsevier.

Eremenko, E. 2014. Personal Communication.

Ezekwe, N. 2011. *Petroleum Reservoir Engineering Practice,* Westford, Massachusetts, USA, Pearson Education, Inc.

*Guidelines for Application of the Petroleum Resources Management System (*PRMS). 2011. SPE. http://www.spe.org/industry/docs/PRMS_Guidelines_Nov2011.pdf (accessed 5 December 2014).

Hamon, G. 2004. *Revisiting Ekofisk and Eldfisk Wettability*. Paper SPE 90014 presented at the SPE Annual Technical Conference and Exhibition held in Houston, Texas, U.S.A, 26-29 September. http://dx.doi.org/10.2118/90014-MS

Haugen, Å. 2010. *Fluid Flow in Fractured Carbonates: Wettability Effects and Enhanced Oil Recovery*. Phd, University of Bergen, Norway.

Hearn, C. L. 1971. *Simulation of Stratified Waterflooding by Pseudo Relative Permeability Curves*. J Pet Technol **23** (7): 805-813. Paper SPE-2929-PA. http://dx.doi.org/10.2118/2929-PA.

International Energy Agency (IEA). 2013. *World Energy Outlook 2013*. OECD/IEA, Paris, France.

Jones, J. 2014. Personal Communication.

Kittilsen, C. E. 2014. *Improved Oil Recovery - The Need for Innovative Solutions In A Changing World*. Specialization Project, Norwegian University of Science and Technology & Weatherford Petroleum Consultants AS, Trondheim, Norway.

Lingen, P. Van, Sengul, M., Daniel, J.M. et al. 2001. *Single Medium Simulation of Reservoirs with Conductive Faults and Fractures*. Paper SPE 68165 presented at the SPE Middle East Show held in Bahrain, 17-20 March. http://dx.doi.org/10.2118/68165-MS.

Morrow, N. R. and Mason, G. 2001. *Recovery of Oil by Spontaneous Imbibition.* Current Opinion in Colloid & Interface Science **6** (4): 321-337. Elsevier.

Norwegian Petroleum Directorate (NPD). 2009. *Why do we not recovery 100 per cent of the oil?* http://www.npd.no/en/Topics/Improved-Recovery/Temaartikler/Whydo-we-not-recover-100-per-cent-of-the-oil/ (accessed 28.11.14).

Norwegian Petroleum Directorate (NPD). 2014a. *Facts 2014, The Norwegian Petroleum Sector.*

Norwegian Petroleum Directorate (NPD). 2014b. *Petroleum Resources on the Norwegian Continental Shelf 2014, Fields and Discoveries.*

Ozoglu-Topdemir, S. 2014. Personal Communication.

Schlumberger. 2014. Schlumberger Oilfield Glossary. http://glossary.oilfield.slb.com/.

Schulte, W.M. 2005. *Challenges and Strategy for Increased Oil Recovery*. Paper IPTC-10146-MS presented at the International Petroleum Technology Conference in Doha, Qatar, 21-23 November. http://dx.doi.org/10.2523/10146-MS.

Settari, A. 2002. *Reservoir Compaction*. Distinguished Author Series (August 2002). SPE 76805. http://dx.doi.org/10.2118/76805-JPT.

Streamsim Inc. 2014. *Streamline-Based Surveillance for Mature Floods*. http://www.streamsim.com/sites/default/files/surveillance.whitepaper.spe166393.pdf (accessed 12 November 2014).

Sylte, J. E., Thomas, L. K., Rhett, D. D. et al. 1999. *Water Induced Compaction in the Ekofisk Field*. Paper SPE 56426 presented at the 1999 SPE Annual Technical Conference and Exhibition held in Houston, Texas, 3-6 October. http://dx.doi.org/10.2118/56426-MS.

Terry, R. E. 2001. *Enhanced oil recovery*. Encyclopedia of Physical Science and Technology *3 (18): 503-518*.

U.S. Energy Information Administration (EIA). 2014. Europe Brent Spot Price FOB, 10.12.2014, http://www.eia.gov/dnav/pet/hist/LeafHandler.ashx?n=pet&s=rbrte&f=a (accessed 13 December 2014).

Zitha, P., Felder, R., Zornes, D. et al. 2011. *Increasing Hydrocarbon Recovery Factors*. SPE Technology Updates 2011.

Appendix A: Figures

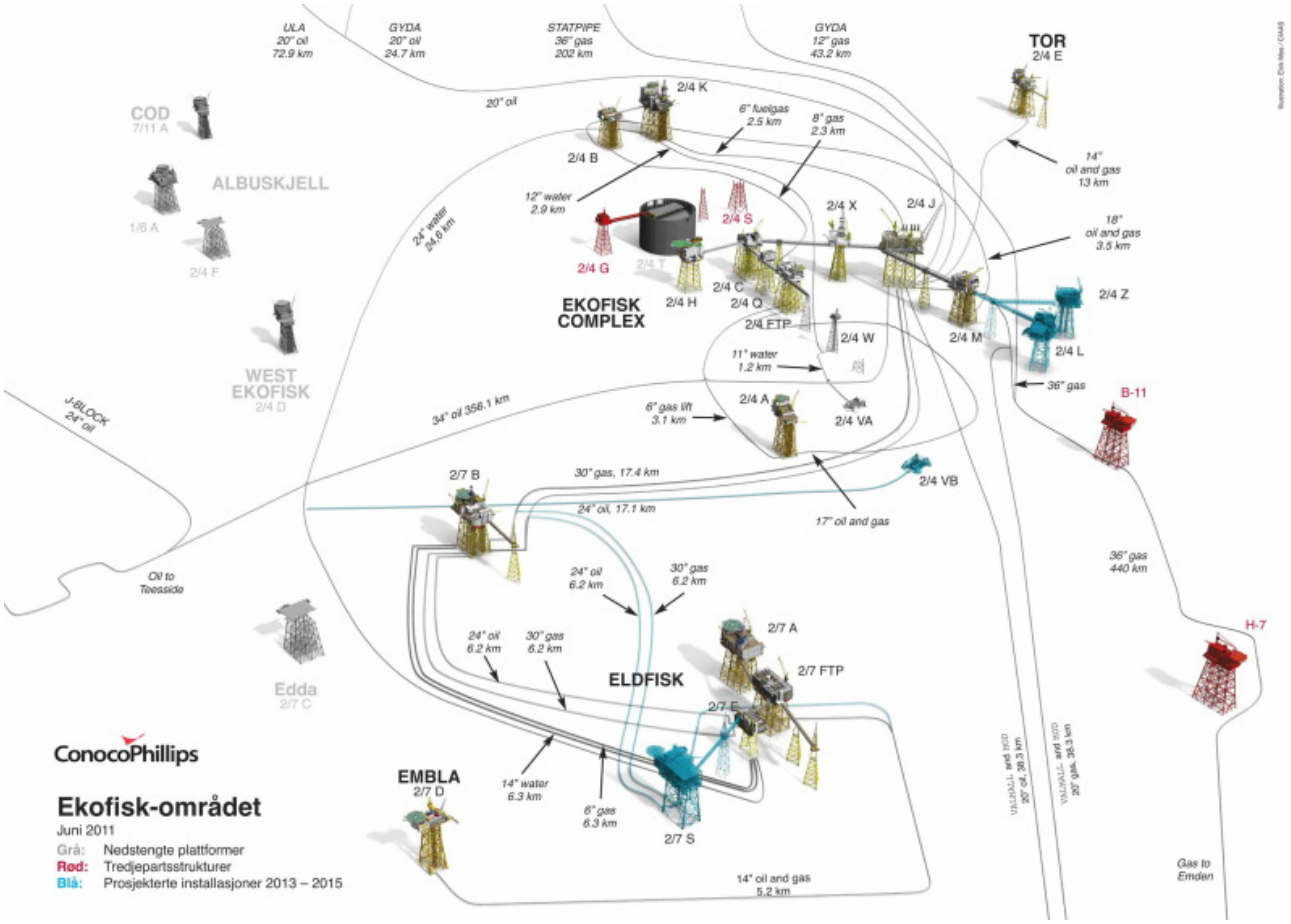

Fig. A.1 The Greater Ekofisk Area. *A schematics of the facilities and transportation infrastructure in the Greater Ekofisk Area. The Ekofisk, Eldfisk, Embla and Tor field are all part of this area. The grey platforms are shut-in, the red are third-party platforms and the blue are planned platforms for installation in 2013-2015 (ConocoPhillips, 2012). Platform 2/4-Z, 2/4-L and 2/7-S have been installed.*

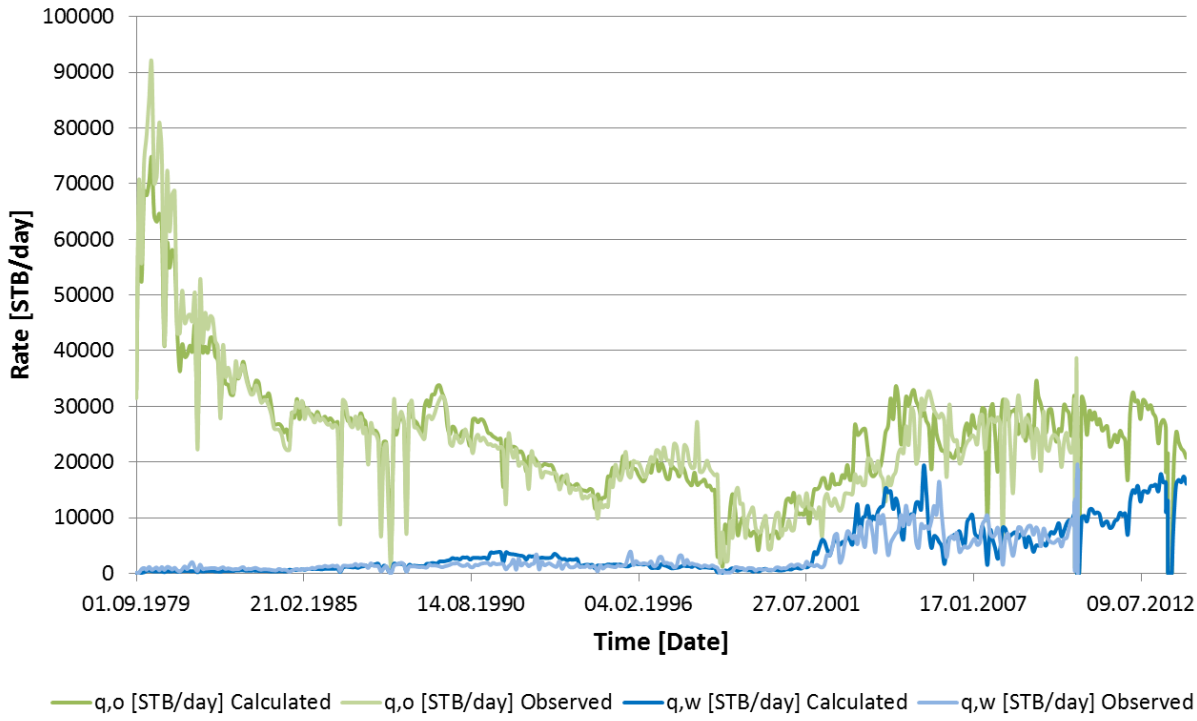

Fig. A.2 History matched oil and water production rates on Alpha. *History matched oil and water production rates vs observed (field data) on Alpha. The observed data ends on 22.06.2010.*

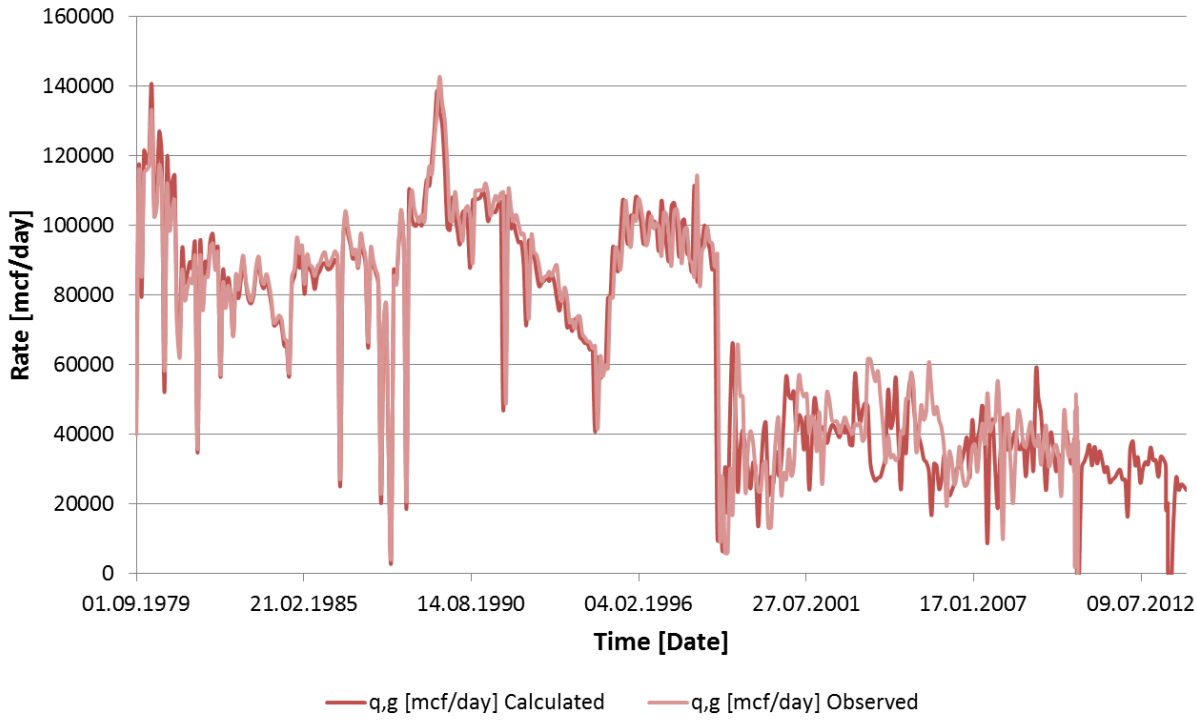

Fig. A.3 History matched gas production rate on Alpha. *History matched gas production rate vs observed (field data) on Alpha. The observed data ends on 22.06.2010.*

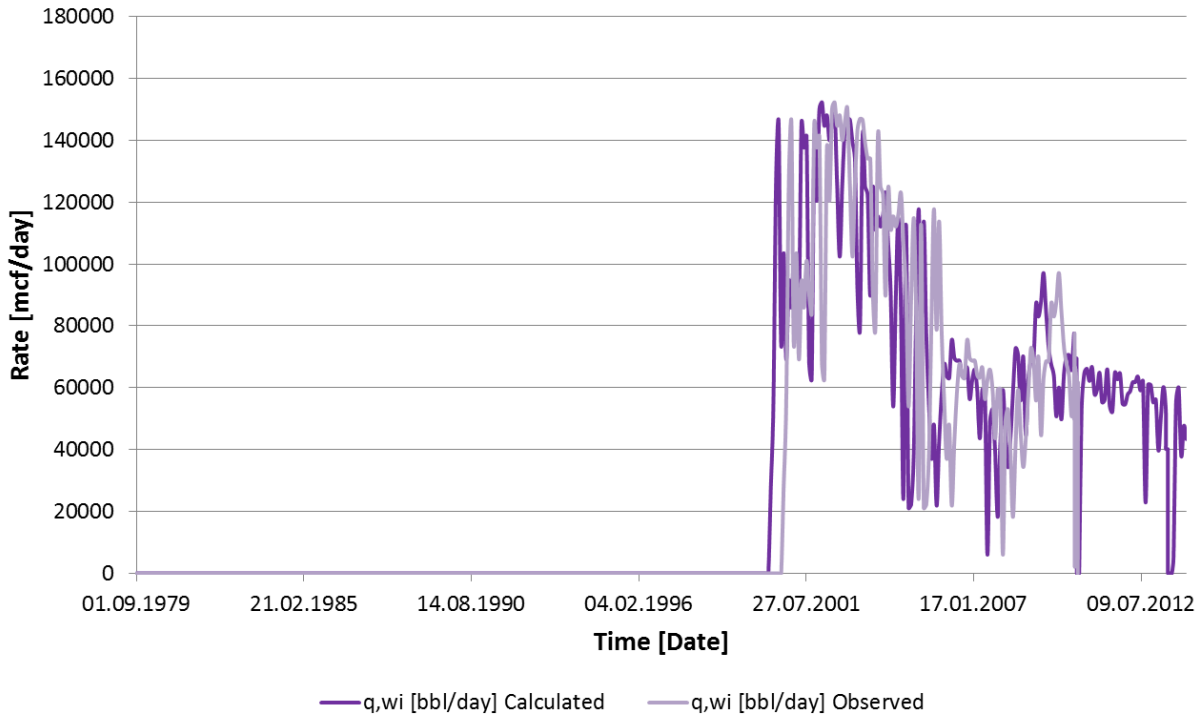

Fig. A.4 History matched water injection rate on Alpha. *History matched water injection rate vs observed (field data) on Alpha. The observed data ends on 22.06.2010.*

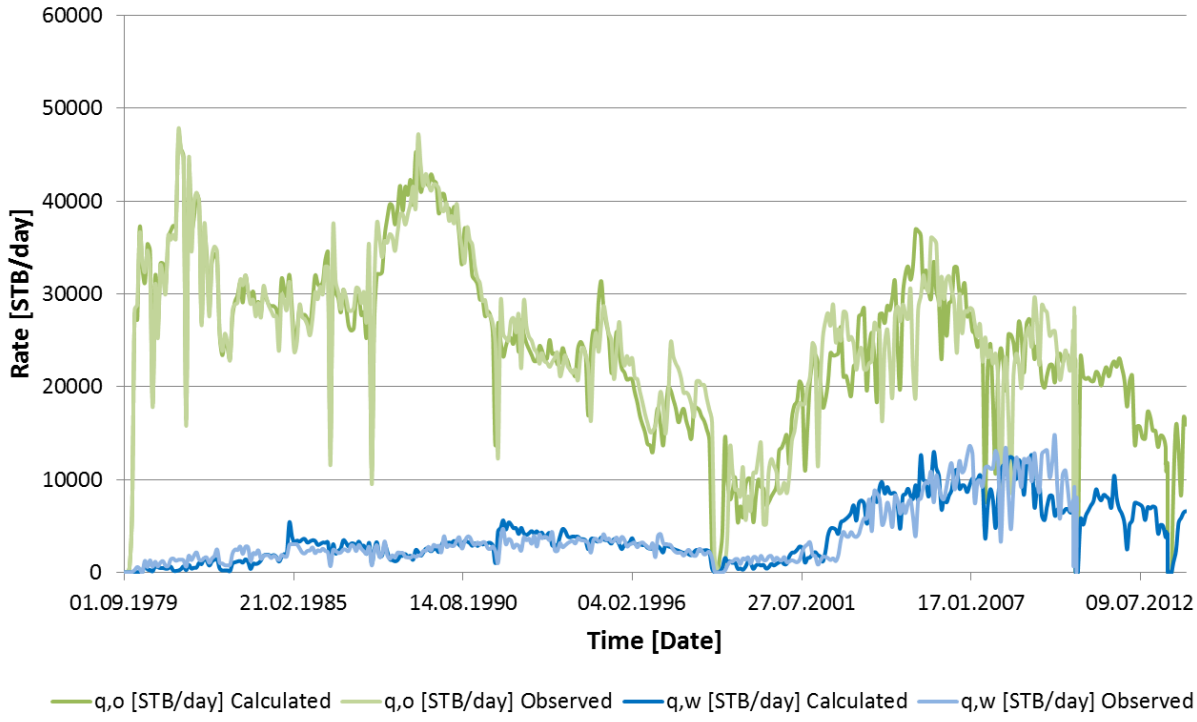

Fig. A.5 History matched oil and water production rates on Bravo. *History matched oil and water production rates vs observed (field data) on Bravo. The observed data ends on 22.06.2010.*

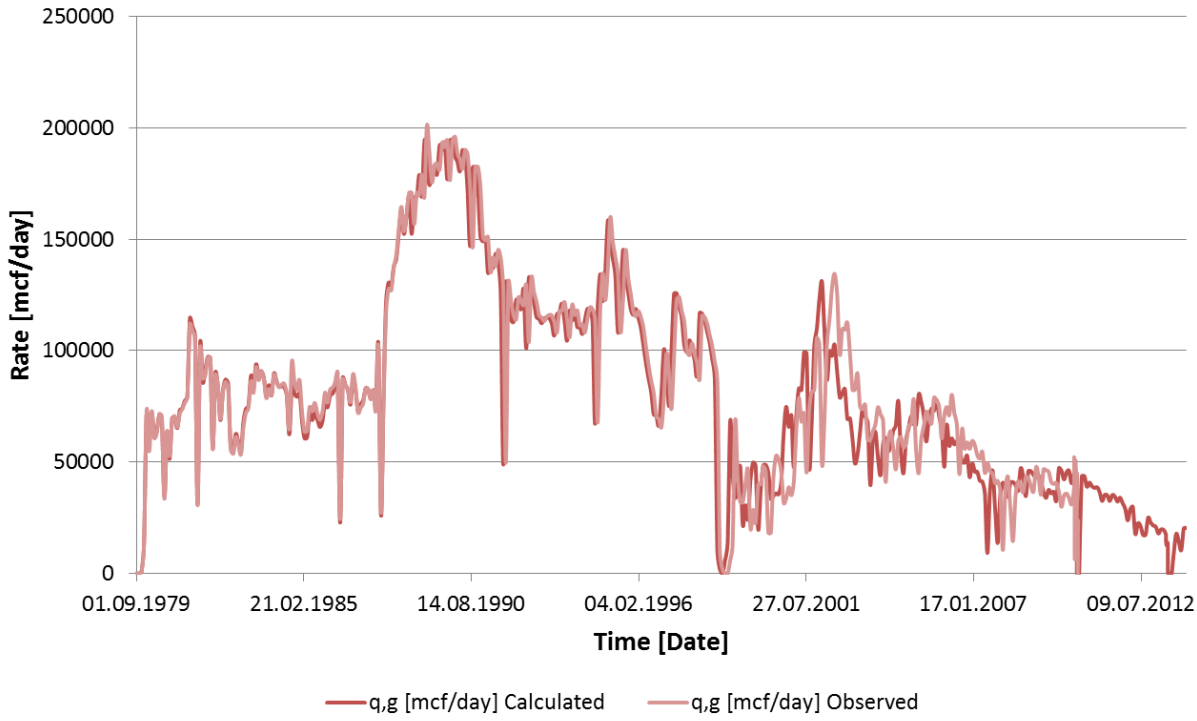

Fig. A.6 History matched gas production rate on Bravo. *History matched gas production rate vs observed (field data) on Bravo. The observed data ends on 22.06.2010.*

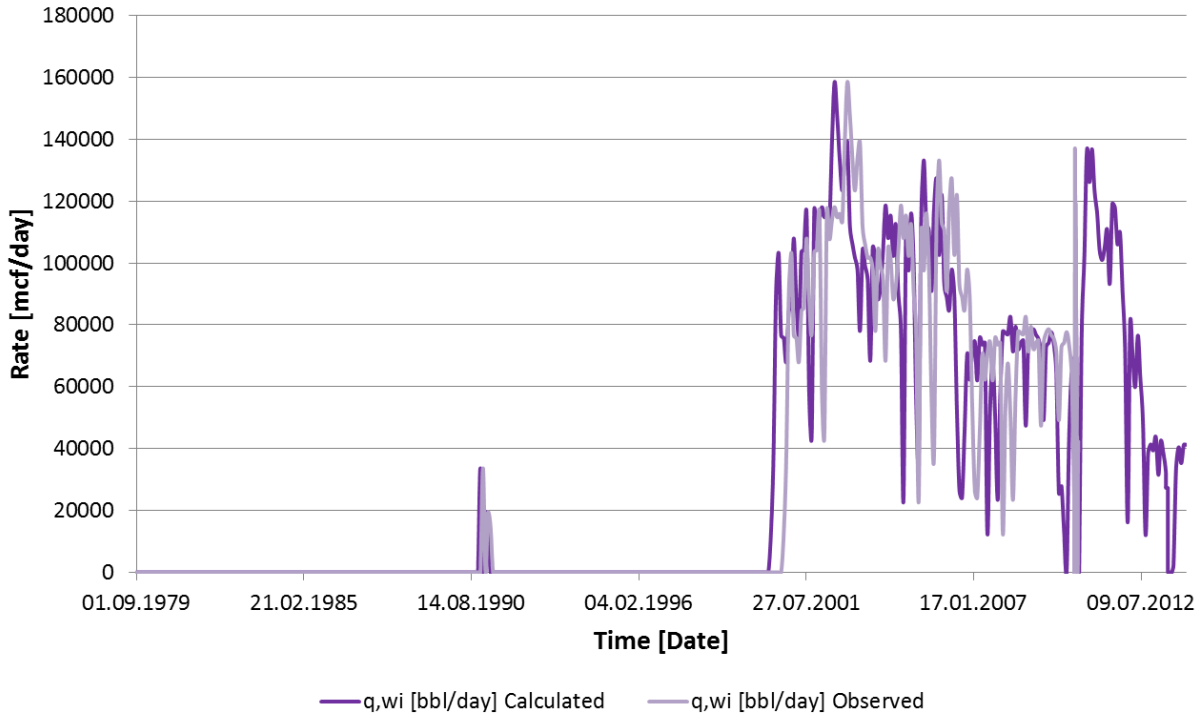

Fig. A.7 History matched water injection rate on Bravo. *History matched water injection rate vs observed (field data) on Bravo. The observed data ends on 22.06.2010.*

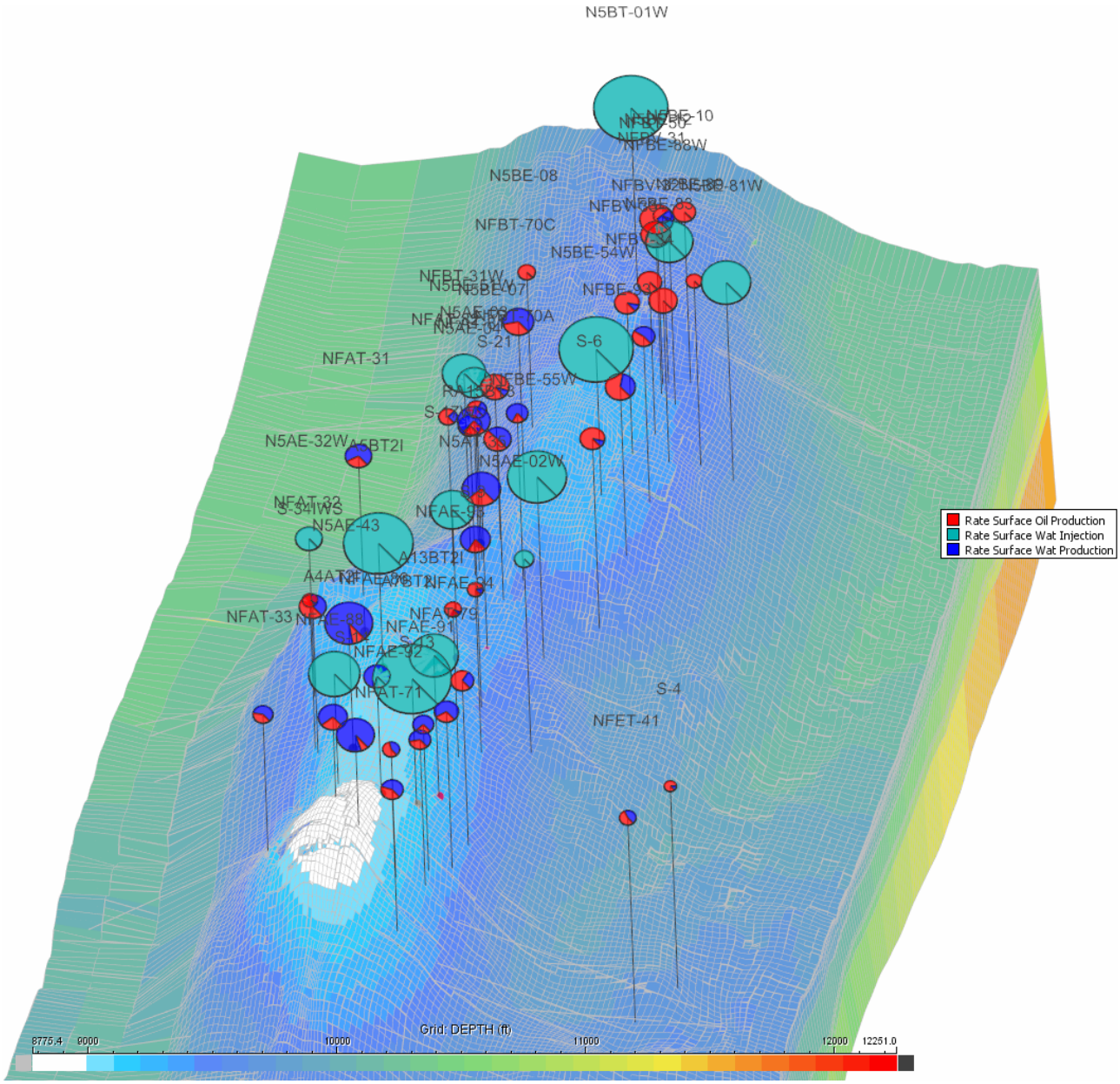

Fig. A.8 Overview of active injectors and producers in 2026. *The figure shows the location of active injectors and producers in 2026 in the Base Case. The bubbles show the relative size of injection or production, and the grid displays the depth.*

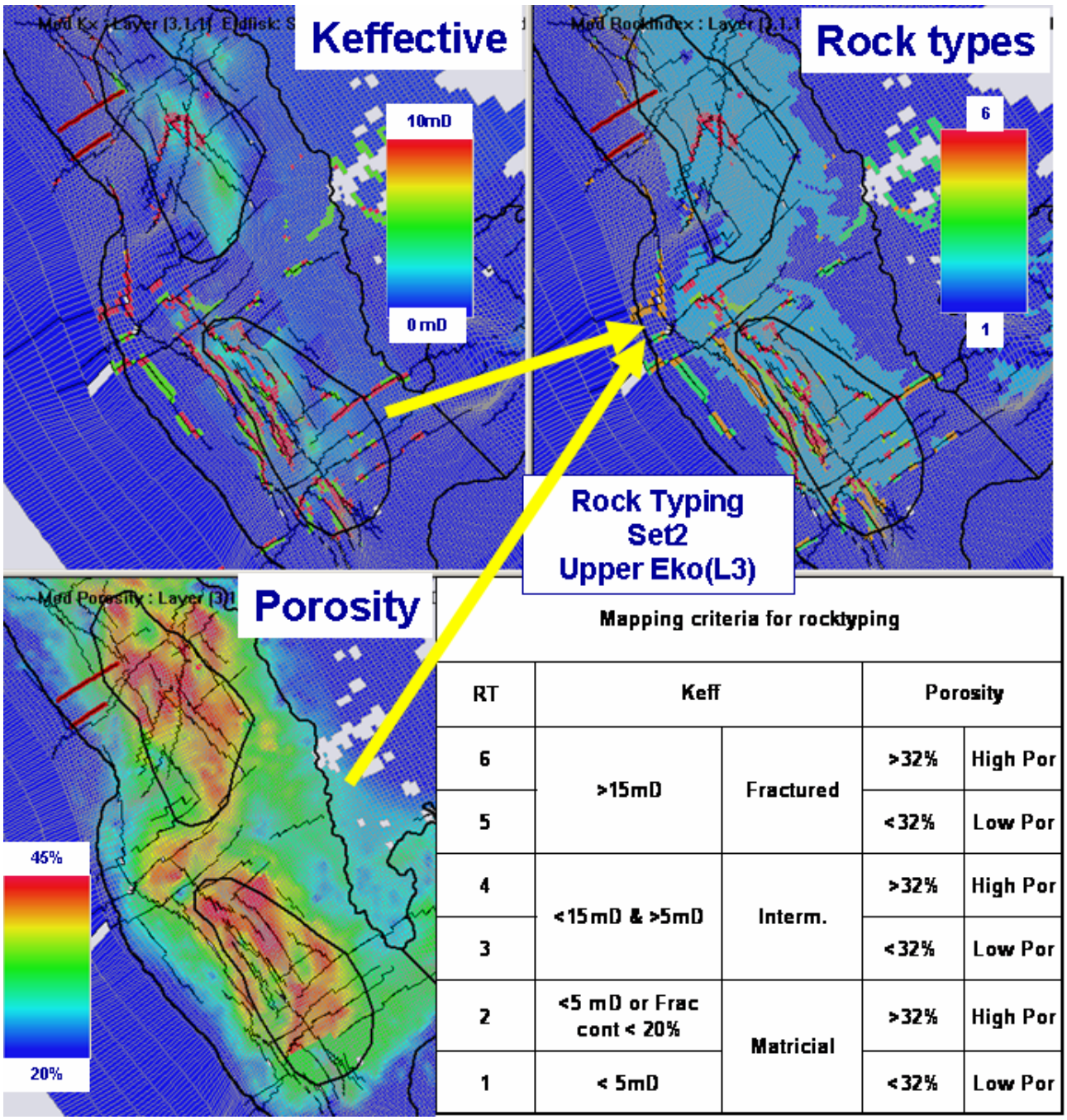

Mapping criteria for rocktyping

RT	Keff		Porosity	
6	>15mD	Fractured	>32%	High Por
5			<32%	Low Por
4	<15mD & >5mD	Interm.	>32%	High Por
3			<32%	Low Por
2	<5 mD or Frac cont < 20%	Matricial	>32%	High Por
1	< 5mD		<32%	Low Por

Fig. A.9 Ekofisk Fm rock typing. *An illustration of how the rock-typing is dervied from permeability and porosity arrays in the upper Ekofisk Fm.*

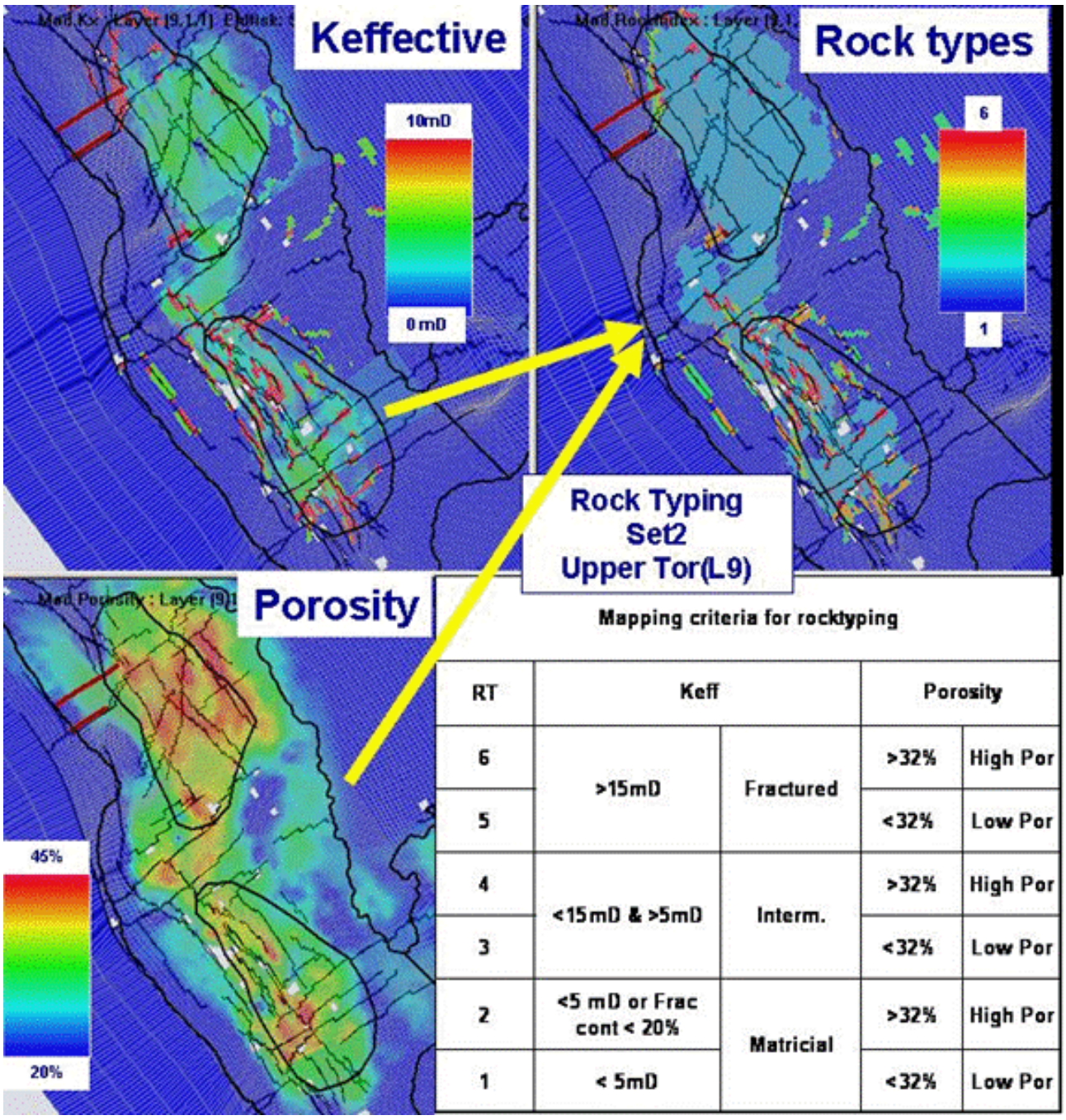

Fig. A.10 Tor Fm rock typing. *An illustration of how the rock-typing is dervied from permeability and porosity arrays in the upper Tor Fm.*

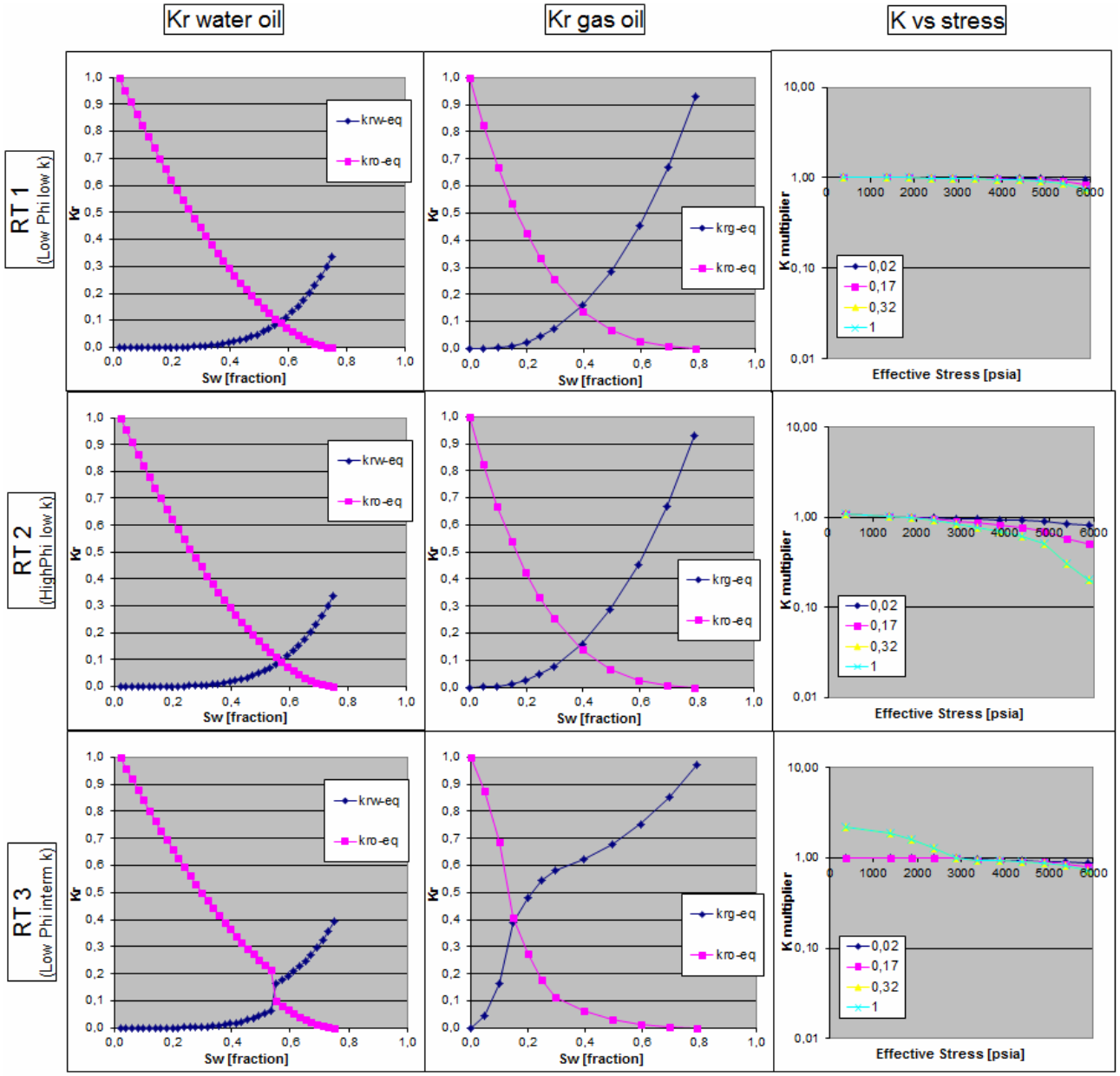

Fig. A.11 Relative permeability and permeability vs stress for rock type 1-3. *Pseudo relative permeability curves for a water-oil system and relative permeability curves for a gas-oil system for rock type 1-3. The permeability vs stress is also given. It shows that with higher k values (higher fracture content) the permeability-multiplier becomes >1 during re-pressurization of the reservoir. The different colored graphs show how the permeability-multiplier change with water content.*

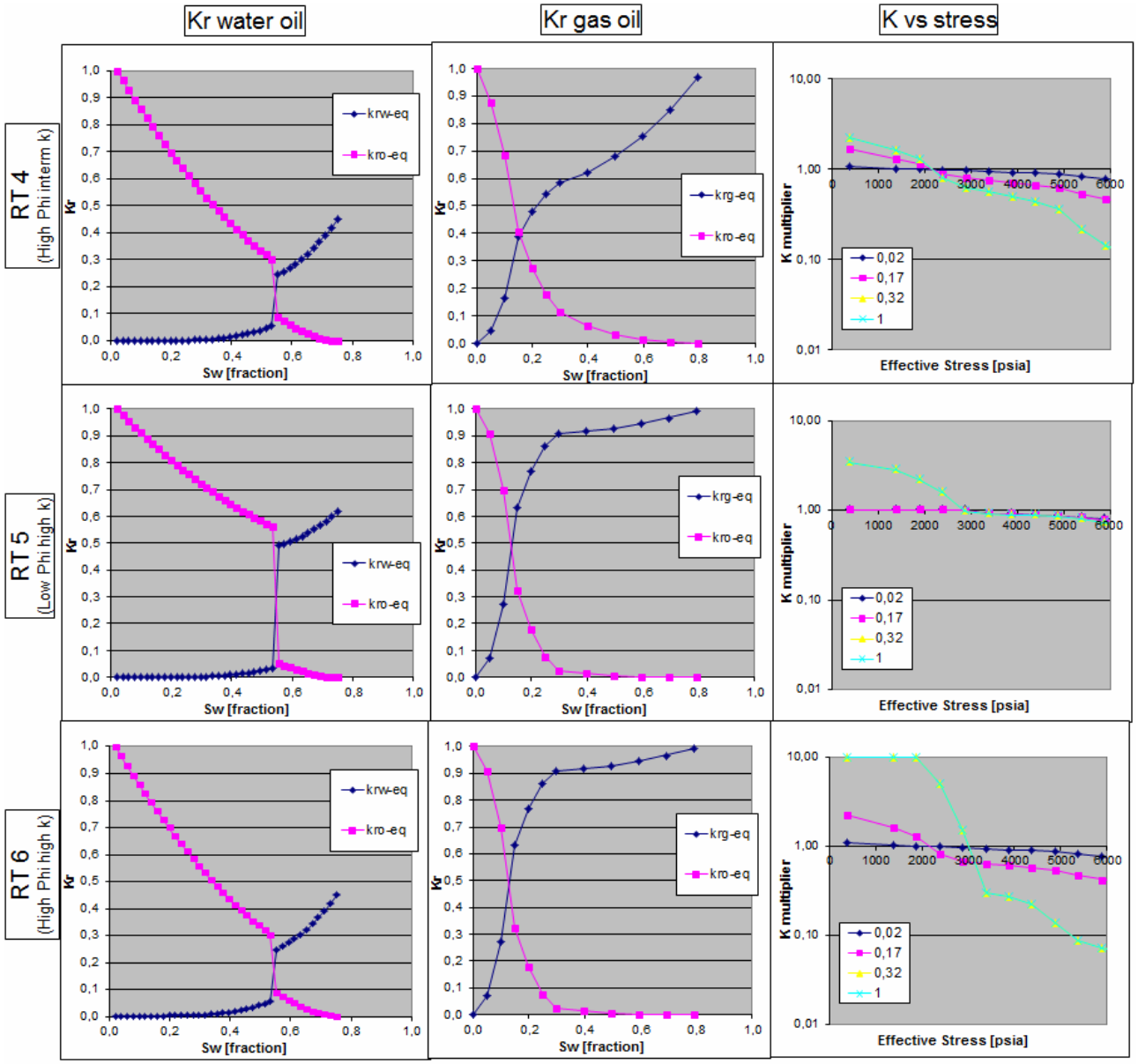

Fig. A.12 Relative permeability and permeability vs stress for rock type 4-6. *Pseudo relative permeability curves for a water-oil system and relative permeability curves for a gas-oil system for rock type 4-6. The permeability vs stress is also given. It shows that with higher k values (higher fracture content) the permeability-multiplier increases during re-pressurization of the reservoir. The different colored graphs show how the permeability-multiplier change with water content.*

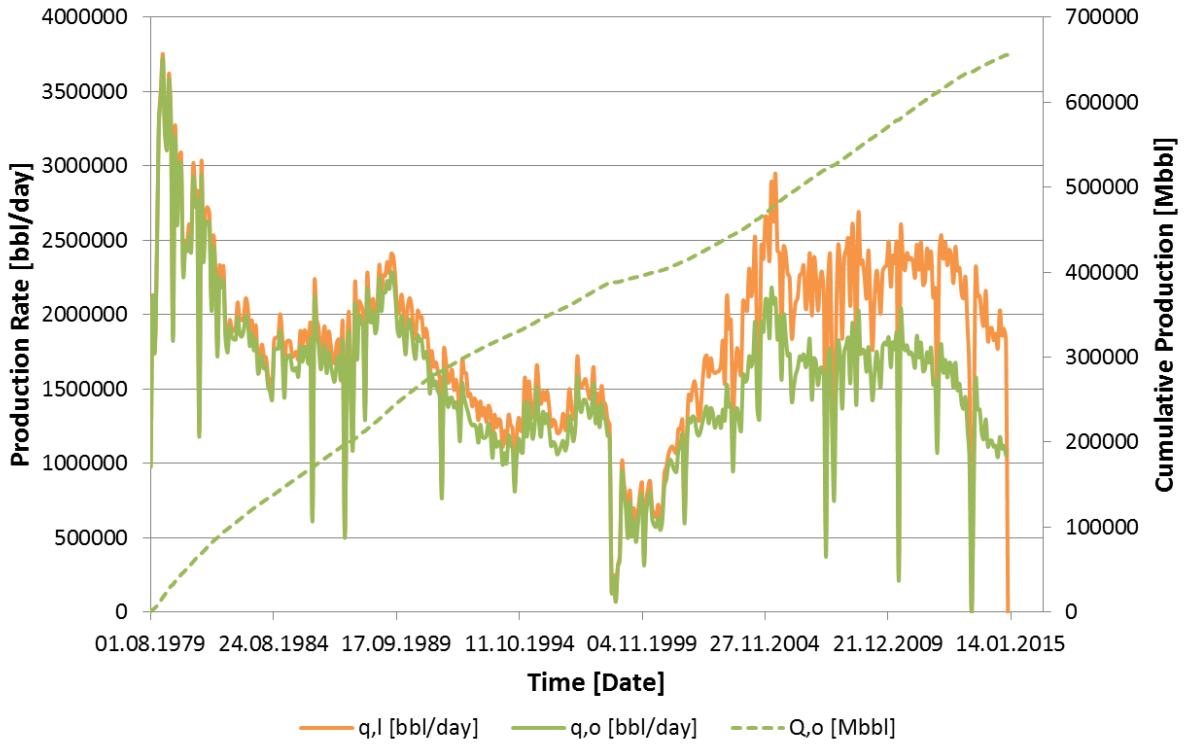

Fig. A.13 Historical field oil and liquid production rate, and cumulative oil production. *WI has resulted in increased oil recovery. At start-up of water injection in year 2000, both the oil and liquid production rate increased.*

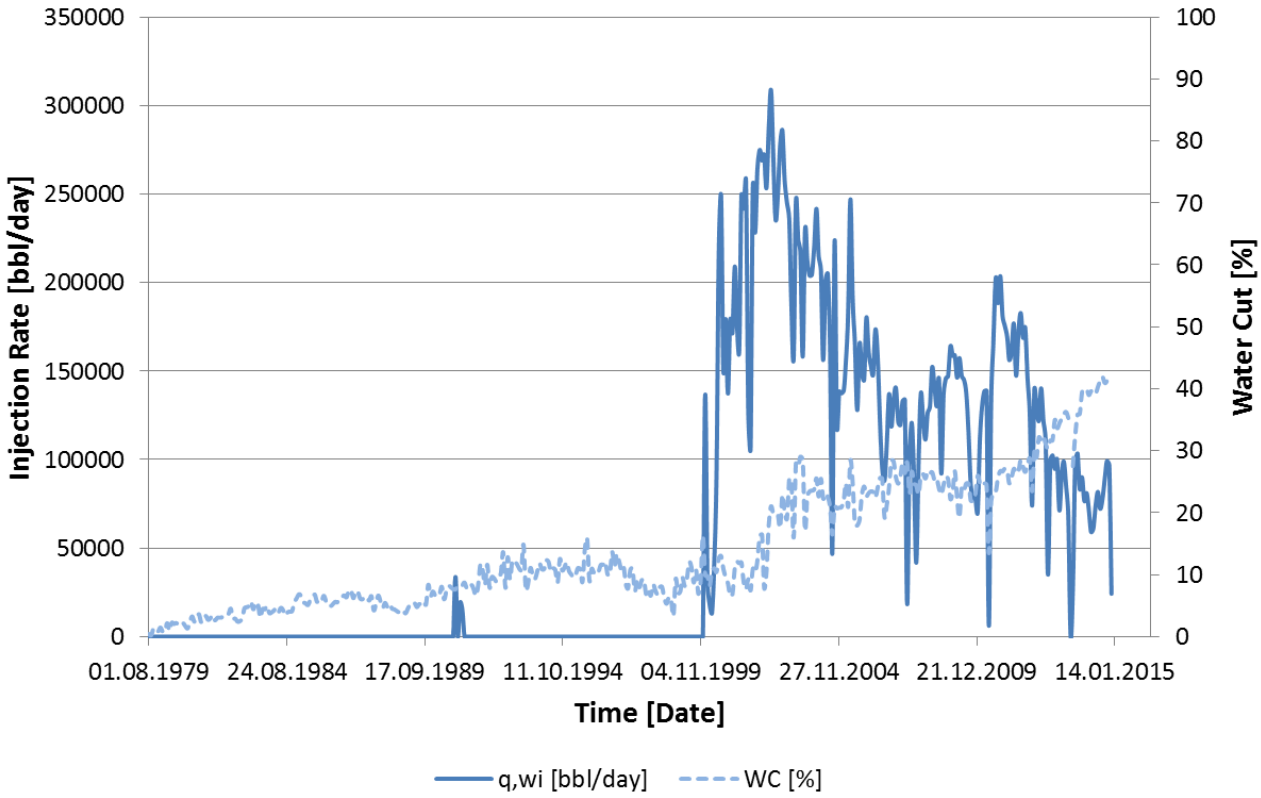

Fig. A.14 Historical field water injection rate and WC. *Start-up of WI was in year 2000. The WC has increased as a result of the waterflood, but is still at a relatively low value (~40 %).*

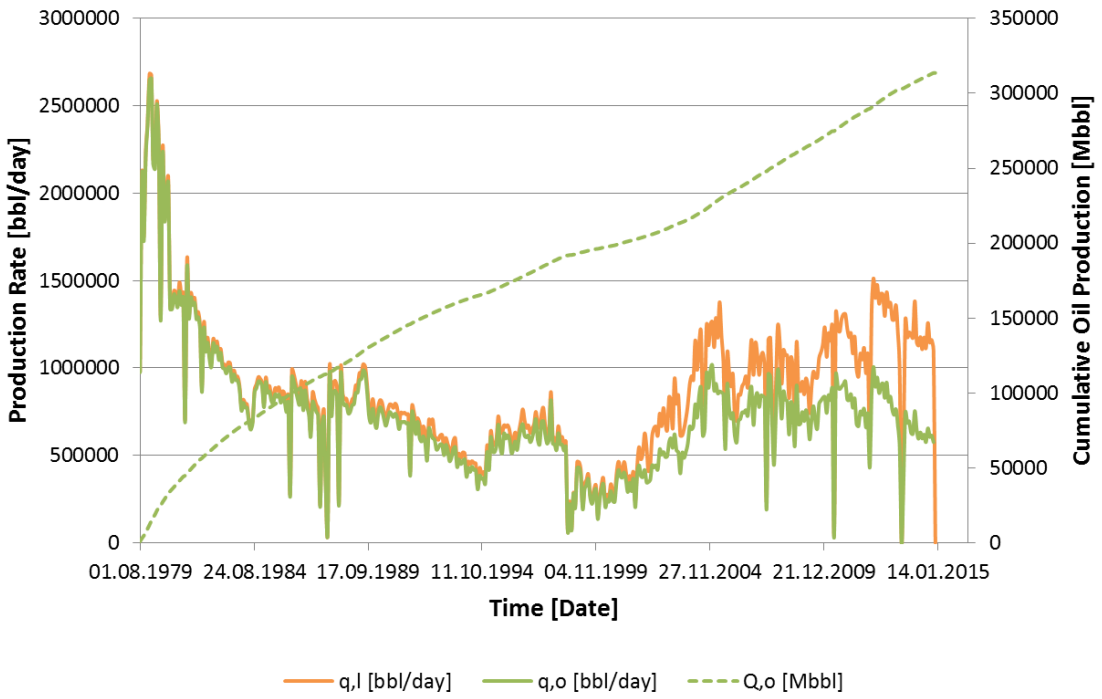

Fig. A.15 Historical Alpha oil and liquid production rate, and cumulative oil production. *WI has resulted in increased oil recovery on Alpha. The oil and liquid production rate have been relatively stable since start-up of WI.*

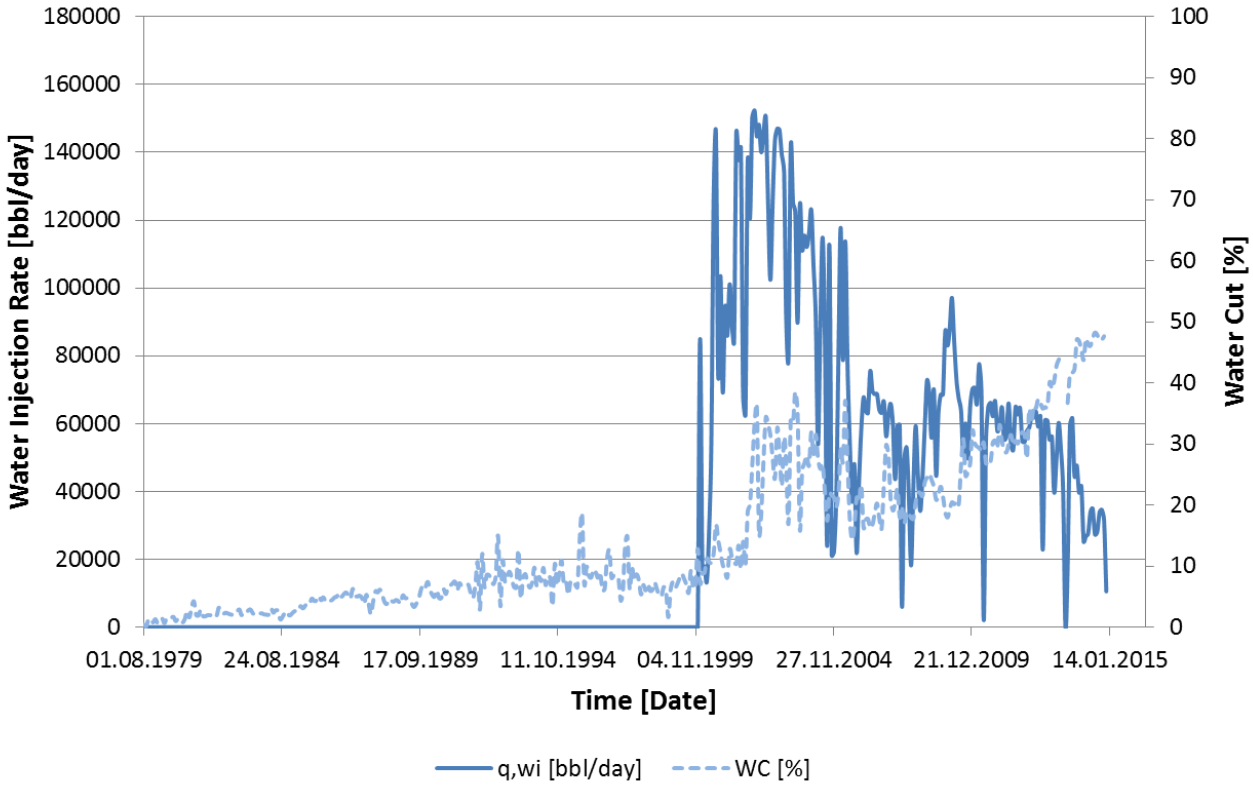

Fig. A.16 Historical Alpha water injection rate and WC. *The WC has increased as a result of the waterflood. On Alpha, the WC has increased while the WI rate has decreased since 2008.*

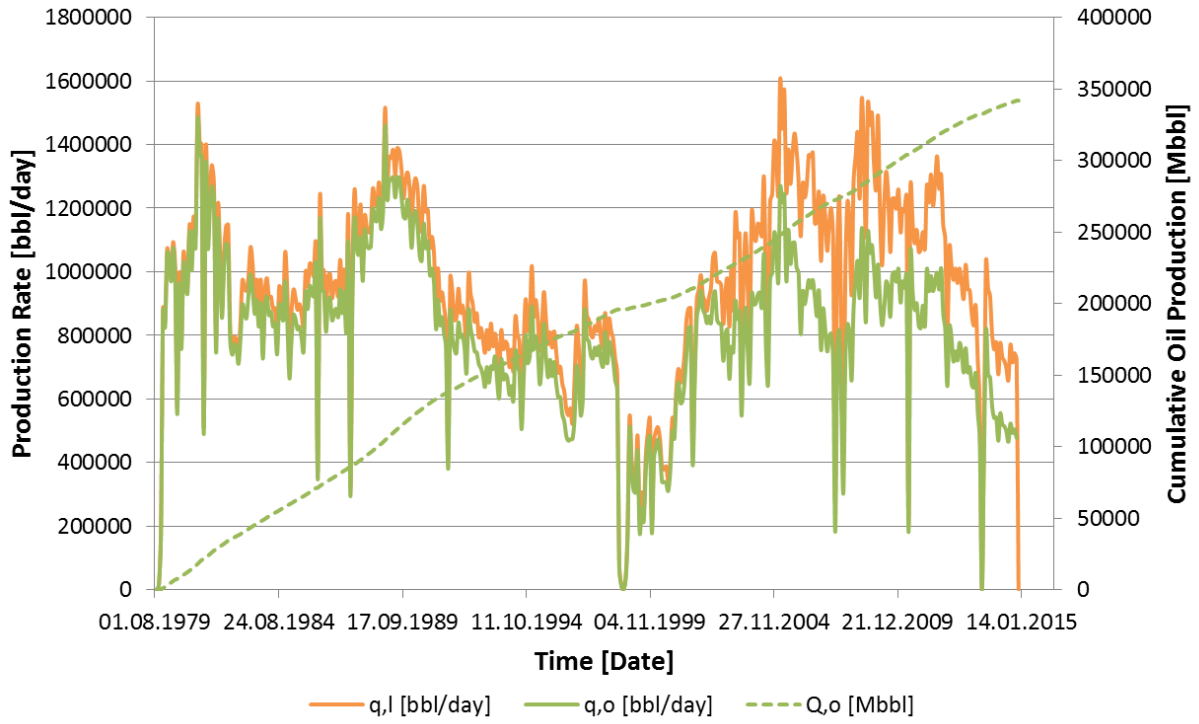

Fig. A.17 Historical Bravo oil and liquid production rate, and cumulative oil production. *WI has resulted in increased oil recovery in Bravo. The oil and liquid production rate has a declining trend.*

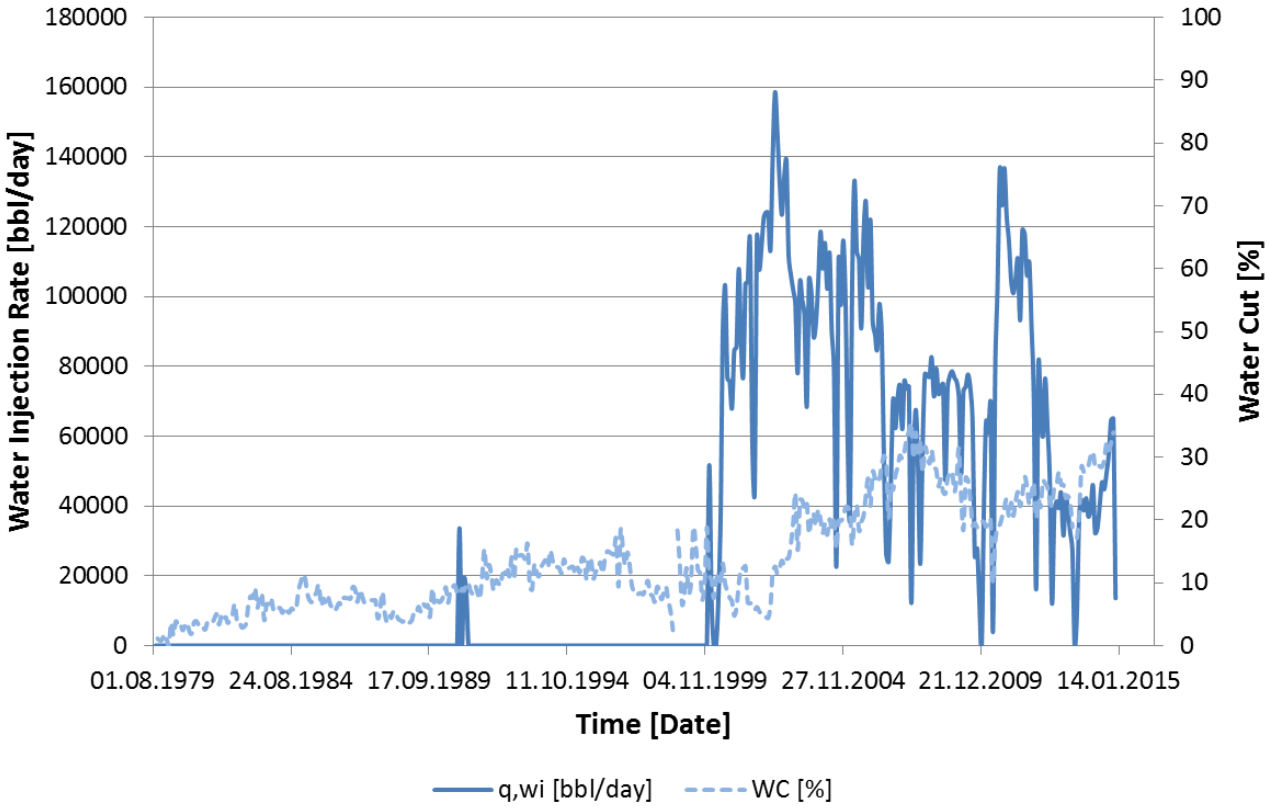

Fig. A.18 Historical Bravo water injection rate and WC. *The WC has increased as a result of the waterflood. Bravo has a relatively stable WC of about 27%.*

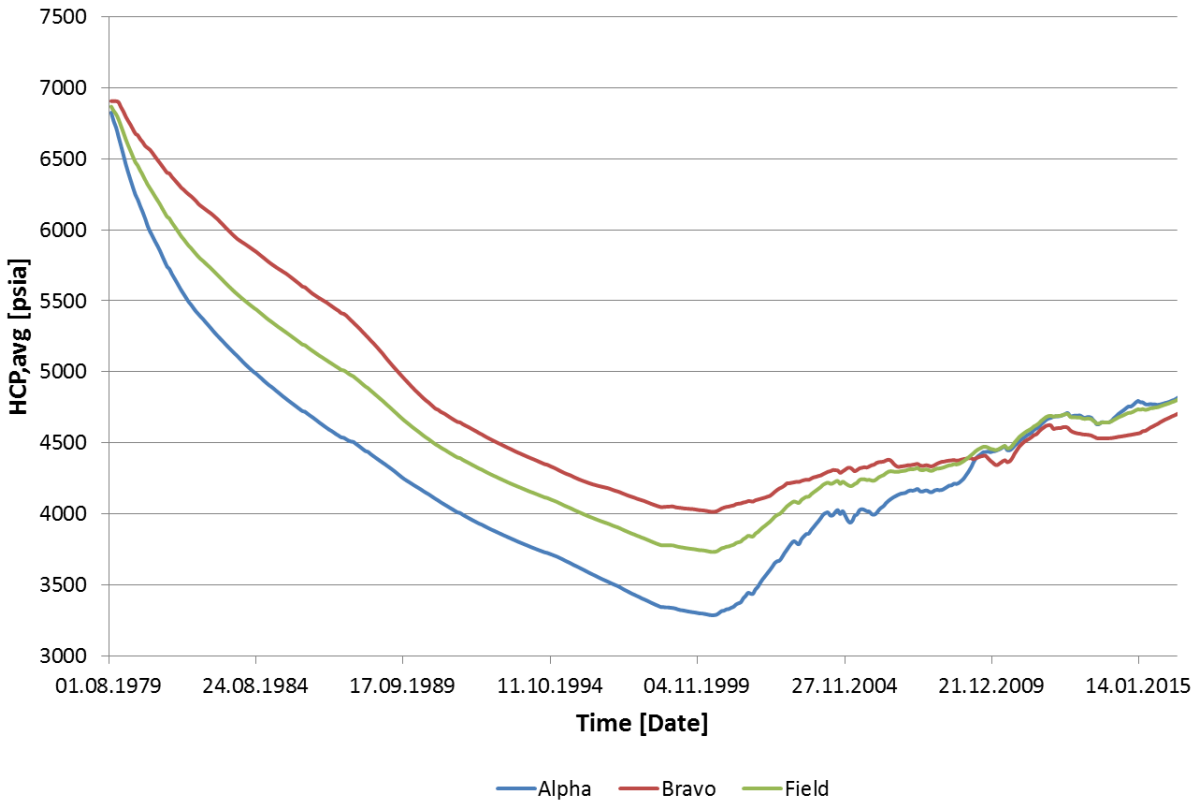

Fig. A.19 Average reservoir pressure from 1979 until 2014. *The figure shows the average pressure in hydrocarbon bearing cells (HCP,avg). It is important to note that there are large pressure differentials on Eldfisk, especially in the Bravo structure, and that this figure only shows the average reservoir pressure.*

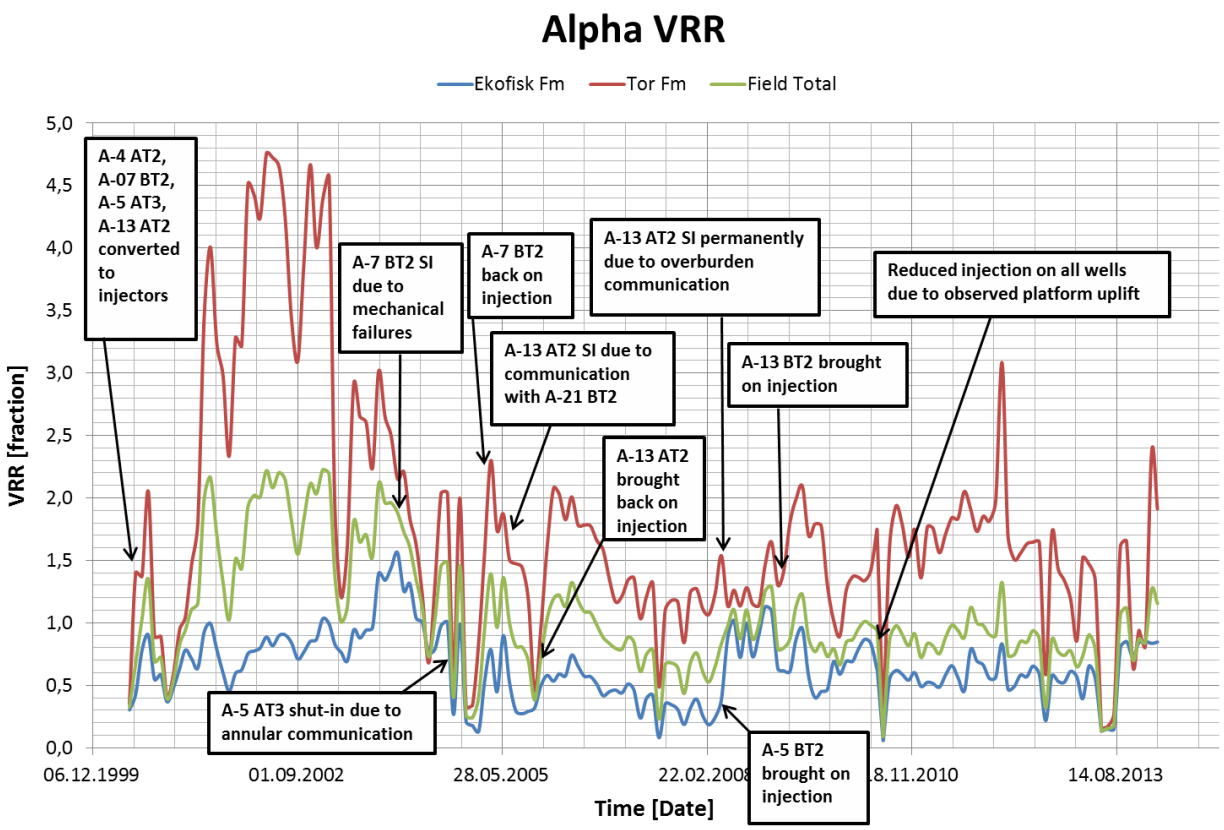

Fig. A.20 Historical Alpha Volume Replacement Ratio (VRR). *The figure shows instantaneous VRR for the Alpha structure, since start of injection. The field average VRR is approximately 1.0. This indicates a good balance in the reservoir in terms of voidage replacement. The highest VRR is in the Tor Fm. Some of the sudden changes in VRR are explained by operational events.*

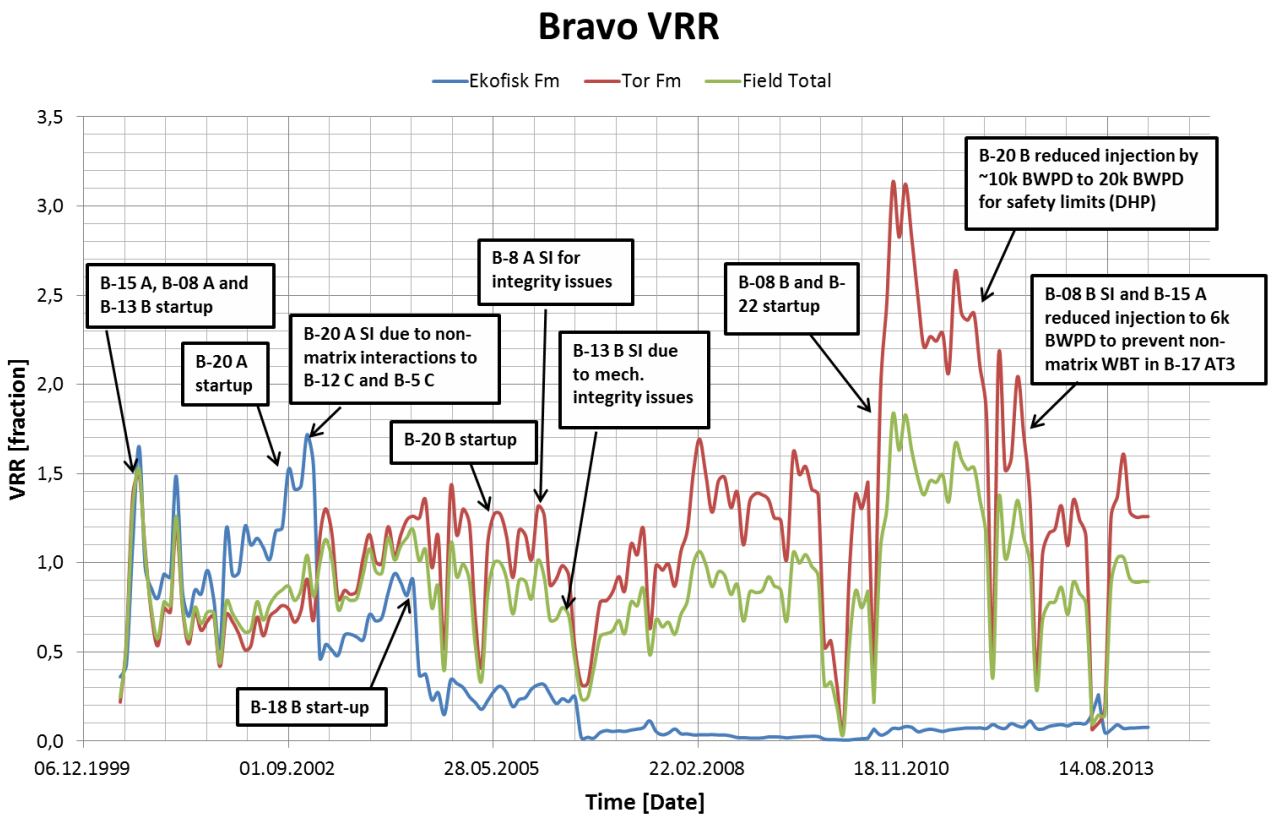

Fig. A.21 Historical Bravo Volume Replacement Ratio (VRR). *The figure shows instantaneous VRR for the Bravo structure, since start of injection. The field average VRR is approximately 1.0. There is a large difference between the Ekofisk Fm and Tor Fm VRR. The Ekofisk Fm is lagging behind in terms of water injection support, and has an average VRR of only ~0.1. Some of the sudden changes in VRR are explained by operational events.*

Appendix B: Tables

Table B.1 Initial Alpha structure volumetrics and permeabilities. The volumetric parameters shown in this table were calculated using a net pay cutoff of Sw < 60 %. Therefore the OOIP is less than the numbers presented in Table 2.1 in chapter 2.2. The average values shown in the table include areas of high pay at the crest (good quality reservoir) and poorer quality pay closer to the flanks (ConocoPhillips, 2012, p.62).

Layer	Formation	Zone	Average Pore Volume Weighted Water Saturation [Fraction]	Average Pore Volume Weighted Porosity [Fraction]	Average Effective Absolute Permeability [mD]	OOIP [MMSTB]
1	Ekofisk	EU1	0,34	0,27	3,0	36,6
2	Ekofisk	EU2	0,22	0,32	4,8	49,6
3	Ekofisk	EU3	0,17	0,36	5,2	125,7
4	Ekofisk	EM1	0,20	0,34	5,5	110,7
5	Ekofisk	EM2	0,17	0,36	5,2	189,1
6	Ekofisk	EL1	0,25	0,30	5,4	33,4
7	Ekofisk	EL2	0,24	0,31	5,8	36,4
8	Ekofisk	EL3	0,25	0,30	4,2	13,8
9	Tor	T1	0,18	0,30	4,9	141,6
10	Tor	T2	0,16	0,30	5,5	94,9
11	Tor	T3	0,15	0,31	5,0	71,2
12	Tor	T4	0,23	0,29	3,3	41,7
13	Tor	T5	0,28	0,27	2,0	1,8
14	Tor	T6	0,40	0,31	9,3	0,8
15	Hod	M	0,34	0,29	8,3	22,8
16	Hod	N1	0,39	0,28	3,1	30,1
17	Hod	N2	0,42	0,28	3,1	15,1
18	Hod	N3	0,45	0,26	4,1	19,4
19	Hod	N4	0,36	0,23	1,8	25,6
Total						1060

Table B.2 Initial Bravo structure volumetrics and permeabilities. The volumetric parameters shown in this table were calculated using a net pay cutoff of Sw < 60 %. Therefore the OOIP is less than the numbers presented in Table 2.1 in chapter 2.2. The average values shown in the table include areas of high pay at the crest (good quality reservoir) and poorer quality pay closer to the flanks (ConocoPhillips, 2012, p.63).

Layer	Formation	Zone	Average Pore Volume Weighted Water Saturation [Fraction]	Average Pore Volume Weighted Porosity [Fraction]	Average Effective Absolute Permeability [mD]	OOIP [MMSTB]
1	Ekofisk	EU1	0,33	0,27	3,7	21,0
2	Ekofisk	EU2	0,24	0,32	3,4	34,5
3	Ekofisk	EU3	0,21	0,35	1,9	104,8
4	Ekofisk	EM1	0,22	0,33	3,2	143,0
5	Ekofisk	EM2	0,25	0,33	2,2	158,8
6	Ekofisk	EL1	0,34	0,28	2,9	71,8
7	Ekofisk	EL2	0,32	0,29	2,6	96,8
8	Ekofisk	EL3	0,27	0,29	5,6	28,0
9	Tor	T1	0,15	0,34	2,9	200,4
10	Tor	T2	0,12	0,35	4,1	187,4
11	Tor	T3	0,12	0,34	4,9	116,2
12	Tor	T4	0,21	0,33	4,9	88,6
13	Tor	T5	0,34	0,34	4,0	24,8
14	Tor	T6	0,31	0,29	0,4	2,2
15	Hod	M	0,51	0,25	1,1	0,3
16	Hod	N1	0,32	0,24	3,9	4,7
17	Hod	N2	0,36	0,26	6,0	1,5
18	Hod	N3	0,28	0,20	2,0	4,9
19	Hod	N4	N/A	N/A	N/A	N/A
Total						1290

Table B.3 Initial Eldfisk East structure volumetrics and permeabilities. The volumetric parameters shown in this table were calculated using a net pay cutoff of Sw < 60 %. Therefore the OOIP is less than the numbers presented in Table 2.1 in chapter 2.2. The average values shown in the table include areas of high pay at the crest (good quality reservoir) and poorer quality pay closer to the flanks (ConocoPhillips, 2012, p.64).

Formation	Average Pore Volume Weighted Water Saturation [Fraction]	Average Pore Volume Weighted Porosity [Fraction]	Average Effective Absolute Permeability [mD]	OOIP [MMSTB]
Ekofisk	0,44	0,30	0,40	21,00
Tor	0,39	0,26	0,60	42,90
Hod	N/A	N/A	N/A	N/A
Total				64

Table B.4 Black oil properties. A summary of black oil properties for the Alpha, Bravo and Eldfisk East structures (ConocoPhillips, 2012, p.60).

Alpha Structure

Variable	Initial	Bubble Point	Current
Pressure (psi)	6860	N/A	5030
Bubble Point (psi)	4843	4843	3770
Formation Volume Factor (rb/stb)	1.65	1.73	1.51
Solution Gas (mscf/stb)	1.35	1.35	1.01
Viscosity (cp)	0.27	0.21	0.33

Bravo Structure

Variable	Initial	Bubble Point	Current
Pressure (psi)	6910	N/A	4880
Bubble Point (psi)	5610	5610	4390
Formation Volume Factor (rb/stb)	1.80	1.85	1.62
Solution Gas (mscf/stb)	1.65	1.65	1.19
Viscosity (cp)	0.21	0.18	0.26

East Eldfisk Structure

Variable	Initial	Bubble Point	Current
Pressure (psi)	6940	N/A	5520
Bubble Point (psi)	3050	3050	3050
Formation Volume Factor (rb/stb)	1.38	1.46	1.40
Solution Gas (mscf/stb)	0.77	0.77	0.77
Viscosity (cp)	0.57	0.33	0.48

Table B.5 Lookup table to generate simulation sensitivity runs. This lookup table was used in SplicerXL to locate well name from well number. Well number 0 was used to create the Base Case.

Well Number	Existing Wells Name	Future Wells Name
0		
1	A1T2	S-14
2	A2B	S-8
3	A3B	S-13
4	A6AT2	S-9
5	A9AT3	S-4
6	A10	S-34IWS
7	A11	S-21
8	A12A	S-6
9	A14B	NFBT-70A
10	A15BT3	NFBT-70C
11	A16A	NFAT-81
12	A17A	NFAE-92
13	A18E	NFAE-88
14	A19BT4	NFBV-33
15	A20B	NFBV-34
16	A22B	N5AE-43
17	A23B	N5AE-04
18	A25T2	NFAE-93
19	A26T2	NFAT-79
20	A27AT2	NFAT-32
21	A28AT2	N5AT-35
22	A29B	NFBE-93
23	A30BT3	N5BE-07
24	B1DT3	NFET-41
25	B2BT3	NFAT-31
26	B3A	NFAE-94
27	B4B	NFAT-33
28	B5C	N5AE-03
29	B6A	NFAE-91
30	B7B	NFAT-71
31	B9A	NFAT-82
32	B10C	NFBE-83
33	B11B	NFBV-31
34	B12C	N5BE-10
35	B14CT2	NFBV-32
36	B16A	NFBT-50
37	B17BT2	NFBE-89
38	B18B	N5BE-12
39	B19B	N5BE-08
40	B21T4	NFAE-86
41		N5AE-31
42		NFBE-07
43		N5AT-72
44		NFAE-70

Table B.6 Conversion value of existing producers. The table shows the field cumulative oil production and the relative difference in the conversion runs to the Base Case (which is referred to as value of injector). The wells are converted on 01/01/2015 and inject until end of simulation in 01/01/2050 (or when the pressure is too high to inject). Also, the field cumulative WI and the relative difference in cumulative WI in the conversion runs to the Base Case is included. MMSTB = 10^6 STB.

Well Name	Conversion Date	Field Cum Oil [MMSTB]	Diff Cum Oil [MMSTB]	Field Cum WI [MMSTB]	Diff Cum WI [MMSTB]
Base Case		939		1886	
A1T2	01.01.2015	938	-0,7	1892	5
A2B	01.01.2015	937	-2,4	1883	-3
A3B	01.01.2015	940	0,6	1898	11
A6AT2	01.01.2015	938	-1,2	1891	5
A9AT3	01.01.2015	940	0,5	1893	7
A10	01.01.2015	939	-0,2	1898	12
A11	01.01.2015	939	0,1	1888	2
A12A	01.01.2015	941	1,5	1892	6
A14B	01.01.2015	939	0,3	1883	-3
A15BT3	01.01.2015	939	-0,2	1891	5
A16A	01.01.2015	939	-0,3	1891	4
A17A	01.01.2015	936	-3,2	1913	27
A18E	01.01.2015	939	-0,2	1889	3
A19BT4	01.01.2015	939	-0,1	1889	3
A20B	01.01.2015	939	-0,4	1890	4
A22B	01.01.2015	940	0,6	1888	2
A23B	01.01.2015	939	-0,1	1893	7
A25T2	01.01.2015	939	0,2	1890	3
A26T2	01.01.2015	939	0,0	1886	0
A27AT2	01.01.2015	932	-6,8	1882	-4
A28AT2	01.01.2015	937	-2,0	1897	11
A29B	01.01.2015	939	0,1	1888	2
A30BT3	01.01.2015	940	0,6	1889	3
B1DT3	01.01.2015	938	-0,8	1888	2
B2BT3	01.01.2015	941	2,2	1899	13
B3A	01.01.2015	939	-0,5	1890	4
B4B	01.01.2015	936	-2,6	1893	7
B5C	01.01.2015	938	-1,3	1903	17
B6A	01.01.2015	939	0,2	1894	8
B7B	01.01.2015	939	0,3	1895	9
B9A	01.01.2015	940	1,3	1895	9
B10C	01.01.2015	940	1,2	1891	5
B11B	01.01.2015	940	0,6	1894	7
B12C	01.01.2015	940	0,7	1893	6
B14CT2	01.01.2015	939	0,3	1896	10
B16A	01.01.2015	938	-1,0	1892	6
B17BT2	01.01.2015	941	2,1	1895	9
B18B	01.01.2015	939	0,4	1892	6
B19B	01.01.2015	939	0,1	1894	7
B21T4	01.01.2015	941	2,3	1900	14

Table B.7 Conversion value of future producers. The table shows the field cumulative oil production and the relative difference in the conversion runs to the Base Case (which is referred to as value of injector). The wells are converted on their individual start up date and inject until end of simulation in 01/01/2050 (or when the pressure is too high to inject). Also, the field cumulative WI and the relative difference in cumulative WI in the conversion runs to the Base Case is included. MMSTB = 10^6 STB.

Well SI	Conversion Date	Field Cum Oil [MMSTB]	Diff Cum Oil [MMSTB]	Field Cum WI [MMSTB]	Diff Cum WI [MMSTB]
Base Case		939		1886	
S-14	01.01.2015	937	-1,7	1873	-13
S-8	05.01.2015	938	-1,6	1884	-3
S-13	10.01.2015	936	-3,3	1887	1
S-9	22.01.2015	938	-1,0	1890	4
S-4	28.04.2015	938	-0,7	1893	7
S-34IWS	31.05.2015	938	-0,9	1911	25
S-21	29.07.2015	940	0,4	1899	13
S-6	07.12.2015	936	-3,4	1886	0
NFBT-70A	06.04.2016	938	-1,6	1895	8
NFBT-70C	14.06.2016	933	-5,8	1873	-13
NFAT-81	05.11.2016	937	-2,4	1890	3
NFAE-92	25.12.2016	935	-3,8	1887	1
NFAE-88	16.02.2017	934	-4,7	1880	-7
NFBV-33	12.04.2017	936	-2,8	1885	-1
NFBV-34	28.05.2017	937	-2,0	1882	-4
N5AE-43	02.08.2017	934	-4,8	1854	-32
N5AE-04	11.01.2018	939	0,1	1882	-4
NFAE-93	03.03.2018	936	-3,6	1882	-4
NFAT-79	22.04.2018	936	-2,7	1879	-7
NFAT-32	13.06.2018	937	-1,9	1906	20
N5AT-35	05.08.2018	938	-1,1	1870	-16
NFBE-93	05.12.2018	930	-9,1	1870	-16
N5BE-07	08.02.2019	937	-2,2	1893	6
NFET-41	02.08.2019	936	-3,2	1893	7
NFAT-31	03.10.2019	939	-0,4	1882	-4
NFAE-94	15.11.2019	933	-6,0	1876	-11
NFAT-33	20.12.2019	937	-1,8	1890	4
N5AE-03	12.02.2020	938	-1,1	1886	0
NFAE-91	31.03.2020	939	-0,3	1884	-2
NFAT-71	20.05.2020	937	-2,2	1892	5
NFAT-82	14.11.2020	937	-2,4	1886	-1
NFBE-83	01.11.2020	936	-3,0	1884	-2
NFBV-31	01.11.2020	934	-4,8	1886	0
N5BE-10	01.01.2021	936	-3,3	1886	0
NFBV-32	01.02.2021	937	-1,9	1887	1
NFBT-50	01.04.2021	932	-6,8	1881	-5
NFBE-89	01.06.2021	938	-1,0	1887	1
N5BE-12	01.07.2021	937	-1,8	1887	0
N5BE-08	01.09.2021	936	-2,6	1887	1
NFAE-86	13.08.2023	938	-0,8	1884	-3
N5AE-31	06.10.2026	940	0,7	1892	6
NFBE-07	07.11.2030	937	-1,7	1887	1
N5AT-72	10.07.2036	938	-1,3	1885	-2
NFAE-70	23.10.2036	936	-2,9	1877	-9

Table B.8 Injector performance data (including successful producer conversions). The table gives an overview of the overall existing injectors, future injectors and successful producer convserions performance data in 2050. It shows the well name, structure, cumulative WI, well value and well life. The table also gives an estimate of the individual injectors contribution to oil production per year (well value/well life). As an example this shows that even though A-5 has the highest value of the existing injectors, it does not contibute as much as the Bravo wells on a yearly basis. For the producer conversions, the well value and well life as producer is also included.

Existing Injectors Value

Structure	Well Name	Cum Water [MMSTB]	Well Value [MMSTB]	Well life [months]	Well Value/Well life [MMSTB/year]
Alpha	A4 AT2	61	0,3	276	0,01
	A5 BT2	154	7,4	420	0,21
	A7 BT2	180	1,3	420	0,04
	A13 BT2	51	1,2	260	0,05
Bravo	B8 B	32	3,9	84	0,56
	B15 A	32	4,4	84	0,63
	B20 B	40	5,9	84	0,84
	B22	40	6,1	84	0,87

Future Injectors Value

Structure	Well Name	Cum Water [MMSTB]	Well Value [MMSTB]	Well life [months]	Well Value/Well life [MMSTB/year]
Alpha	S-17W	55	11,2	411	0,33
	N5AE-32W	24	3,3	399	0,10
	N5AE-02W	8	0,6	365	0,02
Bravo	NFBT-31W	41	5,9	385	0,18
	N5BE-51W	26	6,0	379	0,19
	N5BT-01W	110	4,9	350	0,17
	N5BE-54W	78	3,9	348	0,13
	N5BE-81W	47	3,8	348	0,13
	NFBE-88W	37	5,1	345	0,18
	NFBE-55W	59	5,5	348	0,19

Existing Producers Conversions

Structure	Well Name	Well Value as Producer [MMSTB]	Well Life as Producers [months]	Well Value as injectors [MMSTB]	Cum Water [MMSTB]	Well life [months]	Formation	Well Value/Well life [MMSTB/year]
Bravo	B-2 BT3	0	0	2,2	29,0	420	Tor/Eko	0,06
	B-17 BT2	0	12	2,1	17,4	420	Tor/Eko	0,06
	B-21 T4	-0,3	66	2,3	29,3	420	Eko	0,06

Appendix C: Maps

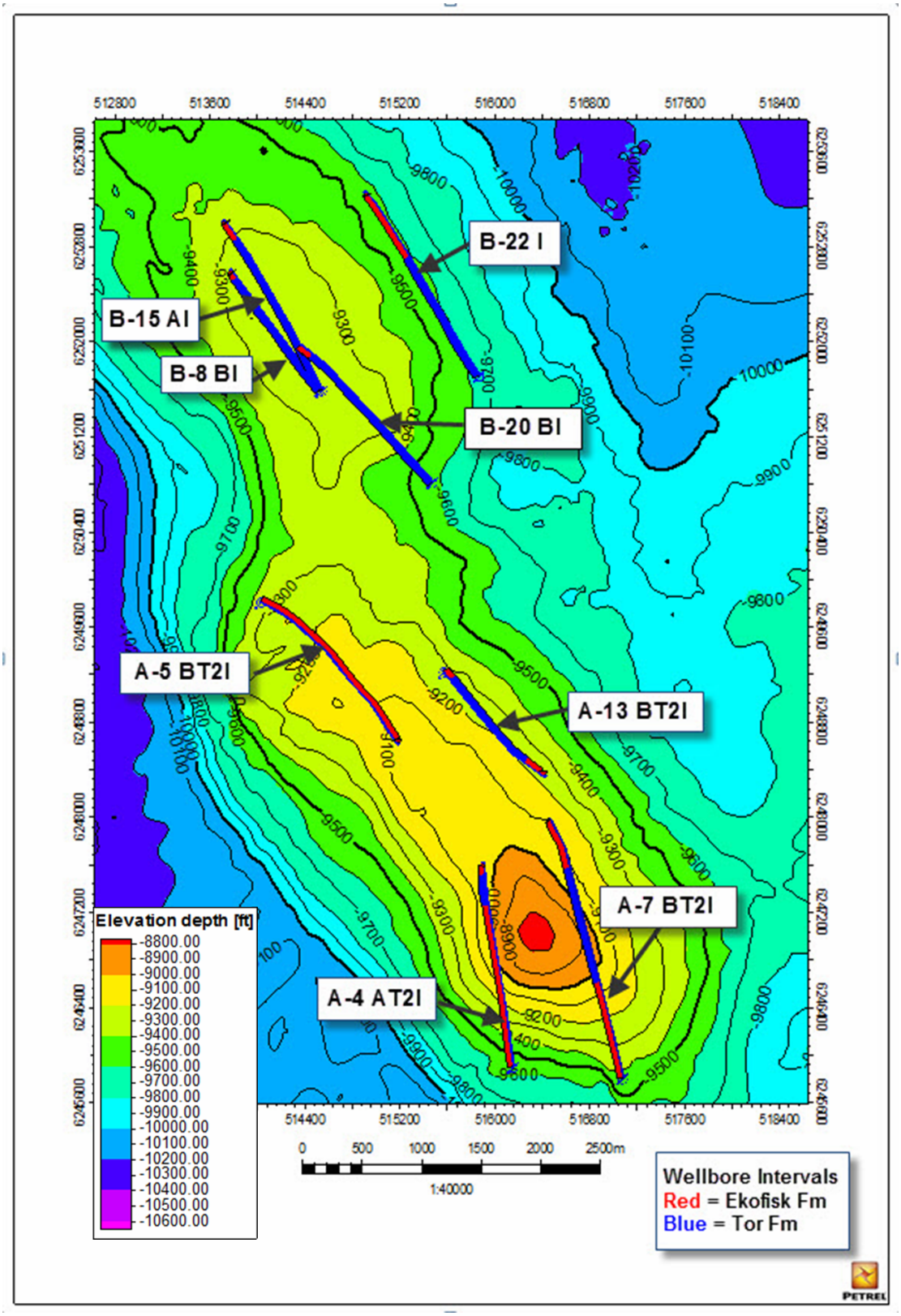

Fig. C.1 Map of injectors showing their presence in the Ekofisk and Tor Fm.. *It becomes visible that the Ekofisk Fm in the Bravo structure has not been a target for water injection.*